

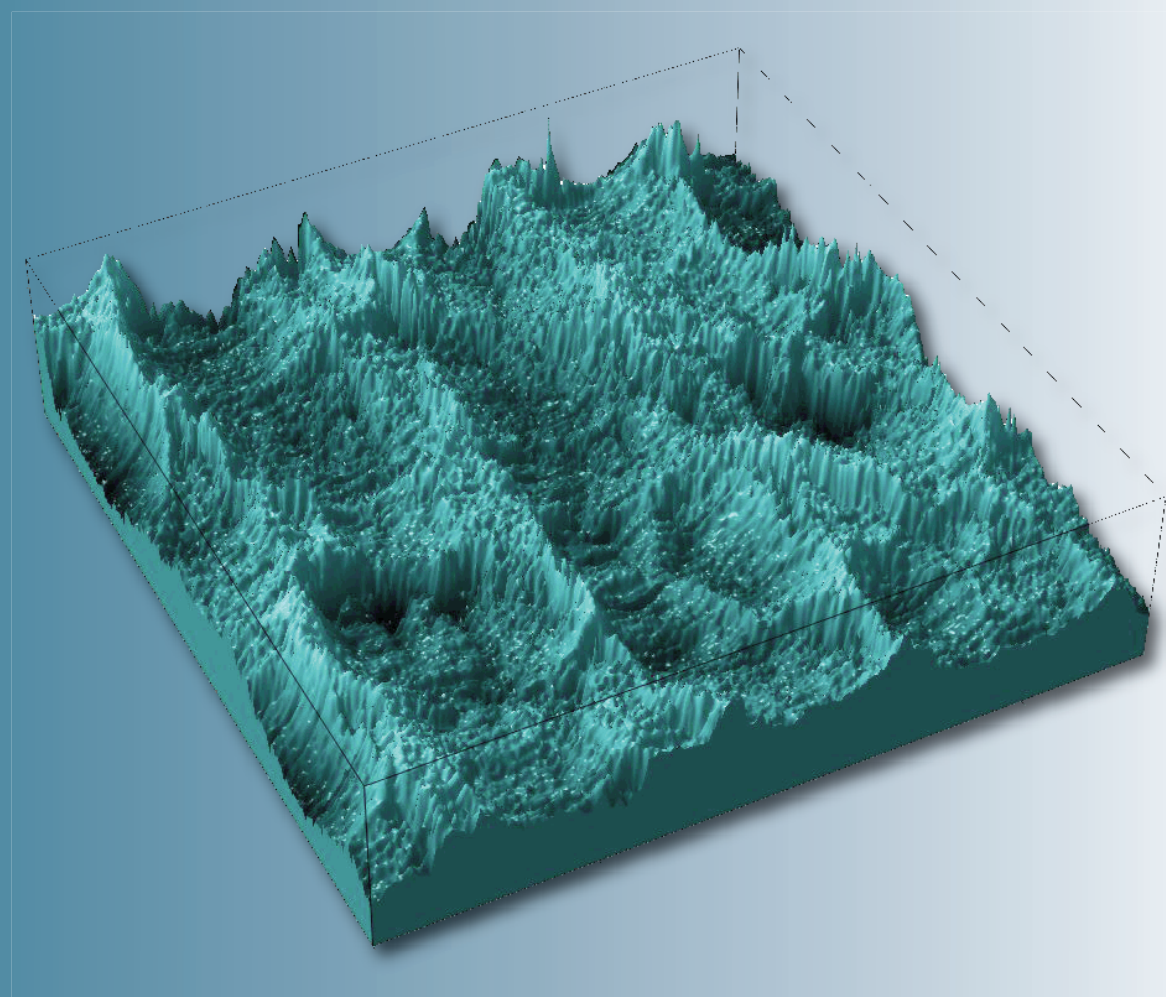


ISSN 1028-8546

Volume XX, Number 1
Section: En
April, 2014

Azerbaijan Journal of Physics

Fizika



www.physics.gov.az

G.M. Abdullayev Institute of Physics
Azerbaijan National Academy of Sciences
Department of Physical, Mathematical and Technical Sciences

Published from 1995
Ministry of Press and Information
of Azerbaijan Republic,
Registration number 402, 16.04.1997

ISSN 1028-8546
vol. XX, Number 1, 2014
Series: En

Azerbaijan Journal of Physics

FIZIKA

*G.M.Abdullayev Institute of Physics
Azerbaijan National Academy of Sciences
Department of Physical, Mathematical and Technical Sciences*

HONORARY EDITORS

Arif PASHAYEV

EDITORS-IN-CHIEF

Nazim MAMEDOV

Chingiz QAJAR

SENIOR EDITOR

Talat MEHDIYEV

INTERNATIONAL REVIEW BOARD

Ivan Scherbakov, Russia
Kerim Allahverdiyev, Azerbaijan
Mehmet Öndr Yetiş, Turkey
Gennadii Jablonskii, Buelorussia
Rafael Imamov, Russia
Vladimir Man'ko, Russia
Eldar Salayev, Azerbaijan
Dieter Hochheimer, USA
Victor L'vov, Israel
Vyacheslav Tuzlukov, South Korea
Majid Ebrahim-Zadeh, Spain

Firudin Hashimzadeh, Azerbaijan
Anatoly Boreysho, Russia
Mikhail Khalin, Russia
Hasan Bidadi, Tebriz, East Azerbaijan, Iran
Natiq Atakishiyev, Mexico
Maksud Aliyev, Azerbaijan
Iskender Djafarov, Azerbaijan
Arif Hashimov, Azerbaijan
Vali Huseynov, Azerbaijan
Javad Abdinov, Azerbaijan
Bagadur Tagiyev, Azerbaijan

Tayar Djafarov, Azerbaijan
Talat Mehdiyev, Azerbaijan
Emil Guseynov, Azerbaijan
Ayaz Baramov, Azerbaijan
Tofiq Mammadov, Azerbaijan
Salima Mehdiyeva, Azerbaijan
Shakir Nagiyev, Azerbaijan
Rauf Guseynov, Azerbaijan
Almuk Abbasov, Azerbaijan
Yusif Asadov, Azerbaijan

TECHNICAL EDITORIAL BOARD

Senior secretary Elmira Akhundova, Nazli Guseynova, Sakina Aliyeva,
Nigar Akhundova, Elshana Aleskerova

PUBLISHING OFFICE

131 H.Javid ave, AZ-1143, Baku
ANAS, G.M.Abdullayev Institute of Physics

Tel.: (99412) 439-51-63, 439-32-23
Fax: (99412) 447-04-56
E-mail: jophphysics@gmail.com
Internet: www.physics.gov.az

It is authorized for printing:

Published at "SƏRQ-QƏRB"
17 Ashug Alessger str., Baku
Typographer : Aziz Gulaliyev

Sent for printing on: ___. 201__
Printing approved on: ___. 201__
Physical binding: _____
Number of copies: ____ 200
Order: _____

THE ANALYSIS OF MAIN ARTIFACTS IN SCANNING PROBE MICROSCOPY (III)

S.D. ALEKPEROV^{1,2}

¹The branch of MSU named by M.V.Lomonosov in Baku

AZ-1141, Baku, F.Agayeva str., 14

²Institute of Physics named by G.B.Abdullayev of Azerbaijan National Academy of Sciences

AZ-1143, Baku, np. G.Javid ave., 33

e-mail: sdalekperov@mail.ru

The analysis of methodology of experiment carrying out in the region of scanning probe microscopy (SPM) is carried out in the article, the main parameters influencing on image quality are revealed. In order to reveal the artifact reason, we consider the main components of SPM signal which are divided on 5 groups: desired signal; noises connected with external influences and temperature drift; distortions connected with piezo-ceramics and piezo-scanner non-perfection; the influence of probe geometry; equipment noises. The main methods of elimination and minimization of the given artifacts are considered. The processes taking place in “needle-surface” system are analyzed in the third part of the article. The estimation of critical parameters of the needle and needle edge and also influence degree of these parameters on the surface at scanning is carried out. It is shown that knowledge of probe geometry allows us to minimize the artifacts connected with probe and also use the probes the more suitable for representation of interesting peculiarities of the investigated sample.

Keywords: scanning probe microscopy (SPM); scanning tunneling microscopy (STM); atomic force microscopy (AFM).

PACS: 81.05.Je, 81.70.-q

IV. THE PROBE SPACE GEOMETRY AND DISTORTIONS OF SPM-SURFACE IMAGES

1. INTRODUCTION

Scanning probe microscopy (SPM) is subdivided into scanning tunnel microscopy (STM) and atomic force microscopy (AFM). Both of a method mutually supplement each other and allow receiving rather extensive information on various characteristics of a surface.

However, from the point of view of the spatial resolution, between them there is an essential difference. If STM really shows the resolution down to atomic, for AFM the level of the molecular-atomic resolution (especially in lateral planes) is while an unattainable level. A principal cause here is that resolution AFM very strongly depends on the geometrical sizes of point of the tip of a microscope. Even though atomic force microscopy [1,2] has been successful in imaging surfaces with atomic resolution, it is still doubtful whether true atomic resolution is really obtained. Most images reported show perfect crystal lattices or defects much larger than atomic scale defects. On the other hand, the situation in scanning tunneling microscopy is quite different and images with point defects are routinely obtained [3].

This is usually attributed to the fact that the tunneling current is laterally localized in an area of few angstroms in diameter, while in atomic force microscopy the effective part of the probing tip is laterally much larger. So the atomic resolution is not obtained by a point interaction but by a superposition (convolution) of several interactions between the atoms in the tip and the sample. This assumption is justifiable if one considers that even in the case of a diamond tip and a diamond sample, using typical loads, the tip-sample contact area is larger than a single-atom one [4,5].

The two surfaces (tip and sample) are generally deformed when they are in contact [6]. For softer materials this tendency for larger contact areas under load is even more prevalent [4]. For materials with layered

structures (e.g. pyrolytic graphite) the assumption that the tip drags a flake of the material as it scans the surface has proved to be very fruitful [7] and provides results in agreement with the experiments. Especially for the layered materials the same considerations of flake-like tips (or multiple-atom tips) can be also applied to the STM imaging mechanism.

However, the usual case in STM pictures is the imaging of single-point defects in a variety of materials. This excludes the possibility of laterally large effective tips as has been shown [8].

In a word, there are two physical mechanisms that make the tip-sample contact area become of some considerable size: a) loads (even the lowest ones) result in a flat contact area of considerable size; b) especially for layered materials the tip drags a flake of the sample probed and this flake is the effective tip.

The main difference between the two cases is that while in the first case the material of the tip is in general different from the material of the sample, in the second case the effective flake like tip is of the same material.

At last, tip with big radius is not able to track precisely sharp relief with big height drops on the surface [9-11], this is third physical factor that makes the tip-sample contact area becomes of considerable size.

Thus, for topographic AFM studies of larger scale structures the macroscopic shape of the tip becomes very important. So, it is necessary to have a limiting small radius of the microscope's tip.

However, as for the further analysis tip parameters are the most important ones, so we can rule out the possibility to study the second factor in the system of “tip-surface”.

2. THE MAIN TYPES OF SPM PROBES

For representation of interesting peculiarities of the investigated samples the different types of SPM probes

are applied. For example, the conducting coatings from different materials (Au, Pt, Cr, W, Ti and etc) are marked o probe for carrying out of electric measurements. For investigation of surface magnetic properties, the probes are covered by thin layers of ferromagnetic materials (Co,

Fe, CoPt, FeCr, CoCr and etc). However, if we consider only space geometry, then all probes can be divided on three main groups in first approximation: 1) probes of pyramidal type; 2) probes of cone type, 3) probes of whisker type.

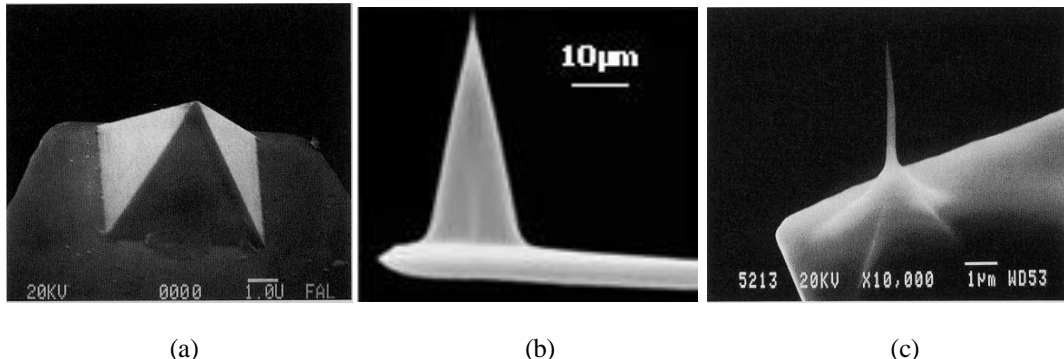


Fig. 1. The images of pyramidal (a), cone (b) and whisker (c) probes in scanning electron microscope.

Let's consider the peculiarities of these probes. The probes of pyramidal type (Fig. 1, a) are pyramids from silicon nitride with square footing with sides approximately 5 μm . The cantilevers with pyramidal probes are obtained by the way of Si_3N_4 spraying in etching pits on Si (100) surface, lithography and following substrate etching. The ratio of sides (height to foundation) is defined by geometry of etching pit and is equal approximately to 1:1 with edge radius near 20÷50 nm. The probes of cone type (Fig.1,b): for preparation of such silicon AFM probes the enough complex technological process including the operations of photolithography, ion implantation, chemical and plasma etching is applied. The probes obtained as a result of plasma etching sharpening, have the cone form with root radius 3÷6 μm and height 10÷30 μm (that gives the side ratio 3÷5/1). The edge radius is approximately 10÷20 nm. The probes of whisker type (Fig. 1, c): these probes have the bif side ratio that allows us to investigate the narrow deepening and cracks on the surface. The length of such probes is 1,5÷2 μm , the side ratio is >10:1 and edge radius is ~10 nm.

The probe obtaining technology for STM is the special area. As a rule, they are prepared from thin tungsten wire. For preparation of sharp probes with big side ratio these wires are sharpened with use of electrochemical etching process.

However all technologies of reception of tips from tungsten until recently had the certain restrictions.

How can we reduce the radius of the tip? If we use most widespread method of electrochemical etching the magnitude of the obtained tip is defined by the relationship:

$$R = D \sqrt{\frac{\gamma \Delta L}{4 \sigma_{ur}}} , \quad (1)$$

where D – diameter of tip wire; ΔL – length of separating part; γ – specific density of tip agent; σ_{ur} – ultimate

resistance to tip agent breakage. For tungsten being one the conventional materials at producing the tip specific weight $\gamma = 1, 89 \times 10^5 \text{ N/m}^3$; $\sigma_{ur} = 7, 11 \times 10^8 \text{ N/m}^2$. It follows that it is possible to obtain the tip with reasonable values of tip radius $\leq 10 \text{ nm}$ from wire of low diameter ($\leq 10^{-4} \text{ m}$). However the tip with such diameter has low mechanic stiffness in longitudinal and lateral direction and mechanical, thermal and quantum fluctuations can worsen stability of atom force microscope operation. Let us evaluate amplitude of longitudinal and lateral oscillations of tip of two tips in diameter 10^{-3} m (Tip1) and 10^{-4} m (Tip2) at their similar length 10^{-2} m . It is known that mean square of amplitude of quantum $\langle X_q^2 \rangle$ and thermal $\langle X_T^2 \rangle$ fluctuations of oscillating system on resonance frequency is defined as

$$\langle X_q^2 \rangle = \frac{\hbar \omega}{K_M} , \quad (2)$$

$$\langle X_T^2 \rangle = \frac{\kappa T}{K_M} , \quad (3)$$

where k – Boltzmann's constant; T – temperature; K_M – effective stiffness of oscillating system; ω_0 – its resonance frequency equal to $\sqrt{K_M/m}$; m – equivalent mass of oscillating system. Lateral K_{ML} and longitudinal K_{MV} stiffness of tip can be determined with sufficient accuracy using the following expressions:

$$K_{ML} = \frac{3\pi E D^4}{64 L^3} , \quad (4)$$

$$K_{MV} = \frac{\pi E D^2}{4L} , \quad (5)$$

where E – Young's modulus, L – tip length. If we substitute in formulae (2 – 5) typical parameter magnitudes we get following values for thermal and quantum fluctuations (Table 1).

Parameter magnitudes	Tip 1		Tip 2	
	Longitudinal oscillations	Lateral oscillations	Longitudinal oscillations	Lateral oscillations
L, (m)	10^{-2}	10^{-2}	10^{-2}	10^{-2}
D, (m)	10^{-3}	10^{-3}	10^{-4}	10^{-4}
K_M , (N/m)	$1,5 \times 10^7$	$3,1 \times 10^4$	$1,6 \times 10^5$	$2,9 \times 10^1$
ω_0 , (Hz)	$3,2 \times 10^5$	$1,2 \times 10^4$	$2,1 \times 10^5$	$2,8 \times 10^3$
$[<X_q^2>]^{1/2}$, (m)	$1,8 \times 10^{-18}$	$3,5 \times 10^{-17}$	$1,7 \times 10^{-17}$	$1,1 \times 10^{-16}$
$[<X_T^2>]^{1/2}$, (m)	$3,3 \times 10^{-14}$	$6,7 \times 10^{-13}$	$3,1 \times 10^{-13}$	$2,1 \times 10^{-11}$

As it follows from Table 1, tip 2 has deficient mechanic stiffness. But if the tip diameter is 10^{-3} m tip radius is prohibitively big (see formula (1)). As it was already marked, the tip should have extremely small radius of a point and simultaneously possess sufficient mechanical stiffness. At manufacturing a tip by a method of electrochemical etching it is not possible to provide performance of both these conditions, since there is a connection between initial diameter of a wire of a tip and the received radius of a point (Fig. 2, a). Therefore, with the purpose of reception of a tip with small radius of a point and high mechanical stiffness the technique in which basis the method of reception of a tip of the step form lays at electrochemical etching (a Fig. 2, b) has been developed. Thus at the initial stage etching goes in regular intervals on all length of the part of a tungsten wire shipped in a solution. After some time the wire is a little extended from a solution and process proceeds, and etching already goes on smaller, in comparison with initial, to diameter. It allows $\sim 8 \times 10^{-4}$ m to spend at initial diameter of a wire a final stage of etching at working diameter $\sim 4 \times 10^{-5}$ m, that as a result gives a tip with small enough radius of a point (≤ 20 nm) and, owing to the geometrical

accuracy. Therefore there are no problems in data interpretation for these two cases. But such "ideal" surfaces which can be investigated a tip of the big radius, in atomic force microscopy meet seldom.

The second case: there has been a recess with sharp edges on the surface; in this case its lateral sizes are bigger than tip ones. The tip falls until back control system touches the recess bottom. Here at the expense of interaction of recess front edge with lateral side of tip we obtain not the image of recess lateral edges but the image of tip lateral surface. There have been taken place size distortion in the direction of scanning surface and data loss as a result. There has been a step with sharp edges up on the surface. The tip is moving over the surface measuring surface relief till the beginning of the interaction of its lateral surface with the step edge. The relief of the tip lateral surface starts to be represented and the value of distortion and data loss depends on the distance between the tip and surface: the less is the distance, the less is distortion. In this case to minimize given distortion it is possible only by means of a tip with small radius of a point.

The third case: the apparent sizes of features can be also affected by the topography around them. For example, if one investigates spherical particles adsorbed on a rough substrate their shape will be partially determined by the topography of the substrate around them (we assume that spherical particles dimensions are in the order of the tip's radius of curvature).

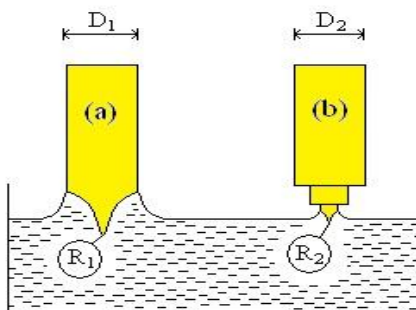


Fig. 2. Classical (a) and step (b) methods electrochemical etchings of tungsten tips.

form, high mechanical stiffness. Those tips allow of artifacts being at the investigation of surfaces with complicated relief to be minimized.

3. THE PROCESSES BEING IN THE SYSTEM "TIP-SURFACE"

Here several various cases can be arisen. The first case is recesses or rises on the surface of half-sphere-typed with the radius much bigger than the tip radius. Here surface topography is tracked with maximum

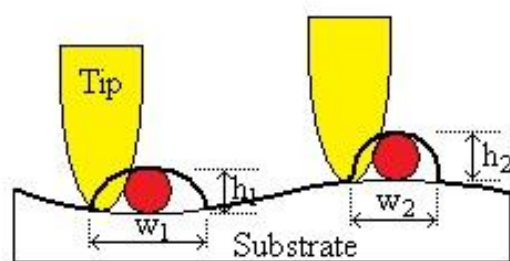


Fig. 3. Effect of the particle shape on the local topography of the substrate.

Fig. 3 shows schematically this distortion: even if two particles are exactly the same, they will be imaged differently if one is on a peak and the other in a valley, due to convolution of the tip and the sample. The thick line shows the apparent height corrugation. The particle in

the valley seems lower ($h_1 < h_2$) and more flattened ($w_1 > w_2$) than the particle on the peak.

The fourth case: a tip with a relatively large cone angle fails to penetrate into deep and narrow grooves on the sample surface. This leads to underestimation of their depth and smoothing of their edges (Fig. 4, a). One point of recess edge touches lateral surface of the tip. Tip displacement trajectory do not describes recess surface, but tip surface. Although the height of protrusions can be recorded quite accurately their edges are being smoothed and their lateral size is overestimated (Fig. 4, b).

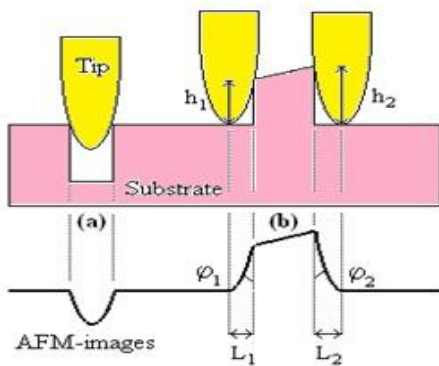


Fig. 4. Effect of tip geometry on imaging (thick line): a) a groove and b) a protrusion.

Due to finite size of the tip artifacts are produced and the resulting image is a convolution between the shape of the tip and the topography of the sample. Therefore is this case interaction between the tip and surface changes from the system "tip-surface" to the system "tip-cluster surface", tip displacement trajectory describes the image of the tip itself. In this case there is a restriction connected with geometry of a tip.

Thus there can be areas in which the image basically is defined by the form of a tip and geometry of its fastening. As a first approximation these so-called "dead zones" can be defined as follows: $L_1 \approx h_1 \times \operatorname{tg}(\varphi_1 - \alpha)$ and $L_2 \approx h_2 \times \operatorname{tg}(\alpha + \varphi_2)$, where α – a corner of fastening of a tip with cantilever. At $\varphi_1 \geq \alpha$, that is typical for the majority industrial cantilevers, having a corner of fastening $\alpha \geq 15^\circ$, the area of "dead zone" L_1 for "step" is defined only by radius of curvature of a tip. The size of area of "dead zone" L_2 for conic tips with a corner of convergence 22° ($\varphi_2 = 11^\circ$) and $\alpha = 20^\circ$ turns out significant and is equal $L_2 \approx 0,6 \times h_2$.

Thus, the brief analysis of the artifacts arising in system "tip-surface" has shown, that accuracy of the decision of a task convolution in SPM to those above, than it is less radius of curvature of a tip and than less corner of convergence of a cone of a tip.

-
- [1] W.A. Lin, E.G. Karpov, H.S. Park. Nano mechanics and materials: theory, multiscale methods (Wiley), 2006, 287 p.
 - [2] Binning G., Quate C.F., Gerber Ch. Phys. Rev. Lett. 1986, 56, 930.
 - [3] Whitman L.J., Stroscio J.A., Dragoset R.A., Cellota R.J. Vac. Sci. Technol. B, 1991, 9, 770.
 - [4] Dou J., Shang W., Chen Z. J. Vac. Sci. Tech. B, 2004, v. 22, no. 2, p. 597.
 - [5] Szczepkowicz A., Bryl R. Phys. Rev. B, 2005, v. 71, no. 113, p. 416.
 - [6] A.L. Volyinski, I.V. Yaminski. High-molecular substances, A, 2005, v. 47, no. 6, p. 747-751.
 - [7] Fu T.-Y., Cheng L.-C., Nien C.-H., Tsong T.T. Phys. Rev. B, 2001, v. 64, no. 113, p. 401.
 - [8] V. Bykov, V. Dremov, V. Losev, S. Saunin. Proceedings of all-Russian Conference "Probe microscopy", Nizhny Novgorod, 2000, 28 Feb.-2 Mar., p. 298-302.
 - [9] G.S. Batoq, A.S. Baturin, V.S. Bormashov, E.P. Sheshin. JTF, 2006, v. 76, no. 8, p. 123-128.
 - [10] K.N. Romanyuk, S.A. Tiyis, B.Z. Olshaneski. FTT, 2006, v. 48, p. 1716-1720.
 - [11] A.Y. Vulf, A.Q. Dideykin and etc. Pisma v JTF, 2006, v. 32, no. 13, p. 12-15.

Received: 11.03.2014

ABOUT POSSIBILITY OF USING A DUAL-FREQUENCY LIQUID CRYSTAL FOR SELECTIVE MODULATION OF RADIATION

T.D. IBRAGIMOV^{a*}, A.R. IMAMALIYEV^a, A.K. MAMMADOV^a, G.M. BAYRAMOV^{a,b}

^aH.Abdullayev Institute of Physics of Azerbaijan National Academy of Sciences,

AZ114, H.Javid Avenue, 33, Baku, Azerbaijan. E-mail:tdibragimov@mail.ru

^bBaku State University, AZ1148, Z.Khalilov street, 23, Baku, Azerbaijan

Transmission spectra of the Al₂O₃ particles-DFLC system in both the ordinary electrooptical cell and the twist-structure were studied. It was shown that for certain changes in the frequency of the applied electric field, a transmission region maximum of the Al₂O₃ particles-DFLC ordinary cell switches from one wavenumber to the other. While the twist-structure of the system at low frequencies passes the light at the same wavenumbers but it becomes practically opaque at high frequencies. The experimental results are explained by the optical homogeneity of the system in a narrow wavelength interval when the refractive indices of the particle material and the matrix are close, and also by reorientation of the liquid crystal molecules as the frequency of the applied voltage changes.

Keywords: dual-frequency liquid crystal, twist-structure, Fredericksz effect, Christiansen effect, small particles, aluminum oxide.
PACS: 42.70.Df; 47.20.Cn; 47.32.Cd; 61.30.Gd.

1. INTRODUCTION

Optical properties of a well-aligned layer of a liquid crystal (LC) are characterized by extraordinary n_e and ordinary n_o refractive indices. Meanwhile, the difference $\Delta\epsilon$ between dielectric permittivity components $\epsilon_{||}$ and ϵ_{\perp} corresponding n_e and n_o defines dielectric anisotropy of LC. Here, $\epsilon_{||}$ and ϵ_{\perp} are measured along and perpendicular to the direction of LC long molecular axes, correspondingly. An electric field can change the orientation of LC molecules (the Fredericks effect), leading to a change in the effective refractive index along the direction of propagation of the light. In this case, the long axes of molecules of LC with positive dielectric anisotropy are aligned parallel to the field direction, while they are aligned perpendicular to the field in LC with negative dielectric anisotropy.

One of widely used effects in LC is the so-called twist-effect. It arises at planar oriented molecules of LC with positive dielectric anisotropy whose directors of molecules are perpendicular each other on opposite electrodes. The formed twist- structure turns a polarization plane of linearly polarized light on angle $\pi/2$. This structure with parallel polarizers is opaque at a lack of electric field while the cell becomes transparent at application of the sufficient magnitude field.

Dual-frequency liquid crystal (DFLC) represents a mixture consisting of molecules of LC with positive and negative dielectric anisotropies. A sign of dielectric anisotropy of such mixture can change from positive to negative magnitudes at a change of an electric field frequency. Possibility of sign inversion of dielectric anisotropy on some crossover frequency f_c allows operating the switching processes in LC.

A use of DFLC expands a span of electrooptical effects and possibility of application of LC in various electrooptical devices. In particular, the DFLC system in combination with the polymer, having refractive index equal to ordinary refractive index of LC, allows operating the transmission of an electrooptical cell [1]. Obtaining of plasmon modulators of high-contrast signals based on DFLC is informed in [2]. The method of phase modulation with the high speed using DFLC is described

in work [3]. This system uses an electronic feedback connection in order to simplify the control. For large phase shifts, phase modulation speeds are an order of magnitude faster than for existing techniques.

The method for tunable filtration of infrared (IR) radiation, based on a combination of the Fredericks effect and the Christiansen effect was proposed in [4]. The latter effect arises if particles are dispersed in a sufficiently transparent medium and the particle sizes are comparable with the wavelength of the incident light. In this case, the system transmits light in a narrow range of wavelengths, where the refractive indices are close for the particle material and the medium in which the particles are dispersed. Here, aluminum oxide is used as a material of particles because of strong change of its refractive index in mid-IR spectral region.

In the given work, possibility of using peculiarities of the novel synthesized DFLC- Al₂O₃ particles system for selective modulation and filtration of infrared radiation are reported.

2. EXPERIMENTAL

The samples were pieces of chemically pure aluminum oxide. After thoroughly grinding in an agate mortar with a small addition of alcohol, the powder obtained was separated according to sedimentation time in a column with hexane according to the expression $t = 18h\eta/(\rho_1 - \rho_2) g d^2$, where h is the height of the column; η is the viscosity coefficient of the liquid; ρ_1 and ρ_2 are the densities of aluminum oxide and hexane; g is the gravity acceleration; d is the transverse dimension of the particles. The obtained fractions were dried under a vacuum of 10⁻² Torr at $T= 50^\circ\text{C}$ for a week. A dual-frequency liquid crystal was developed for experiments. It consists of three components: 4-n-pentyl-4'-cyanobiphenyl (5CB), 4-hexyloxyphenyl ester 4'-hexyloxy-3-nitrobenzoic acid (C2), 4-n-pentanoyloxybenzoic acid-4-hexyloxyphenyl ester (H22) with molar ratio of 1:1:1.5, correspondingly.

The cells for optical measurements had a “sandwich” structure with conductive p-type germanium substrates transparent in the mid-IR range. Two types of

substrates were used for the cells. Ones were not specially treated while substrates of another type (for twist-effect) were rubbed by diamond paste. The aluminum oxide particles were allowed to settle on the lower germanium plate in the column with hexane. Then the substrate was dried for 3 days at $T = 40^{\circ}\text{C}$. Two holes were first drilled into the upper plate, and then it was carefully laid on the dispersing layer and both plates were tightly pressed together. In this case, the processed substrates had rubbed surfaces with perpendicular directions each other for the twist-effect. The cell thickness was about 35 μm . Copper tubes were inserted into the holes for filling the cell with liquid crystal. The cemented cell was filled with liquid crystal at the isotropic phase. An alternating voltage of sine form was applied to the cell with the Al_2O_3 particles - liquid crystal system using a AWG 5002C Arbitrary Waveform generator (Tektronix).

The transmission spectra were recorded on a IKS-29 double-beam spectrophotometer in the IR range 4000-400 cm^{-1} . The resolution and accuracy of the frequency determination was within 1 cm^{-1} . The radiation was linear polarized for a twist-effect and unpolarized for the ordinary cell, and it normally fell to the cell surface. In order to record the transmission spectrum only of the particles - LC system, the same cell but unfilled was placed in front of the reference beam of the spectrophotometer. The refractive indices of LC matrix

were determined by interference method [5] on the spectrophotometer using IR polarizer.

3. RESULTS AND DISCUSSION

Earlier we developed dual-frequency liquid crystal consisting of 4-n-pentyl-4'-cyanobiphenyl (5CB), 4-hexyloxyphenyl ester 4'-hexyloxy-3-nitrobenzoic acid (C2), and 4-n-pentanoyloxy-benzoic acid-4'-hexyloxyphenyl ester (H 22) was developed and its basic dielectric characteristics were determined [6]. It was shown that the point of crossing of dispersive curves (crossover frequency) corresponds to transition of the mixture from the state of positive dielectric anisotropy to negative one and makes up 104 kHz at temperature 23°C . The optimal frequencies for switching of the mixture from the state with positive anisotropy to the state with negative dielectric anisotropy are 1 kHz and 1 MHz at room temperature.

The preliminary study of transmission spectra of the mixture has shown that it is practically transparent up to 1800 cm^{-1} at small layer thickness except for a set of the bands corresponding to vibrations of groups CH_2 , CH_3 and NO_2 [7]. Calculations of n_o and n_e from the interference pattern of transmission spectra have shown that they have values 1.64 and 1.78, accordingly.

The transmission spectra of aluminum oxide particles with average size of $15\mu\text{m}$ in the mixture 5CB-C2-H22 at room temperature are shown in Fig. 1.

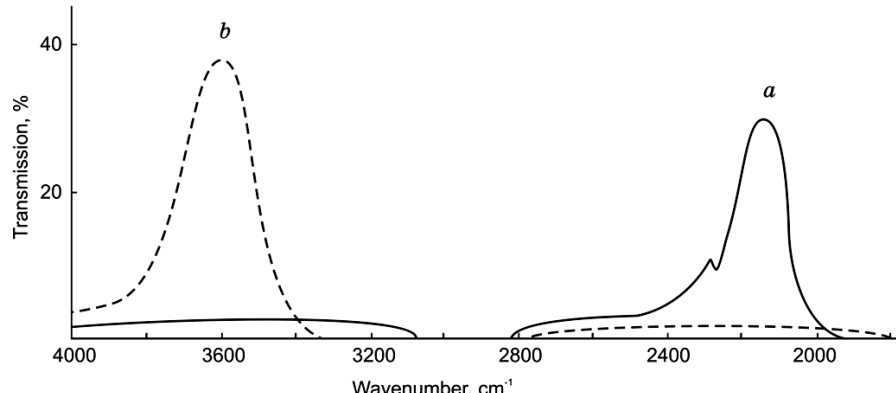


Fig.1. Transmission spectra of mixture 5CB - C2 - H22 with aluminum oxide particles at different frequencies of the applied electric field with voltage of 9 V: a - 1 kHz; b - 1 MHz.

In this case, the total particle weight was selected so that particles settled on the substrate with an effective thickness of four monolayers. The voltage applied to the cell was 9 V. One can see, at a frequency of 1 kHz, a transmission band is observed with maximum at 2154 cm^{-1} . The extinction on the long-wavelength wing of the band is determined by two factors: light scattering on the dispersion medium and absorption of its particles. Therefore transmission on a long-wavelength part of this band is less than on its short-wavelength part. An increase of the layer thickness of small particles leads to a decrease of a half-width and an intensity of the transmission band owing to absorption by the particle material. An increase

in particle size results in a decrease of the intensity and the bandwidth narrowing of the transmission band for the same sample weight. All the indicated characteristic features are consistent with the behavior of the change in the transmission spectra of the Christiansen effect for the solid particles - liquid system [8]. For all changes in the cell filling conditions, the wavenumber of the transmission band maximum remains practically unchanged.

The transmission peak is also observed at the same wavenumber in the transmission spectrum of the twists-cells with the composite at the same frequency (1 kHz) (Fig.2).

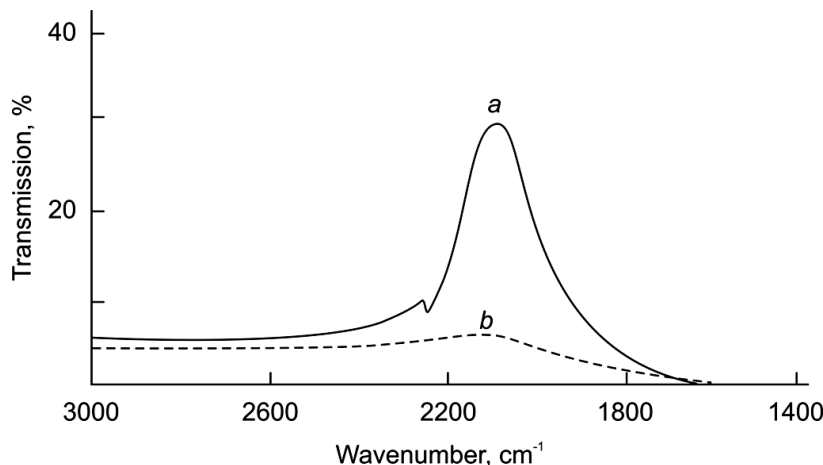


Fig.2. Transmission spectra of the twist-cell with the mixture 5CB - C2 - H22 and aluminum oxide particles at different frequencies of the applied electric field with voltage of 9 V: a - 1 kHz; b - 1 MHz.

Switching the frequency on 1 MHz at the same voltage changes a transmission band maximum to 3638 cm^{-1} at an ordinary cell. While the twist-cell do not practically passes the light. It is explained by different orientation of LC molecules at different frequencies. LC molecules at low frequencies are sure to orient perpendicular to the substrate surface because it has positive dielectric anisotropy at these frequencies. At that case, the effective refractive index corresponds to ordinary refractive index n_o . While at high frequencies of applied electric field, the LC molecules are oriented parallel to the substrate surface owing to its negative dielectric anisotropy and the effective refractive index has surface average value $n_s = 1/2(n_o + n_e)$. The polarization plane of polarized light passing through the twist-structure turns on angle $\pi/2$, and it is extinguished at parallel polarizers. In this case its full clearing does not occur because of presence of aluminum oxide particles. Comparison of experimental and calculated data shows their good accordance.

4. CONCLUSIONS

A study of transmission spectra of the aluminum oxide particles-DFLC system in both the ordinary electrooptical cell and the twist-structure was shown that for certain changes in the frequency of the applied electric field the transmission region of the Al_2O_3 particles -DFLC ordinary cell switches from one wavenumber to the other. While the twist-structure of the system at low frequencies passes the light at the same wavenumbers but it becomes practically opaque at high frequencies. The experimental results are explained by the optical homogeneity of the system in a narrow wavelength interval when the refractive indices of the particle material and the matrix are close, and also by reorientation of the liquid crystal molecules as the frequency of the applied voltage changes.

Acknowledgements

The work has been supported by Scientific and Technology Center in Ukraine (grant no 5821).

- [1] *D. Coates, P. Nolan.* Electrooptical liquid crystal system containing dual frequency liquid crystal mixture, US Patent 5621552 (1997).
- [2] *J.S. Smalley, Y. Zhao, A.A. Nawaz, Q. Hao, Y. Ma, I.-Ch. Khoo, T.J. Huang.* High contrast modulation of plasmonic signals using nanoscale dual-frequency liquid crystals, Optics Express 19 (2011) 15265-15274.
- [3] *A.K. Kirby, G.D. Love.* Fast, large and controllable phase modulation using dual frequency liquid crystals, Optics Express 12 (2004) 1470-1475.
- [4] *T.D. Ibragimov.* Christiansen effect in the particles Al_2O_3 – liquid crystal system, Journal of Applied Spectroscopy. 76 (2009) 793-796.
- [5] *T.D. Ibragimov, G.G. Kurbanova, V.S. Gorelik.* Raman scattering in gallium selenide and sulfide films, Physica Status Solidi B 155 (1989) 113–116.
- [6] *T.D. Ibragimov, G.M. Bayramov, A.K. Mamedov.* Dielectric properties of dual-frequency liquid crystal 5CB-C2-H22. Azerbaijani Journal of Physics. V.18, No1, (2012), 16-18.
- [7] *N. Kirov, P. Simova.* in: Vibrational Spectroscopy of Liquid Crystals, Publishing House of the Bulgarian Academy of Sciences, Sofia, 1984, pp. 43–54.
- [8] *R.H. Clark.* A theory for the Christiansen filter, Applied Optics 7 (1968) 861-868.

Received: 15.01.2014

THE SPECTRA OF OPTICAL PARAMETERS OF Bi_2Te_3 SINGLE CRYSTALS AND FILM COMPOUNDS

N.Z. JALILOV, G.M. DAMIROV

*Institute of Physics of
Azerbaijan National Academy of Sciences
AZ-1143, Baku, G.Javid ave., 33*

The reflection spectra $R(E)$ of single crystals Bi_2Te_3 of n- and p-types parallel and perpendicular to C axis and its film samples in beam energy interval $1\div 6$ eV falling normally on the surface, are measured in the work. The spectra of their optical parameters and values of optical transitions in the investigated samples are defined by Kramers-Kroning method on the base of $R(E)$. The dependence of spectra of investigated parameters on their structural differences is defined.

Keywords: dispersion, optical parameters, bismuth telluride.

PACS: 78.20.Ci; 78.40.Fy; 78.66.Jg

INTRODUCTION

There are series of works on investigation of optical properties of single crystals and Bi_2Te_3 films [1-4]. The data on thermoelectric materials on the base of Bi_2Te_3 are given in the work. The results on study of its band structures are given [2-4]. The bismuth telluride is the semiconductor having the well thermoelectric properties. It belongs to crystal group of $A_2^V B_3^{VI}$ type. Its crystalline structure is formed by repetition of five-layer packages which are quintets, consisted of atoms placed in consequence----- $\text{Te}^{(1)} - \text{Bi} - \text{Te}^{(2)} - \text{Bi} - \text{Te}^{(1)}$

The bismuth telluride is known as effective material for thermoelectric transformers. This material is simply prepared in the form of enough perfect single crystals and obtain both n- and p-types by doping way [1,5].

Bi_2Te_3 crystals have the packet structure and connection between neighbor packages has the Van der Waals-covalent character [6].

The additional bond exists between packages because of transition of one p-electron on d-levels and overlapping of some d-levels with valence band. This condition causes the significant metallic properties and comparatively small energy values of forbidden bands in interval $0,15\div 0,35$ eV.

With optical point of view, Bi_2Te_3 and its analogues are the uniaxial crystals. The dielectric constant in them is second order tensor and depends on incident wave direction in respect of optical axis C. In work [3] the optical properties of bismuth telluride are investigated in region of higher frequencies.

In work [2] Bi_2Te_3 crystal bond structure is theoretically calculated in work [2]. The absence of data about value of spin-orbit interaction (Δ) and complexity of chemical bond character between Bi_2Te_3 atoms causes the significant difficulty.

The bismuth telluride and solid solutions on its base are used at preparation of different energy transformers [5]. Mainly the monocrystalline or polycrystalline Bi_2Te_3 and its solid solutions with Bi_2Se_3 are used.

The monocrystalline samples Bi_2Te_3 are easily chipped on cleavage planes [0001] forming the mirror surface, stable to oxidation, that it is very important for carrying out of optical measurements and doesn't require the special chemical treatment.

The study of Bi_2Te_3 bond structure hasn't achieved such level as germanium of $A^{III}B^V$ compound that is connected with complexity of its crystalline and band structure [1]. This makes necessary the new investigations in this direction.

The aim of the given work is the measurement of Bi_2Te_3 crystal reflection coefficient of n- and p-types parallel and perpendicular to C axis, and also the measurement of its polycrystalline film samples and definition of spectra of their optical parameters on the base of reflection coefficient.

EXPERIMENT TECHNIQUE

The chip of single crystals having the specular smooth surface is used for measurement of reflection coefficient $R(E)$. The reflection coefficient is measured by double-beam spectroscopy method. The crystals are doped by Cl impurities having n-type conduction and Tb impurities, which have p-type conduction.

The technology of single crystals and Bi_2Te_3 films is described in works [1,7,8].

The single crystals are obtained by Bridgman method as in work [1] and films of thickness $0,3\mu\text{m}$ of Bi_2Te_3 polycrystalline compound on cleavage surface of rock salt crystals are obtained by its sublimation in vacuum.

The definition methods of optical parameters are given in work [9] and procedure is described in work [10].

For calculation of optical parameters, as usual, the special computer programs are applied. The optical parameters of investigated materials are calculated on programs consisted by author of work [11]. These programs are checked at calculation of optical parameters of series of materials in works [12-16].

RESULTS AND THEIR DISCUSSION

The reflection coefficients $R(E)$ of Bi_2Te_3 monocrystalline compound of n- and p-types parallel and perpendicular to C axis and also its film samples of n- and p-types are measured in present work. Spectra of their optical parameters: absorption coefficient α , real ϵ_1 and imaginary ϵ_2 parts of dielectric constants, indexes of absorption κ and refraction n , effective number of valence electrons $n_{ef}(E)$ taking part in transitions up to the given

THE SPECTRA OF OPTICAL PARAMETERS OF Bi₂Te₃ SINGLE CRYSTALS AND FILM COMPOUNDS

energy E , effective static dielectric constant $\varepsilon_{0,\text{eff}}(E)$, functions of characteristic volume - $\text{Img } \varepsilon^{-1}$ and surface $\text{Img}(\varepsilon+1)^{-1}$ electron losses, optical conduction $\varepsilon_2 E$ reflected light phase θ , integral function of connected density of states $\varepsilon_2 E^2$ and electro-optical differential functions (α, β), are defined. Only spectra of reflection coefficients $R(E)$, imaginary and real parts of dielectric constant, functions of characteristic volume $\text{Img } \varepsilon^{-1}$ and surface $-\text{Img}(\varepsilon+1)^{-1}$ electron loss, spectra of electro-optic differential functions (α, β), spectra of optic conduction σ of massive and film samples, are shown on fig.1-10 for brevity.

The values of interband optical transitions in Bi₂Te₃ single crystals and film compounds in energy interval 1÷6eV of n- and p-types, parallel and perpendicular to C axis are defined on maximums of optical conduction.

The presented data give the possibility to compare the optical spectra, transitions of Bi₂Te₃ single crystals and its film samples. The authors of work [3] for case of high energies for monocrystalline have found Bi₂Te₃ transitions 1,4eV and 1,1eV. From this, one can conclude that values of some Bi₂Te₃ optical transitions at transition of material from crystalline state to non-crystalline one remain the same.

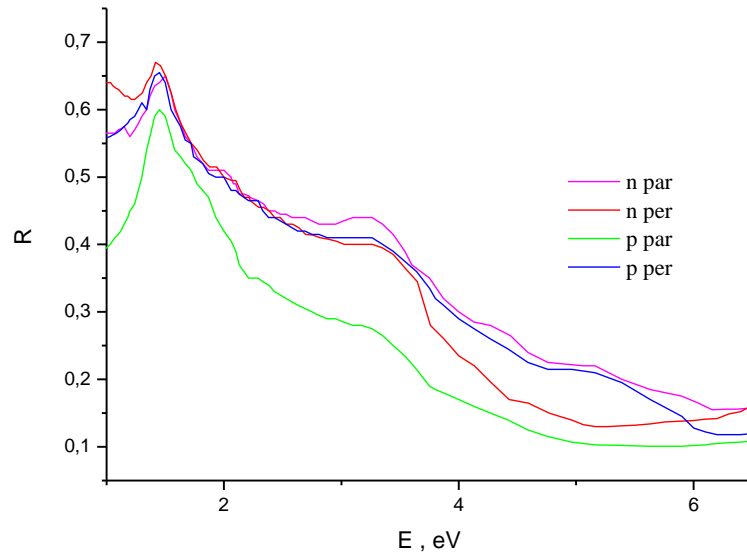


Fig.1. The reflection spectra of Bi₂Te₃ of single crystals of n- и p-types parallel and perpendicular to C axis.

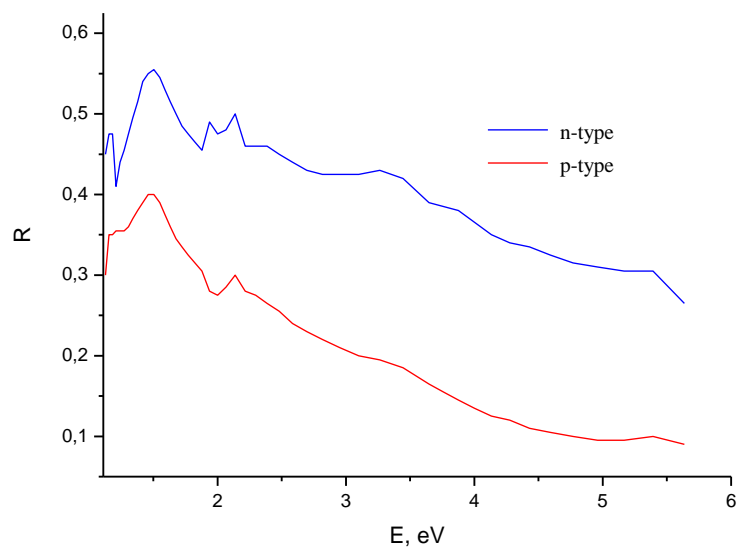


Fig.2. The reflection spectra of Bi₂Te₃ film compound of n- and p-types

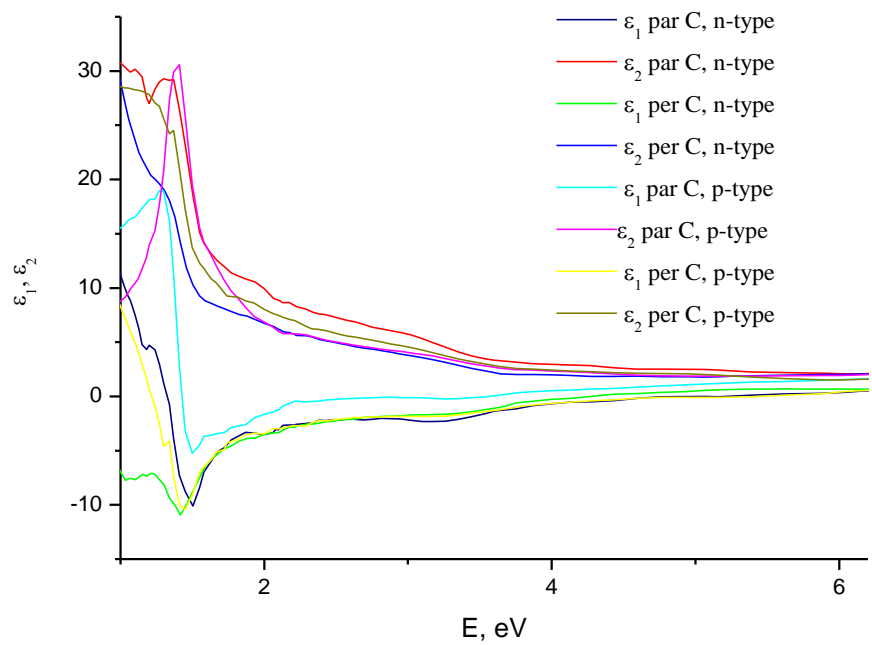


Fig.3. The spectra of coefficients ε_1 and ε_2 of Bi_2Te_3 single crystals of n- и p-types parallel and perpendicular to C axis.

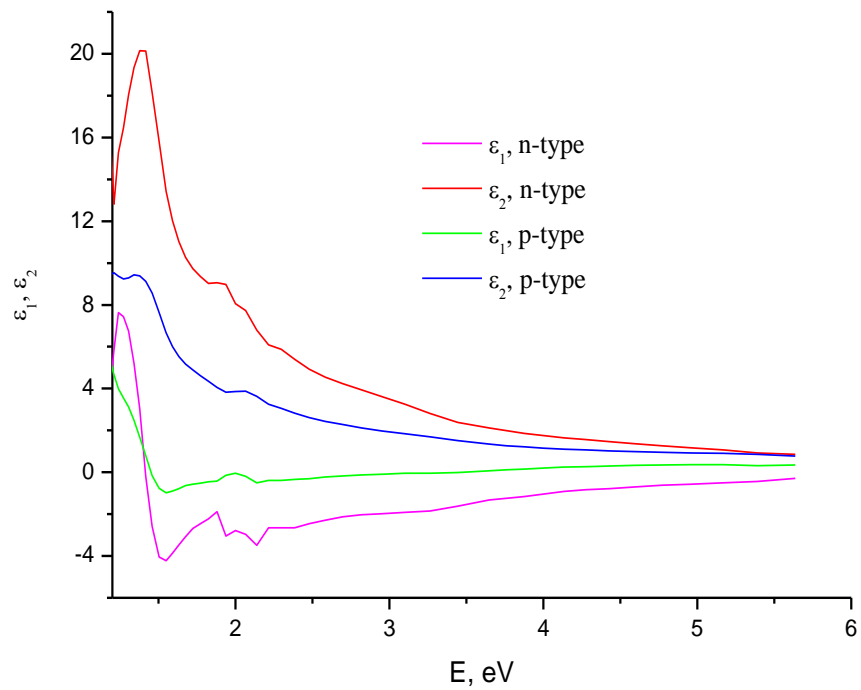


Fig.4. The spectra of coefficients ε_1 and ε_2 of Bi_2Te_3 film compound of n- and p-types.

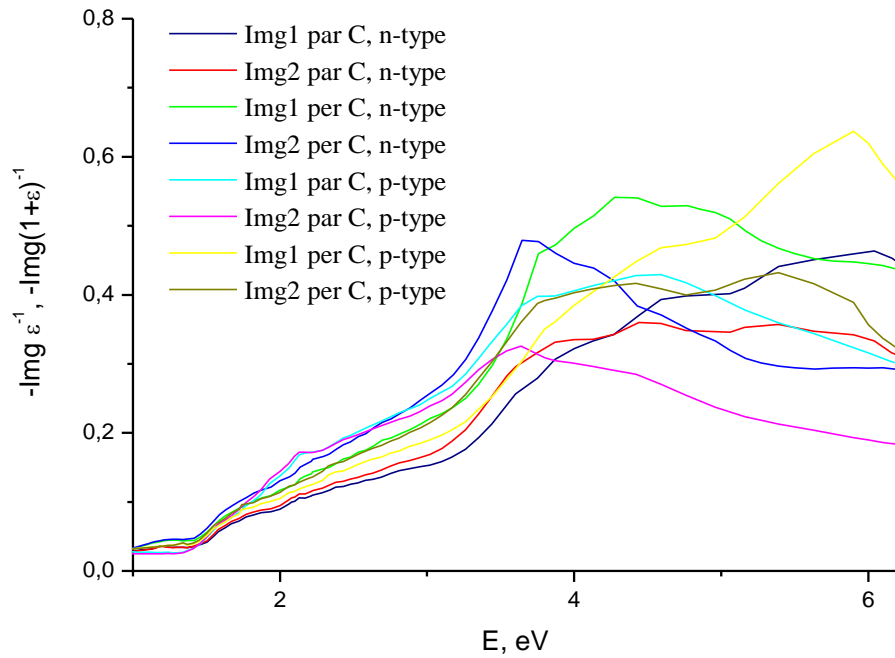


Fig.5. The spectra of Img1 ($-\text{Img}\epsilon^{-1}$) and Img2 ($-\text{Img}(1+\epsilon)^{-1}$ of Bi_2Te_3 single crystals of n- and p-types parallel and perpendicularly to C axis.

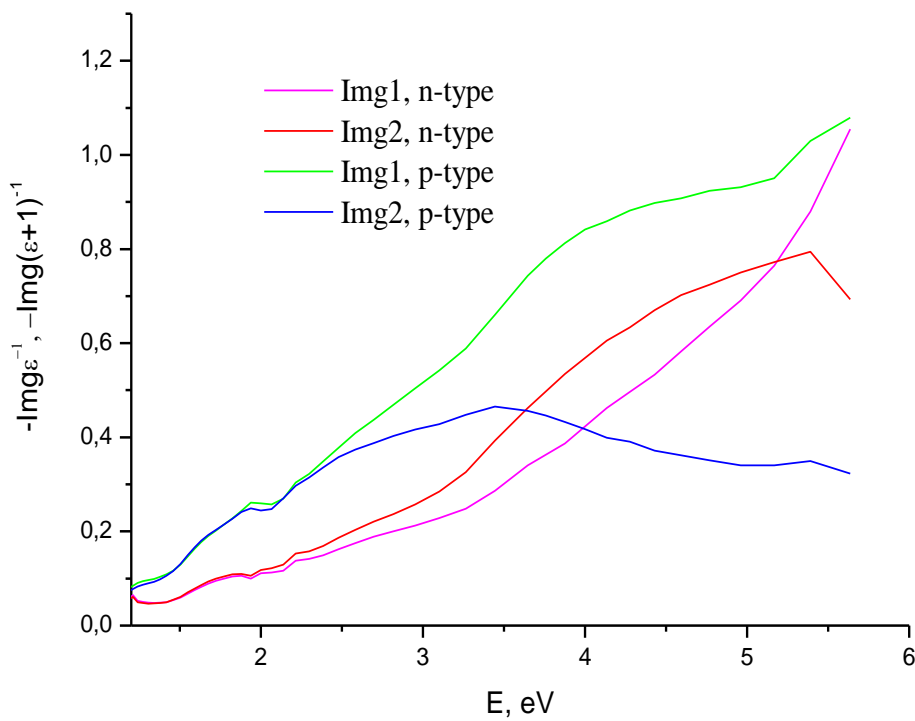


Fig.6. The spectra of Img1 ($-\text{Img}\epsilon^{-1}$) and Img2 ($-\text{Img}(1+\epsilon)^{-1}$ of Bi_2Te_3 film compound of n- and p-types.

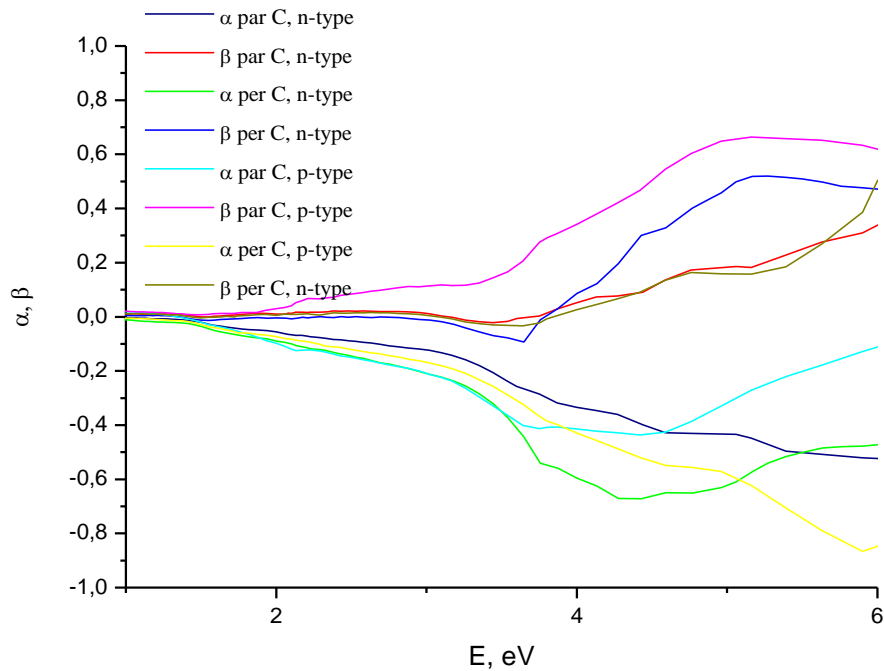


Fig.7. The spectra of electro-optic coefficients α and β of Bi_2Te_3 single crystals of n- and p-types parallel and perpendicularly to C axis.

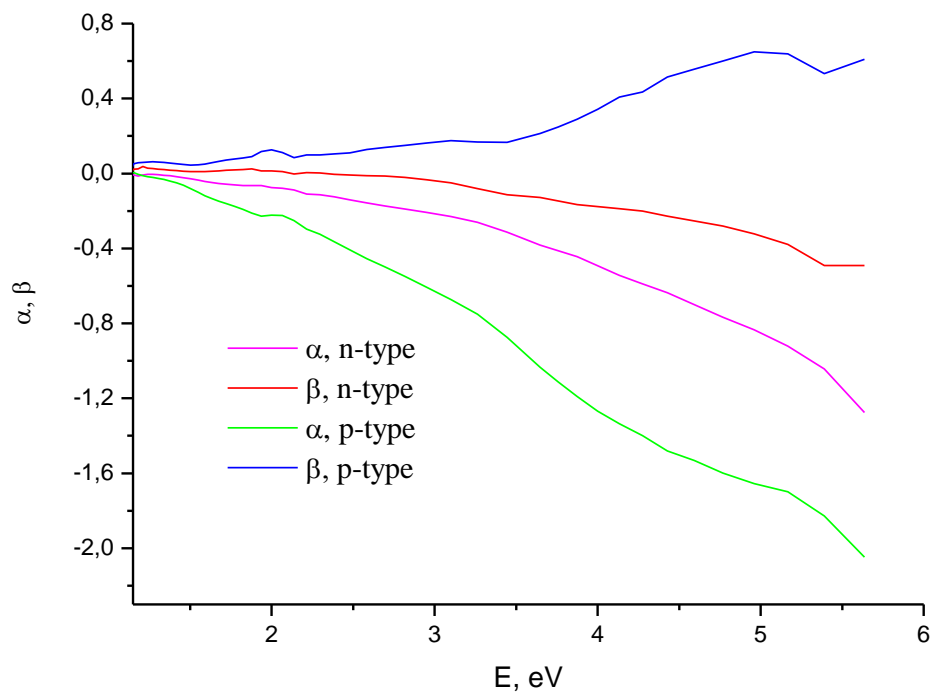


Fig. 8. The spectra of electrooptic coefficients α and β of Bi_2Te_3 film compound of n- and p-types.

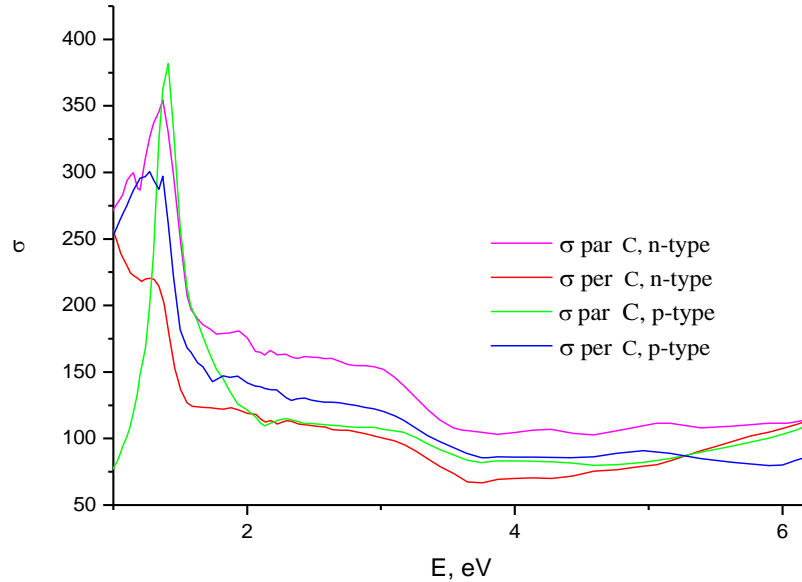


Fig. 9. The spectra of optical conduction σ of Bi_2Te_3 single crystals of n- и p-types parallel and perpendicular to C axis.

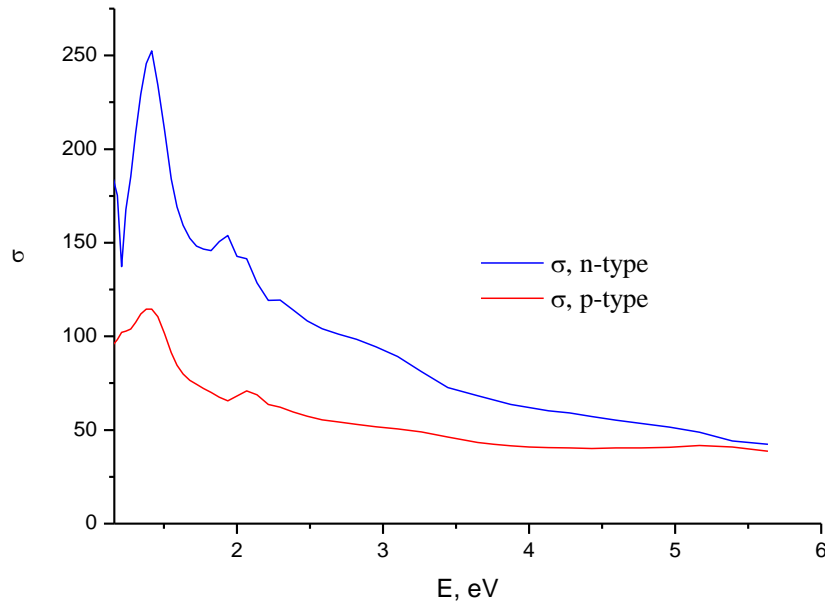


Fig. 10. The spectra of optical conduction σ of Bi_2Te_3 film compound of n- and p-types.

As it is mentioned in [17] in energy region of interband transitions $E > E_g$ (E_g is forbidden band width) the study of absorbing transitions in materials is impossible because of absorption big value. The reflection remains the unique effective method.

The analytical singularity of imaginary part of complex dielectric constant $\varepsilon_2(E)$ and functions connected with dN/dE state densities are almost coincide and the interband distance gradient makes contribution in dN/dE functions:

$$\frac{dN_{ij}}{dE} \sim \int \frac{dS_k}{|\nabla_k E_{ij}|}, \quad (1)$$

where $E_{ij}(k) = E_j(k) - E_i(k)$ is distance between conduction and valence bands. dN/dE values near critic points in k-space defined by $|\nabla_k E_{ij}| = 0$ expression and also the positions of critic points and transition types can be calculated theoretically.

The analysis of $\varepsilon_2(E)$, dN/dE functions and reflection coefficient $R(E)$ shows that placement and character of maximums in these spectra are similar or very close ones. That's why one can define the values of corresponding interband spaces and band nature with the help of direct comparison of the experimental data in $E > E_g$ region with theoretical calculations of dN/dE

function. As it is mentioned in [18] the resonance frequency E_0 presents itself that one at which the conduction $2nkE$ achieves the maximum by which the interband transitions are defined.

For non-crystalline materials the high transparency in wide energy region is typical one and some methods of E_g definitions are known. Its evaluation on level of $\alpha(E)$ absorption coefficient of long-wave edge is the one of them. E_g exact value for non-crystalline semiconductors is debatable one and usually the discussion of $\alpha(E)$ spectrum character in Urbah and Tauc models is carried out without E_g evaluations [19, 20].

As it is mentioned in [19], $N(E)$ state density is the similarly applied perception for crystalline and non-crystalline substances. On having results of experimental data, state density variation in non-crystalline body insignificantly differs from corresponding one in crystal. The thin structure in first case can be blurred and the local states can appear in forbidden band. The band structure is saved as it is defined by short-range order of atoms in materials.

The author [21] mentions that it is impossible to differentiate the principal boundary between monocrystalline, polycrystalline and amorphous substance states. The presence of band structure i.e. the forbidden and conduction bands can be obtained from the fact of existence of atom short-range order and for such conclusion there is no necessary to require the periodical atom placement.

As authors [22-24] show, the structure of unorderd binary compound can be considered as the assemblage of different basis clusters presented in structural matrix with different statistic weight and put into effective medium. As authors [25] mention, the short-range order makes the main contribution into electron state density. However, as the short-range order in binary compounds can significantly change from node to node in amorphous substance structural matrix, especially statistics of basis clusters defines the final density of electron states. So, the low-molecular structural configurations that is accompanied by definite success in energy, can appear alloy cooling or in the process of amorphous substance formation. The ambiguity of structural ordering in composition amorphous solid states by A_xB_{1-x} can be considered as their general property. The peculiarity of short-range order range near each node are caused firstly, by physical methods of A_xB_{1-x} system preparation and secondly, by chemical ordering principle, taking under consideration "rule 8-N" [19] and by bond energy values of neighbor atoms.

The destruction of ideal structure in non-crystalline solid body takes place in systems including the atoms with lone-electron pairs. Often, the electron pair at bond opening remains on the one of fragments, i.e. the heterolytic bond opening takes place. The one positive- and one negative-charged defect centers in short-range

order regions appear. The energy necessary for bond opening is partly compensated because of lone-electron pair existence of atoms being in nearest surrounding and number of chemical bonds doesn't change.

Thus, there is a structural disorder in homogeneous non-crystalline materials of stoichiometric composition of different types. It reveals in the form of positive-and negative-charged defect centers as in the case of point defects in crystals.

As a result, the reaction defects the formation of which is characterized by less change of free energy, dominate.

The short-range order idea at formation of electron energy bands is the one of fundamental conceptions in unordered system physics. This idea has the experimental and theoretical confirmation on the example of numerous non-crystalline solid and liquid semiconductors [26].

The formation mechanism of valence and conduction bands in non-crystalline semiconductors has been formulated by authors [27,28]. The similarity of main peculiarities of spectral dependence of imaginary part of dielectric constant $\varepsilon_2(E)$ for non-crystalline semiconductors and their crystalline analogues is mentioned in works of these authors. This similarity is demonstrated by author [27] on example of selenium. The analogous conclusion is made in relation to $a\text{-As}_2\text{S}_3$ and $a\text{-As}_2\text{Se}_3$ in works [27, 28]. Only maximum smoothing takes place for cases of amorphous materials in their $\varepsilon_2(E)$ but similarity of curves for amorphous and crystalline samples saves.

Nowadays, it is established that one can pointedly change the optic, photoelectric and electric properties of non-crystalline semiconductors changing the chemical composition.

The change of concentrations of charged defect centers D^+ and D^- (U^1 are centers) in them takes place and these defects form from initial neutral ones D^0 by the reaction:



which can be intrinsic, impurity or mixed defects giving the possibility to control by their physical property.

CONCLUSION

Thus, reflection coefficients $R(E)$ of Bi_2Te_3 single crystals and its film samples of n- and p-types in beam energy interval 1-6eV normally falling on the surface, are measured. For Bi_2Te_3 single crystals, the measurements are carried out parallel and perpendicular to C axis.

It is shown that values of some optical transitions of Bi_2Te_3 from crystalline state to non-crystalline one for non-crystalline samples save.

-
- [1] B.M. Qolzman, B.A. Kudinov, I.A. Smirnov. Poluprovodnikovie termoelektricheskoe materialov na osnove Bi_2Te_3 (M.: Nauka,1972), s.216. (In Russian).
- [2] P.M. Lee, L. Pincherle. Pros. Phys. Soc. **81**, 461 (1963).
- [3] D.I. Greenaway and G. Harbecke. I. Phys. Chem. Solids Pergamon Press, **26**, 1585 (1965).

THE SPECTRA OF OPTICAL PARAMETERS OF Bi_2Te_3 SINGLE CRYSTALS AND FILM COMPOUNDS

- [4] *E.V. Oleshko, V.N. Korolishin.* FTT, 27, 2856 (1985). (In Russian).
- [5] *V.L. Qurevich.* Kinetika fononix system. (M.: Nauka, 1980) 14. (In Russian).
- [6] *E. Mooser, W.C. Pearson.* Phys. Chem. Solids 7, 5 (1958).
- [7] *B.M. Qolchman, Z.M. Dashevskiy, V.I. Kaydanov, N.V. Kolomoech.* Plenochnie termoelementi: fizika i primenenie (M.: Nauka, 1985) s.233. (In Russian).
- [8] *S.A. Semiletov.* Trudi instituta kristalloqrafi, 10, 74 (1954). (In Russian).
- [9] *V.V. Sobolev, V.V. Neoshkalenko.* Elektronnaya struktura poluprovodnikov. (Kiev, nauk. Dumka, 1988). (In Russian).
- [10] Opticheskoe svoystva poluprovodnikov, *pod red. Bira* (IL, M, 1970).
- [11] *N.Z. Jalilov.* Trudi X Mejd. konf. «Opto-nanoelektronika, nanotexnologii i mikrosistemi» (Ulyanovsk, 2008) 46-47. (In Russian).
- [12] *N.Z. Jalilov, G.M. Damirov.* Труды X Mejd. konf. «Opto–nanoelektronika, nanotexnologii i mikrosistemi» (Ulyanovsk, 2008) 45. (In Russian).
- [13] *N.Z. Jalilov, G.M. Damirov.* FTP, 45, 500 (2011). (In Russian).
- [14] *N.Z. Jalilov, G.M. Damirov.* Izv. NAN Azerb., seriya fiz.-mat. I texn., fiz. I astr., XXVIII, №5, 134 (2008); XXIX, 125 (2009). (In Russian).
- [15] *N.Z. Jalilov, M.A. Maximudova.* Izv. NAN Azerb., seriya fiz.-mat. i texn., fiz. i astr., XXX, 71 (2010). (In Russian).
- [16] *N.Z. Jalilov, S.I. Mextieva, H.M. Abdullaev.* Izv. NAN Azerb., seriya fiz.-mat. i texn., fiz. i astr., XXVII, 114 (2007). (In Russian).
- [17] *J.C. Phillips.* Phys. Rev. 125, 1931 (1962), 133, A452 (1964).
- [18] *T.Moss, Q. Barrel, B. Ellis.* Poluprovodnikovaya optoelektronika (M., Mir, 1976). (In Russian).
- [19] *H. Mott, E. Devis.* Electronnie prochessi v nekristallicheskix veshestvax. (M., Mir, 1982). (In Russian).
- [20] Pod red. K.D. Chendina. Elektronnje yavleniya v xalkogenidnix stekloobraznix poluprovodnikax. (SPB.: Nauka 486 (1996). (In Russian).
- [21] *A. Rouz.* Osnovi teorii fotoprovodimosti, Izd., Mir, M. (1966). (In Russian).
- [22] *Yu.N. Shunin, K.K. Shvarths.* JSX, 27, №6, 146-150 (1986). (In Russian).
- [23] *K.K. Shvarth, Yu.N. Shunin, Ya.A. Teteris.* Izv. AN. LatSSR, ser. fiz. I tex. nauk, №4, 51-57 (1987). (In Russian).
- [24] *K.K. Shvarths, F.V. Pirgorov, Yu.N. Shunin, J.A. Teteris.* Cryst. Latt. Def. Amorph. Mat., 17, 133-138 (1987).
- [25] *Yu.N. Shunin, K.K. Shvarths.* FTP, 23, №6, 1049-1053 (1989). (In Russian).
- [26] *A.I. Qurbanov.* Kvantovo – elektronnaya teoriya amorfniix provodnikov. M., L.: Izd.AN SSSR, 1966, 250 s. (In Russian).
- [27] *M. Kastner.* Phys. Rev. Lett., 1972, 26, N7, p.355.
- [28] *R.E. Drews, R.L. Emerald, M.L. Slade, R. Zallen.* Solid State Comm., 1972, 10, N3, p.293.

Received: 10.02.2014

THE STUDY OF PHASE EQUILIBRIUM IN TlSe-FeSe SYSTEM, ELECTRIC AND THERMAL PROPERTIES OF TlFeSe₂

F.M. SEIDOV, E.M. KERIMOVA, R.G. VELIYEV, N.Z. GASANOV, K.M. GUSEYNNOVA

Institute of Physics of Azerbaijan NAS, AZ-1143, Baku, G.Javid ave., 33

E-mail: nazimgasanov55@gmail.com

The phase equilibrium in TlSe-FeSe system is studied and it is established that at component ratio 1:1 the compound TlFeSe₂ is formed, the solubility of FeSe in TlSe at room temperature is 12 mol%. It is shown that TlFeSe₂ compound is the semiconductor of p-type, activation energy of TlFeSe₂ eigen conductivity is 0,68 eV. The phonon scattering mechanism is revealed as a result of thermal conduction investigation in temperature interval 90-600K in TlFeSe₂ compound.

Keywords: crystal growth, phase diagram, electric conduction, thermal conduction.

PACS: 61.66.Fn, 64.70.Dv, 65.40.-b, 72.20.-i

The iron-thallium chalcogenides are representatives of new class of semiconductor materials [1-10]. It is known that TlSe lattice consists of two independent structural units: eight topwood with ion bond between M-C (metal – chalcogen, Tl¹⁺-Se) and tetrahedron with covalent bond between M-C (Tl³⁺-Se).

The change of trivalent thallium ions in tetrahedral by corresponding elements of III^B sub-groups and also by trivalent elements (Fe, Sm, Yb) not including the one-valent Tl¹⁺ ions in eight topwood is more rational and practically possible for control by semiconductor properties at cation change in structures of TlSe type.

In this connection, the phase equilibrium in TlSe-FeSe system and also electric and thermal properties of TlFeSe₂ single crystals is studied in the present paper.

14 samples for state diagram construction of TlSe-FeSe system are prepared. The compound alloys Tl_xFe_{1-x}Se ($0 \leq x \leq 1$) are synthesized by direct alloying of high purity elements in quartz ampoules vacuumed up to $1,3 \cdot 10^{-2}$ Pa.

The alloy synthesis regime is chosen based on melting points of initial components: 603K for TlSe and 1290K for FeSe. Each alloy is heated higher melting points of initial compounds, kept at this temperature during 5-6 hours and then temperature in furnace is slowly decreased up to room temperature. The synthesized alloys for homogenization are annealed during 21 days at temperature 410K for alloys enriched by thallium and during 23 days at 840K for alloys enriched by iron.

The obtained samples are investigated by the method of differential-thermal analysis (DTA). DTA are carried on installation HTP-64 allowing the fix the temperature of phase transformations with accuracy $\pm 3-5$ K. The heating velocity is 2-4K/min. The temperature is controlled by Pt-Pt/Rh-thermo-couple graduated on standard substances in interval 472-1560K.

The state diagram of TlSe-FeSe system constructed on DTA results is shown on fig.1. As it is followed from diagram, TlFeSe₂ compound at component ratio 1:1 forms with congruent melting at temperature 872K. The homogeneity region for the given compound is absent. The solid solutions up to 12 mol% FeSe at temperature 300K form on the base of TlSe. Non-invariant peritectic point corresponds to (TlSe)_{0,7}(FeSe)_{0,3} and temperature 673K.

The simple eutectics of (TlSe)_{0,44}(FeSe)_{0,56} composition melting at temperature 830K forms between TlFeSe₂ and FeSe.

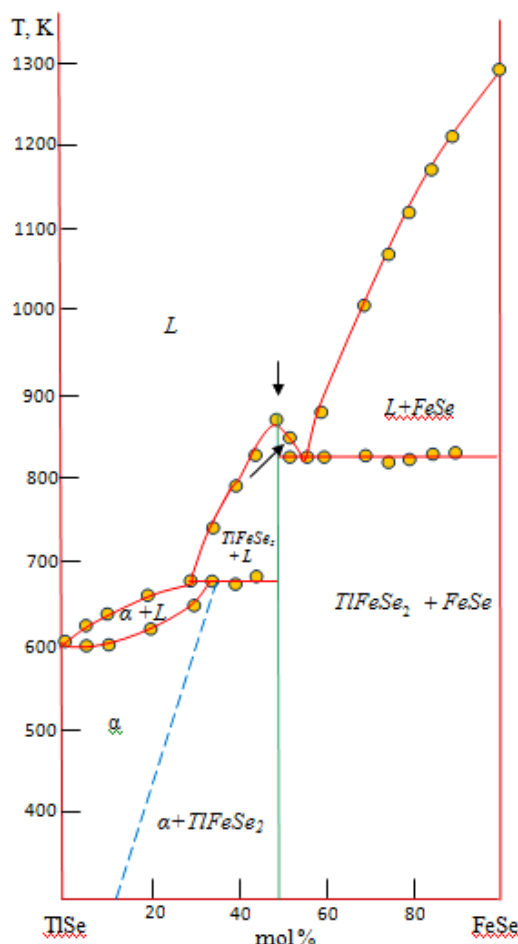


Fig.1. State diagram of TlSe-FeSe system.

Single crystals grown up by modified Bridgman-Stockbarger method in specially prepared ampoules from melted quartz are obtained for investigation of electric and thermal properties of TlFeSe₂ compound. The interior walls of ampoules are covered by graphite layer. The ampoules are put in vertical two-band furnace. The equilibrium temperature in upper high-temperature zone is set on 25-30K higher substance melting point (T_m) and temperature of low-temperature region is less than T_m on

30-40K. The transition band with temperature gradient ~20K/cm is between these two bands. The ampoule with substance with the help of special mechanism is introduce along axis of tube furnace in upper high-temperature band. After 15-20-hour regime stabilization this ampoule is moved into low-temperature band with velocity 0,8 mm/h. During 7-8 days the ampoule passing through transition crystallization band ends up in low-temperature furnace band. Further, the temperatures of both bands slowly decrease up to room one (2-3 days). TlFeSe₂ ingots obtained by such way are constructed from long (~10cm) finer fibers oriented along ampoule, forming the monolithic crystal. Roentgenographic analysis of alloys is carried out on installation URS-55 in CuK_α radiation in chamber RKD-57.3. According to data of Roentgenographic analysis TlFeSe₂ compound crystallizes in monoclinic singony with parameters of elementary cell: $a=12,08\text{\AA}$; $b=5,48\text{\AA}$; $c=7,10\text{\AA}$; $\beta=118,48^\circ$.

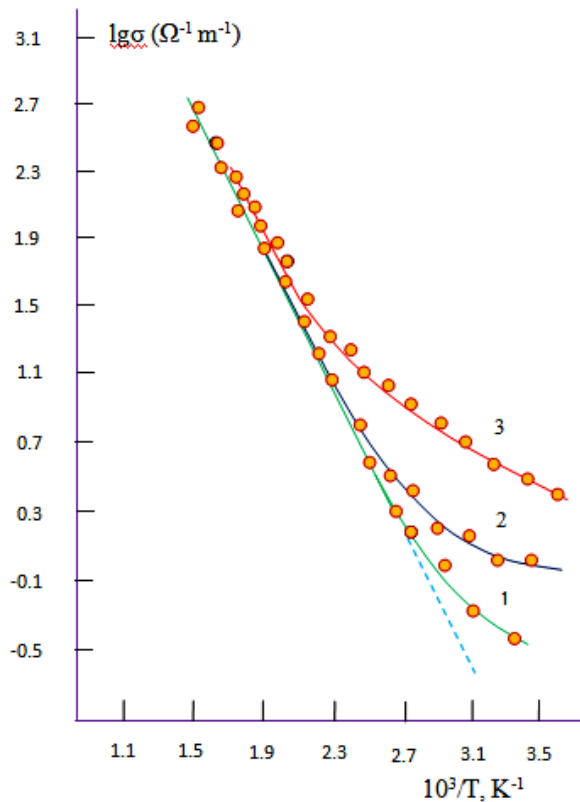


Fig.2. Temperature dependences of electric conduction of three samples of TlFeSe₂ single crystals.

The electric and thermal properties of obtained TlFeSe₂ single crystals are studied. The character temperature dependences of electric conduction for three samples of TlFeSe₂ compound are shown on fig.2. The low-temperature branches of $lg\sigma=f(10^3/T)$ dependence are caused by the presence of impurity centers of acceptor type in crystals. Exponential growth of electric conduction with temperature increase in high temperature region is connected with revealing of eigen conduction.

The forbidden gap of TlFeSe₂ compound defined from inclination of these curves is 0,68eV.

The heat conduction measurements of TlFeSe₂ crystals are carried out in temperature interval 90-600K. The heat conduction of investigated samples is measured in stationary mode by comparison method of two identical melted quartz etalons. The choice of melted quartz in the capacity of etalon is explained by the fact that coefficient of its heat conduction is one order by the value with heat conduction of the investigated samples. The temperature dependences of general TlFeSe₂ crystal heat conduction are presented on fig.3. In temperature interval 90-600K it corresponded to the lattice component because of the possible electron component of heat conduction in the given temperature region is small one ($\alpha_e \sim 10^{-7} \text{ Wt/mK}$). From fig.3 it is seen that observable temperature dependence of thermal conduction coefficient in TlFeSe₂ crystal obeys to Eyken law ($\alpha \sim T^{-1}$) showing on dominating role in thermal transfer of three-phonon processes on

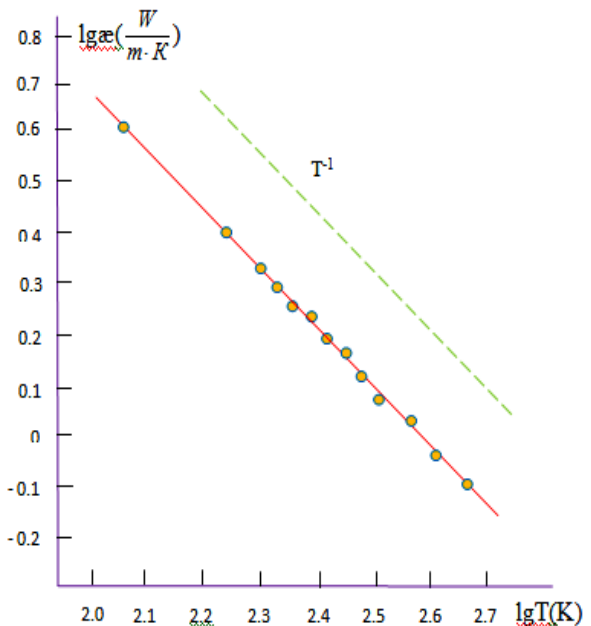


Fig.3. The temperature dependence of thermal conduction coefficient of TlFeSe₂ single crystal.

CONCLUSION

By DTA method it is revealed that in TlSe – FeSe system at component ratio 1:1 TlFeSe₂ compound with congruent melting forms and 12 mol% FeSe is dissolved in TlSe at room temperature. It is shown that TlFeSe₂ compound is semiconductor of p-type and activation energy of TlFeSe₂ eigen conduction is 0,68 eV. It is established, that measured general thermal conduction of TlFeSe₂ crystal in temperature interval 90-600K corresponds to lattice component.

[1] *Kutoglu*. Synthese und Kristallstrukturen von TlFeS₂ und TlFeSe₂, Z. Naturwissench., 1974, v.B61, pp.125-126.

[2] *K. Klepp, H. Boller*. Die Kristallstruktur von TlFeS₂ und TlFeSe₂, Z. Monatsh. Chem., 1979, v.110, pp.1045-1047.

- [3] *G.I. Makovechkiy, E.I. Kasinskiy.* Izv. AN SSSR, seriya «Neorgan. materiali », 1984, t.20, vip.10, s.1752-1753. (In Russian).
- [4] *G.D. Sultanov, G.D. Guseynov, E.M. Kerimova.* Konf. po materialovedenie xalkoqenidnix I kislorodsoderjashix poluprovodnikov, Chernovchi, 1986, s.195. (In Russian).
- [5] *M.A. Aldjanov, M.D. Nadjaf-zade.* FTT, 1990, t.32, №8, s.2494-2495. (In Russian).
- [6] *A.I. Djabbarli, E.M. Kerimova, F.M. Seyidov, A.K. Zamanova.* Neorgan materiali, 1996, t.32, №1, s.118-119. (In Russian).
- [7] *R.G. Veliyev, E.M. Kerimova, F.M. Seyidov. R.Z. Sadixov.* Fizika, 2008, t.14, №3, s.14-16. (In Russian).
- [8] *R.G. Veliyev, E.M. Kerimova, M.Yu. Seyidov., F.M. Seyidov, N.Z. Gasanov, R.Z. Sadixov, A.A. Isaeva.* Sbornik dokladov mejdunarodnoy nauchnoy konferenchii FTT - 2009, Minsk, 2009, s.130-132. (In Russian).
- [9] *R.G. Veliyev, M.Yu. Seyidov, N.Z. Gasanov, F.M. Seyidov.* The magneto-dielectric properties of compounds and alloys in the systems of $TlInS_2$ - $TlFeS_2$, $TlInS_2-TlFeSe_2$, J.Alloys Comp., 2010, v.506, No.2, p.800-803.
- [10] *F.M. Seyidov. E.M. Kerimova, N.Z. Gasanov.* Neorgan materiali, 2011, t.47, №12, s.1429-1432. (In Russian).

Received: 03.03.2014

ENERGY SPECTRUM OF CHARGE CARRIERS IN SINGLE CRYSTAL ALLOYS $\text{Bi}_{1-x}\text{Sb}_x$ ($0 \leq x \leq 0,25$) AT TEMPERATURE T=77-300K

B.A. TAIROV, H.A. GASANOVA, V.I. EMINOVA, F.H. MAMMADOV

Institute of Physics of Azerbaijan NAS, H. Javid ave., 33, Baku, AZ-1143

btairov@physics.ab.az, rasulova.khayala@mail.ru

The resistivity components ρ_{ij} , Hall coefficient R_{ijk} and magnetoresistance $\rho_{ij,kl}$ in monocrystalline alloys $\text{Bi}_{1-x}\text{Sb}_x$ at temperatures of 77 -300K are measured. The possibility of quantitative interpretation of galvanomagnetic effects in bismuth and $\text{Bi}_{1-x}\text{Sb}_x$ alloys with $x \leq 0,09$ based on the model of electron Fermi surface in the form of three ellipsoids and for holes in the form of ellipsoid of rotation. In alloys and antimony of electron Fermi surfaces remain the same as in the bismuth; for holes in antimony these are in the form of six ellipsoids of general type and an ellipsoid of rotation. Hole Fermi surface in $\text{Bi}_{1-x}\text{Sb}_x$ with $0,16 \leq x \leq 0,25$ is represented as three ellipsoids of general type being presumably in Σ point of Brillouin zone (BZ). The angle of inclination of the electron ellipsoids decreases with antimony content increase. The analysis of anisotropy of hole mobilities allows us to assum that hole ellipsoids in $\text{Bi}_{1-x}\text{Sb}_x$ alloys with $0,16 \leq x \leq 0,25$ are less anisotropic ones than the hole ellipsoids in $\text{Bi}_{1-x}\text{Sb}_x$ with $0 \leq x \leq 0,16$, so for anisotropy hole mobility in $\text{Bi}_{1-x}\text{Sb}_x$ alloys with $0,16 \leq x \leq 0,25$ we have $v_2/v_1=0,05$ and $v_3/v_1=0,5$ and in $\text{Bi}_{1-x}\text{Sb}_x$ alloys with $0 \leq x \leq 0,16$ we have $v_2/v_1=0,009$ and $v_3/v_1=0,7$.

Keywords: solid solution, charge carriers

PACS: 64.75.Nx; 72.20.Pa

INTRODUCTION

Recently the interest in bismuth and $\text{Bi}_{1-x}\text{Sb}_x$ alloys has grown [1-2]. The small value of thermal conductivity and the small effective mass of electrons in $\text{Bi}_{1-x}\text{Sb}_x$ solid solutions allows us to use them in infrared sensors and thermoelectric generators, the characteristics of which are directly connected with energy spectrum and charge carrier scattering mechanism.

Therefore, in this paper, the study of galvanomagnetic effects in n - $\text{Bi}_{1-x}\text{Sb}_x$ to identify the energy spectra in these crystals, is carried out.

EXPERIMENTAL RESULTS AND DISCUSSION

The components of electric conduction, magnetoresistance and Hall coefficient are measured at constant current in magnetic fields 0-0,2Tl. The measurements are carried out in solenoid, the homogeneous field region of which is 0,15-0,2 along solenoid axis, its inner diameter is 0,1m.

It should be noted, that the values of the coefficients ρ_{ijk} and $\rho_{ij,kl}$ given in the paper, correspond to the conditions of a weak magnetic field. To obtain these values, the dependence of corresponding galvanomagnetic coefficient on the field is always taken. Moreover, the condition for weak magnetic field, i.e. the independence of R_{ijk} Hall coefficient and $\rho_{ij,kl}$ magnetoresistance, is controlled.

For quantitative interpretations of the experimental results on the galvanomagnetic properties of $\text{Bi}_{1-x}\text{Sb}_x$ the relations [3,4,5] between the components of the galvanomagnetic coefficients with electron and hole kinetic parameters

It should be noted that the given relations [3,4,5] remain in force in NENP model, as it is revealed in [6] that the presence of three symmetrically placed ellipsoids in $\text{Bi}_{1-x}\text{Sb}_x$ almost softens the anisotropy of kinetic coefficients associated with the deviation of the dispersion law from ellipsoid form. Therefore, at

calculation of kinetic phenomena, one can restrict by ENP and EP models. Such interpretation from one hand allows us to judge about correctness of the choice of energy spectrum model by the agreement of the experimental and calculated values, since at the assumption of relaxation time isotropy of carries the mobility tensor components characterize the components of the effective mass tensor.

To calculate the parameters of the energy spectrum of charge carriers in bismuth-antimony alloys on the base of experimentally obtained values of the galvanomagnetic coefficients, it is necessary to concentrate on the most obvious its model, which further will be confirmed by the comparison of experimental and calculated values. Firstly, let's go back to the schemes which demonstrate the energy spectrum variation of $\text{Bi}_{1-x}\text{Sb}_x$ alloys on the its composition (Fig. 1). As it is seen from the figure at the content of antimony 6 at.%, the gap between the valence and the conduction bands opens, while the gap width is determined by L_a conduction band and T valence band. According to the model of Fermi surface (like pure bismuth) should include three ellipsoids of general type for electrons, inclined in respect of the basal plane, and the ellipsoid of rotation with axis in trigonal direction for holes.

When the content of antimony (8-12 at.%), the gap is determined between L_a and L_s energy distances, and the hole Fermi surface should be presented by three ellipsoids similar to electron one. However, T and Σ hole bands being near the bottom of the conduction band have the significantly higher density of states than L_s , whereby in alloys with antimony content up to 12 atm.%, they can play a major role in the transfer phenomena at temperatures higher than 77K.

The new hole band the extremum of which presumably is H or Σ points begins to play role at further antimony content increase [9,10]. The question, whether the new appeared hole band is one with extremum in H point as in pure antimony, which falls with antimony

concentration increase on energy scale or this band is one with extremum in точке Σ point which rises from valence

band depth of pure bismuth, is still open.

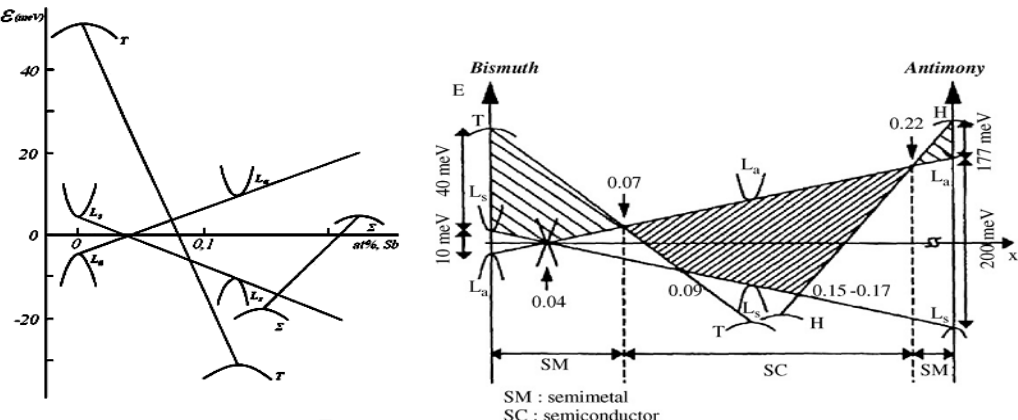


Fig.1. The schemes of energy spectrum reconstruction of bismuth-antimony alloys at increase of antimony concentration [7,8].

Note that the energy indirect gap between bands with extremum L_a point and appeared band decreases and is equal to zero at 22at% Sb with antimony content increase. $Bi_{1-x}Sb_x$ alloys become the semimetals at further antimony content increase. According to above mentioned we use the model representing electron Fermi surface in the form of three ellipsoids general type easily inclined in respect to trigonal axis and placing in Brillouin zone in L point for interpretation of galvanomagnetic properties of $Bi_{1-x}Sb_x$ ($0,15 \leq x \leq 0,25$) alloys. Hole Fermi surface is represented by three or six ellipsoids general type inclined in respect to trigonal axis and placing in Σ and H points of BZ.

For antimony the electrons are in L point and holes are in H and GT points of Brillouin zone.

For interpretation of some $Bi_{1-x}Sb_x$ alloy properties especially at doping it is suggested that the carriers of additional bands take part in transfer phenomena are also used in works [11-12].

Thus, in general case the energy spectrum model of charge carrier in $Bi_{1-x}Sb_x$ alloys should take under consideration the possibility of charge carrier placement in L_a , L_s , T , Σ , H and GT bands.

Such model in general case can be described by three mobility components of L_a electrons (μ_1, μ_2, μ_3), three mobility components of L_s , Σ , H holes and Σ electrons (v_1, v_2, v_3), incident angle of electron and hole ellipsoids ϕ_e, ϕ_g correspondingly, concentration N_e, N_g and finally, by two mobility components of holes T and GT ($v_1 = v_2, v_3$) and concentration.

The ratios between above mentioned energy spectrum parameters and galvanomagnetic coefficients can be obtained in the assumption of contribution independence into general charge carriers of different types.

The ratios obtained by such way are given in references [3,4,5].

The formula of the electric conduction expansion in the magnetic field is convenient by the fact that the obvious additivity of carrier contributions of separate bands is reflected. However, in experiment the resistance components in magnetic field, which are connected by ratio symmetry with corresponding components of electric conduction for D_{3d} crystals [13].

The ratios given in [13] towards with following condition:

$$N_e = N_g + N_g' \quad (1)$$

represent themselves the 13 levels with 13 unknown values (left parts of equations are experimentally obtained coefficients).

Thus, the solution of this nonlinear system of equations should lead to concrete definition of energy spectrum parameters. However, in analytical form it is impossible to solve this system of equation and that's why for this aim, the special programs with following solution selection which corresponds to physical meaning of obtained values are used.

The investigations of galvanomagnetic properties of $Bi_{1-x}Sb_x$ alloys are carried out in complex with dispersion definition of Electromagnetic Magnetoplasma Waves (EMPW) the results of which are described in [14,15,16]. The important factor is the fact that EMPW propagation in Bi-Sb crystals is practically defined by parameters of energy spectrum of L electrons and waves in hole plasma damp because of less hole mobilities (in undoped alloys).

The definition of L electron parameters is also carried out with computer use and results of these experiments are used for the solving of above mentioned system of equations.

Such use of investigation results of EMPW dispersion allows us to compare the correspondence of defined parameters by these two methods.

As it is show in [17], the valence band in L point should be almost "mirror" for m_1 and m_3 directions in respect of conduction band and for m_2 direction the effective mass of halls is bigger in two times than one of electrons.

That's why component ratios of L hole mobilities in m_1 and m_3 directions are equal to ones of L electron mobilities. Thus, the mobility structure of electrons and holes in L is defined.

The values of experimental and calculated values of galvanomagnetic coefficients for Bi, Sb and $Bi_{1-x}Sb_x$ alloys with antimony content 0÷25 at.% at temperature

ENERGY SPECTRUM OF CHARGE CARRIERS IN SINGLE CRYSTAL ALLOYS Bi_{1-x}Sb_x(0,≤x≤0,25) AT TEMPERATURE...

77K are given in table 1. As it is seen from the table, for all alloy compositions the experimental and calculated values are in well agreement. It is necessary to note that agreement is achieved only in narrow interval of values of concentration and charge carrier mobility, which are given in table 2.

The values of experimentally defined and calculated galvanomagnetic coefficients in Bi_{1-x}Sb_x alloys at T=77 K (σ_{II} , σ_{33} are measured with delicacy3%, σ_{123} , σ_{231} – 5%, $\sigma_{II,22}$ – 10%, $\sigma_{II,II}$ and $\sigma_{33,II}$ – 15%, $\sigma_{II,33}$ and $\sigma_{33,33}$ – 20%; the dimension is σ_{ij} - $\Omega^l cm^l$, σ_{ijk} – $cm C^{-1} \Omega^2$, σ_{ijkl} – $cm^3 C^2 \Omega^3$.

Table1.

at.% Sb	type	$\sigma_{II} \times 10^{-5}$	$\sigma_{33} \times 10^{-5}$	$\sigma_{231} \times 10^{-7}$	$\sigma_{123} \times 10^{-6}$
0	Exp.	32,32	26,57	9,99	3,75
	Calc.	32,39	26,54	9,52	3,57
6	Exp.	12,44	15,94	8,7	2,77
	Calc.	11,8	14,64	8,72	2,98
9	Exp.	6,67	7,94	5,45	2,22
	Calc.	6,65	7,82	6,16	2,15
12	Exp.	4,8	5,3	2,72	0,84
	Calc.	4,6	5,4	3,07	0,83
16	Exp.	5,15	5,7	2	0,68
	Calc.	4,87	6,1	2,06	0,6
18	Exp.	6,25	7,8	2,2	0,58
	Calc.	6,03	7,7	2,26	0,59
20	Exp.	7,4	9,1	1,82	0,53
	Calc.	7,1	8,9	1,9	0,53
22	Exp.	7,94	9,6	1,28	0,34
	Calc.	7,53	9,38	1,38	0,31
25	Exp.	8,1	10,2	0,69	0,21
	Calc.	7,27	9,1	0,86	0,19
100	Exp.	141	198	0,63	7,2

Continuation of Table 1.

at.% Sb	Type	$\sigma_{II,33} \times 10^{-6}$	$\sigma_{33,II} \times 10^{-8}$	$\sigma_{II,II} \times 10^{-8}$	$\sigma_{II,22} \times 10^{-8}$	$\sigma_{33,33} \times 10^{-6}$
0	Exp.	220	34,66	19,92	59,4	106,24
	Calc.	200	35	17,8	54	108
6	Exp.	245	76,2	29,4	82,7	192
	Calc.	244	72,8	26	79,4	143
9	Exp.	284	70,4	35,7	95,2	171
	Calc.	278	79,1	28,6	86,1	155
12	Exp.	96	30,9	17,26	49,5	62
	Calc.	100	32	17,06	47,9	71
16	Exp.	34	10,7	5,84	14,2	19
	Calc.	39	14,3	5,1	15,6	20
18	Exp.	17,5	10,3	3,55	11,1	10,5
	Calc.	23,81	11,9	4,21	12,8	12
20	Exp.	11	7,5	2,62	7,85	8
	Calc.	17,23	7,2	2,6	7,85	7
22	Exp.	8,6	2,9	1,74	4,3	5,72
	Calc.	10,6	3,5	1,26	3,83	7,23
25	Exp.	5,3	1,16	1,01	1,97	2,23
	Calc.	4,35	1,47	0,53	1,6	2,98
100	Exp.	12,5	0,38	0,1	0,32	3,5
	Calc.	11,3	0,45	0,08	0,34	2,5

Table 2.
Kinetic parameters of charge carriers for $\text{Bi}_{1-x}\text{Sb}_x$ alloys at $T=77 \text{ K}$

at.% Sb	0	6	9	12	16	18	20	22	25	100
φ_s	$7^010'$	$6^040'$	$6^030'$	$5^050'$	5^0	$4^040'$	$4^010'$	$4^06'$	$4^06'$	$6^023'$
φ_g					7^0	16^0	16^0	16^0	16^0	24^0
$\mu_1, \text{m}^2/\text{V}\cdot\text{s}$	74	120	172	179	90	71,5	52	34,4	23,2	1,83
$\mu_2, \text{m}^2/\text{V}\cdot\text{s}$	0,74	1,08	1,84	0,63	0,81	0,643	0,468	0,309	0,209	0,037
$\mu_3, \text{m}^2/\text{V}\cdot\text{s}$	37	84	112	92	63	50	36,4	24,1	16,2	1,42
$v_1, \text{m}^2/\text{V}\cdot\text{s}$				57	30	18	13	9,1	5,8	2,313
$v_2, \text{m}^2/\text{V}\cdot\text{s}$					0,24	1,5	0,9	0,65	0,455	0,29
$v_3, \text{m}^2/\text{V}\cdot\text{s}$					29	15	9	6,5	4,55	2,9
$v'_1, \text{m}^2/\text{V}\cdot\text{s}$	12,3	9,9	15,2							
$v'_2, \text{m}^2/\text{V}\cdot\text{s}$	12,3	9,9	15,2							
$v'_3, \text{m}^2/\text{V}\cdot\text{s}$	0,984	0,792	1,2							
N_s, m^3	$4,5 \times 10^{23}$	$1,1 \times 10^{23}$	$4,05 \times 10^{22}$	$2,4 \times 10^{22}$	$4,95 \times 10^{22}$	$8,21 \times 10^{22}$	$1,33 \times 10^{23}$	$2,1 \times 10^{23}$	$3,04 \times 10^{23}$	39×10^{24}
N_g, m^3					$2,4 \times 10^{22}$	$4,95 \times 10^{22}$	$8,21 \times 10^{22}$	$1,33 \times 10^{23}$	$2,1 \times 10^{23}$	$3,04 \times 10^{23}$
N'_g, m^3	$4,5 \times 10^{23}$	$1,1 \times 10^{23}$	$4,05 \times 10^{22}$							$4,88 \times 10^{24}$

CONCLUSION

On obtained results, one can make the conclusions:

1. The possibility of quantitative interpretation of galvanomagnetic effects in bismuth and $\text{Bi}_{1-x}\text{Sb}_x$ alloys with $x \leq 0,09$ based on the model of electron Fermi surface in the form of three ellipsoids and holes in the form of an ellipsoid of rotation, is shown.
2. In alloys and antimony of electron Fermi surface remains the same as in the bismuth; for holes in antimony these surfaces are presented in the form of six types of ellipsoids and an ellipsoid of rotation.
3. Hole Fermi surface in $\text{Bi}_{1-x}\text{Sb}_x$ with $0,16 \leq x \leq 0,25$ is represented as three ellipsoids of general type, being presumably in Σ point of BZ.

4. The angle of inclination of electron ellipsoids decreases with antimony content increase. We note that a similar conclusion was reached in [18], where the dependence of angle of inclination of electron Fermi surface on composition for $\text{Bi}_{1-x}\text{Sb}_x$ alloys ($0 \leq x \leq 0,22$) is defined by dispersion investigation method EMPV.
5. Based on the analysis of hole mobility anisotropy one can suggest that hole ellipsoids in $\text{Bi}_{1-x}\text{Sb}_x$ alloys with $0,16 \leq x \leq 0,25$ less anisotropic than the hole ellipsoids $\text{Bi}_{1-x}\text{Sb}_x$ with $0, \leq x \leq 0,16$ since anisotropy hole mobility in alloys for with $\text{Bi}_{1-x}\text{Sb}_x$ $0,16 \leq x \leq 0,25$ $v_2/v_1 = 0,05$ and $v_3/v_1 = 0,5$ and in $\text{Bi}_{1-x}\text{Sb}_x$ alloys with $0, \leq x \leq 0,16$. $v_2/v_1 = 0,009$ and $v_3/v_1 = 0,7$.

-
- [1] *Lu Li, J.G. Checkelsky, Y.S. Hor, C. Uher, A.F. Hebard, R.J. Cava, N.P. Ong.* Science, **321** (5888), 547 (2008).
- [2] *D.Sh. Abdinov, T.D. Aliyeva, N.M. Axundova, M.M. Tagiyev.* Izv NAN Azerbaijana, Ser. Fizika, **I** (5), **41** (2003). (in Russian)
- [3] *S.J. Freedman, H.J. Juretschke.* Galvanomagnetic Effects and Band Structure of Antimony.-Phys. Rev., 1961, v. 124, N.5, p.1379-1386.
- [4] *B. Abeles, S. Meiboom.* Galvanomagnetic effects in bismuth.-Phys. Rev., 1956,v.101, N.2, p.544-550.
- [5] *R.N. Zitter.* Small – Field Galvanomagnetic Tensor of Bismuth at $4,2^0\text{K}$. - Phys. Rev., 1962, v. 127, N.5, p.1471-1480.
- [6] *I.M. Golban.* Issledovanie yavleniy perenosa v kristallakh tipa vismuta. Avtoreferat diss. na zvanie kand. Fiz.-mat. Nauk. Kishinyov, 1982. (in Russian)
- [7] *N.B. Brandt, S.M. Chudinov, V.G. Karavaev.* JETF, 1976, t. 70, s. 2297-2317. (in Russian)
- [8] *Soma Dutta, V. Shubha, T.G. Ramesh.* Effect of pressure and temperature on thermopower of Bi–Sb alloys. Elsevier Physica B. 405, 2010, p. 1239–1243
- [9] *N.B. Brandt, S.M. Chudinov, V.G. Karavaev.* JETF, 1971, t. 61, v.2, s. 689-704. (in Russian)
- [10] *N.B. Brandt, Kh. Dittman, Ya.G. Ponomaryov.* FTT, 1971, t.13, v.10, s. 2860-2872. (in Russian)
- [11] *V.S. Voloshin, V.M. Grabov, G.A. Ivanov, V.A. Kulikov, Yu.N. Saraev, I.I. Fadeeva.* Tezisi dokladov po poluprovodnikam s maloy shirinoy zapreshennoy zoni. Lvov, 1969. (in Russian)
- [12] *A.A. Averkin, Yu.G. Vorov, G.A.Ivanov, B.L. Naletov and A.R. Regel.* FTT, 1971, t.13, n.12, s. 3644. (in Russian)
- [13] *H.J. Juretschke* Acta Crystallogr., 1955, v.8, n.11, p.716-722.
- [14] *R. Brazis, J. Pozela, B. Tairov and M. Shakhtakhtinskii.* Phys.Stat. Sol. (b), 1974, v.62, n2, p. 697-708.

ENERGY SPECTRUM OF CHARGE CARRIERS IN SINGLE CRYSTAL ALLOYS Bi_{1-x}Sb_x(0<x≤0.25) AT TEMPERATURE...

- [15] *Yu.K. Pojela, V. Rauka, B.A. Tairov, R. Tolutis*
Dispersiya magnitoplazmennikh voln v Bi_{0,92}Sb_{0,08}
pri vsestoronnem sjatii. Lit. Fiz. Sb., 1973, t.13, v.4,
s. 535-543. (in Russian)
- [16] *V.Paulavichus, Yu.K. Pojela, R. Tolutis, B.A. Tairov,*
Vliyanie osobennostey zonnoy strukturi Bi_{0,99}Sb_{0,11}
na dispersiyu rasprostranyayushikhsya v nem
magnitoplazmennikh voln. Lit. Fiz. Sb., 1976, t.15,
v. 5, s. 771-779. (in Russian)
- [17] *M.I. Belovalov, N.B. Brandt, V.S. Vavilov,*
Ya.G. Ponomarev. JETF, 1977, t.73, n.2(8), s.721-
731. (in Russian)
- [18] *W. Braune, B. Fellmuth, N. Kubicki, R. Herrman.*
Phys. Stat. Sol. (b), 1982, v.110, n.2, p. 549-556.

Received: 03.02.2014

A MICROSCOPIC THEORY OF LOCAL SPIN EXCITATIONS IN A RECTANGULAR FERROMAGNETIC SEMICONDUCTOR NANOWIRES

V.A. TANRIVERDIYEV, V.S. TAGIYEV

*Institute of Physics of the National Academy of Sciences of Azerbaijan, Baku Az -1143,
Baku, H.Javid ave.33, E-mail : solstphs @physics.ab.az.*

A Green function analysis is used to study spin-waves excitations in a ferromagnetic semiconductor nanowires. The expression of Green function for different spins of ferromagnetic nanowires are derived. The nanowire is modeled as having a cubic cross section. The results are illustrated numerically for a particular choice of parameters

Keywords: A. Magnetic material

PACS: 75.70. Ak

INTRODUCTION

Nowadays preparation magnetic materials in the nanometer scale can be achieved by different techniques. Both semiconductors and magnetic materials play an important role in modern electronics. Although progress has been made in the understanding magnetic nanostructured materials studies of magnetic semiconductors nanotubes and nanowires (NWs) are still at a nascent stage [1-3]. Ferromagnetic semiconductors NWs can bring interesting applications to future magnetic recording media and electronic devices.

The interplay of magnetism and semiconducting properties has been observed in magnetic semiconductors. However, investigation of nanostructures have shown a

noticeable difference in their static magnetic properties as well as the significant advantage of nanosized structures over the bulk state [4-6].

RESULTS AND DISCUSSION

Theoretically, various nanowires can be modeled as having a chosen shape and size cross section (in the x - y plane) with a finite number spins arranged [7,8]. These layers are stacked vertically to form a long nanowire extending in the z direction from $-\infty$ to ∞ .

As indicated in fig. 1. we consider a simple cubic ferromagnetic semiconductor nanowires. The full Hamiltonian of system is expressed as the sum of tree terms:

$$H_M = -\frac{1}{2} \sum_{i,j} J_{i,j} S_i S_j - \sum_i g_i \mu_B H_0 S_i^z, \quad H_E = \sum_{i,j,\sigma} t_{i,j} a_{i\sigma}^\dagger a_{j\sigma} - g_e \mu_B H_0 \sum_i S_i^z, \quad H_I = -\sum_i I_i S_i S_i \quad (1)$$

H_M is the Heisenberg Hamiltonian for the localized spins of d or f type, H_E describes the kinetic and Zeeman energy of conduction s type electrons. The most important term is an s-d (or s-f) interaction Hamiltonian H_I . Here J_{ij} is the exchange coupling between sites

labeled i and j , $S_{i(j)}$ and $s_{i(j)}$ are the spins operators of localized spins and conduction electrons, respectively. Also, H_0 is externally applied field in the along the nanowires under consideration, t_{ij} is a hopping term and I_i is a contact interaction energy.

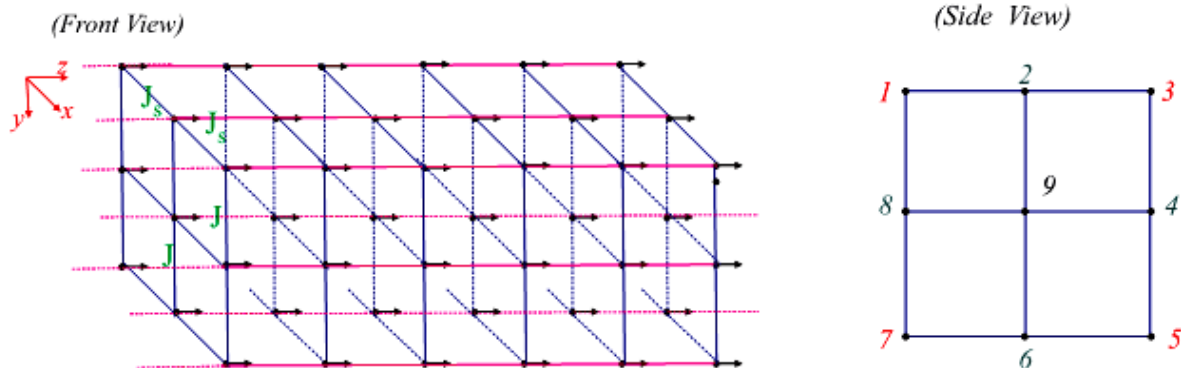


Fig. 1. Model of simple cubic ferromagnetic semiconductor nanowires. The nanowires are infinite in the direction to the axes z .

A MICROSCOPIC THEORY OF LOCAL SPIN EXCITATIONS IN A RECTANGULARFERROMAGNETIC SEMICONDUCTOR...

To study of the spin excitations of the system we introduce two type Green's function $G_{i,j}(t) = \langle\langle S_i^+(t) | S_j^-(0) \rangle\rangle$ and $G'_{i,j}(t) = \langle\langle S_i^+(t) | S_j^-(0) \rangle\rangle$. Using Fourier transform the Green function's equation of motion in the random-phase- approximation at $T \ll T_c$ we obtain the following combined equation [9,10]:

$$\left\{ \omega - g_i \mu_B H_0 - I_i \langle S_i^z \rangle - \frac{I_i^2 \langle S_i^z \rangle \langle S_i^z \rangle}{\omega - g_e \mu_B H_0 - I_i \langle S_i^z \rangle} - \sum_{\delta} J_{i,i+\delta} \langle S_{i+\delta}^z \rangle \right\} G_{i,j}(\omega) + \langle S_i^z \rangle \sum_{\delta} J_{i,i+\delta} G_{i,i+\delta}(\omega) = 2 \langle S_i^z \rangle \delta_{ij} . \quad (2)$$

Employing the equation (2) for the nanowires under consideration one obtains the following system equations:

$$\begin{cases} (\Omega - 4J_s \langle S^z \rangle) G_{n,m}^{1,\tau} + J_s \langle S^z \rangle (G_{n,m}^{2,\tau} + G_{n+1,m}^{1,\tau} + G_{n-1,m}^{1,\tau}) = \delta_{n,m}^{1,r} \\ (\Omega - 4J_s \langle S^z \rangle - J \langle S^z \rangle) G_{n,m}^{2,\tau} + J_s \langle S^z \rangle (G_{n,m}^{1,\tau} + G_{n,m}^{3,\tau} + G_{n+1,m}^{2,\tau} + G_{n-1,m}^{2,\tau}) + J \langle S^z \rangle G_{n,m}^{9,\tau} = \delta_{n,m}^{2,r} \\ (\Omega - 4J_s \langle S^z \rangle) G_{n,m}^{3,\tau} + J_s \langle S^z \rangle (G_{n,m}^{2,\tau} + G_{n,m}^{4,\tau} + G_{n+1,m}^{3,\tau} + G_{n-1,m}^{3,\tau}) = \delta_{n,m}^{3,r} \\ (\Omega - 4J_s \langle S^z \rangle - J \langle S^z \rangle) G_{n,m}^{4,\tau} + J_s \langle S^z \rangle (G_{n,m}^{3,\tau} + G_{n,m}^{5,\tau} + G_{n+1,m}^{4,\tau} + G_{n-1,m}^{4,\tau}) + J \langle S^z \rangle G_{n,m}^{9,\tau} = \delta_{n,m}^{4,r} \\ (\Omega - 4J_s \langle S^z \rangle) G_{n,m}^{5,\tau} + J_s \langle S^z \rangle (G_{n,m}^{4,\tau} + G_{n,m}^{6,\tau} + G_{n+1,m}^{5,\tau} + G_{n-1,m}^{5,\tau}) = \delta_{n,m}^{5,r} \\ (\Omega - 4J_s \langle S^z \rangle - J \langle S^z \rangle) G_{n,m}^{6,\tau} + J_s \langle S^z \rangle (G_{n,m}^{5,\tau} + G_{n,m}^{7,\tau} + G_{n+1,m}^{6,\tau} + G_{n-1,m}^{6,\tau}) + J \langle S^z \rangle G_{n,m}^{9,\tau} = \delta_{n,m}^{6,r} \\ (\Omega - 4J_s \langle S^z \rangle) G_{n,m}^{7,\tau} + J_s \langle S^z \rangle (G_{n,m}^{6,\tau} + G_{n,m}^{8,\tau} + G_{n+1,m}^{7,\tau} + G_{n-1,m}^{7,\tau}) = \delta_{n,m}^{7,r} \\ (\Omega - 4J_s \langle S^z \rangle - J \langle S^z \rangle) G_{n,m}^{8,\tau} + J_s \langle S^z \rangle (G_{n,m}^{7,\tau} + G_{n,m}^{1,\tau} + G_{n+1,m}^{8,\tau} + G_{n-1,m}^{8,\tau}) + J \langle S^z \rangle G_{n,m}^{9,\tau} = \delta_{n,m}^{8,r} \\ (\Omega - 6J \langle S^z \rangle) G_{n,m}^{9,\tau} + J \langle S^z \rangle (G_{n,m}^{2,\tau} + G_{n,m}^{4,\tau} + G_{n,m}^{6,\tau} + G_{n,m}^{8,\tau} + G_{n+1,m}^{9,\tau} + G_{n-1,m}^{9,\tau}) = \delta_{n,m}^{9,r} \end{cases} \quad (3)$$

here $\Omega = \omega - g_i \mu B_0 - I \langle S^z \rangle - I^2 \langle S^z \rangle \langle S^z \rangle / (\omega - g_e \mu B_0 - I \langle S^z \rangle)$, also n and m are layer indices, while $1, \dots, 9$ and τ label the position of the spins in layers n and m , respectively.

The system is also periodic in the z direction, which lattice constant is a . According to Bloch's theorem has been employed for plane waves in order to receive the system equations [10,11]

$$G_{n\pm 1,m}^{(1,2,3,4,5,6,7,8,9),\tau} = \exp[\pm ika] G_{n,m}^{(1,2,3,4,5,6,7,8,9),\tau} \quad (4)$$

Using (4) the Green function are obtained by solving the equations (3):

$$\begin{aligned} G_{n,n}^{\tau,\tau}(\omega) &= \sum_{\substack{l=1 \\ l \neq 4}}^7 \left(\frac{a(\omega_{kl}^+)}{\omega - \omega_{kl}^+} + \frac{a(\omega_{kl}^-)}{\omega - \omega_{kl}^-} \right); \quad \tau = (1,3,5,7) \\ a(\omega_{kl}^{\pm}) &= \frac{2J_s^4 \langle S^z \rangle^4 (\Omega_{kl} - \Omega_b) + 4J_s^2 \langle S^z \rangle^2 (\Omega_{kl} - \Omega_t) (J^2 \langle S^z \rangle^2 + \alpha(\Omega_{kl})) + (4J^2 \langle S^z \rangle^2 + \alpha(\Omega_{kl})) (\Omega_{kl} - \Omega_t)^2 (J \langle S^z \rangle - \Omega_{kl} + \Omega_t)}{(\omega_{kl}^{\pm} - \omega_{kl}^{\mp}) / (\omega_{kl}^{\pm} - g_e \mu B_0 - I \langle S^z \rangle) \cdot \prod_{\substack{j \neq l \\ j \neq 4}} (\Omega_{kl} - \Omega_{kj})} \\ \alpha(\Omega_{kl}) &= (\Omega_{kl} - \Omega_b) (J \langle S^z \rangle - \Omega_{kl} + \Omega_t) \end{aligned}$$

$$\begin{aligned} G_{n,n}^{\tau,\tau} &= \sum_{\substack{l=1 \\ l \neq 5}}^7 \left(\frac{b(\omega_{kl}^+)}{\omega - \omega_{kl}^+} + \frac{b(\omega_{kl}^-)}{\omega - \omega_{kl}^-} \right); \quad \tau = (2,4,6,8) \\ b(\omega_{kl}^{\pm}) &= \frac{2J_s^4 \langle S^z \rangle^4 (\Omega_{kl} - \Omega_b) + 2J_s^2 \langle S^z \rangle^2 (\Omega_{kl} - \Omega_t) (J^2 \langle S^z \rangle^2 + 2\alpha(\Omega_{kl})) + (3J^2 \langle S^z \rangle^2 + \alpha(\Omega_{kl})) (\Omega_{kl} - \Omega_t)^2 (J \langle S^z \rangle - \Omega_{kl} + \Omega_t)}{(\omega_{kl}^{\pm} - \omega_{kj}^{\mp}) / (\omega_{kl}^{\pm} - g_e \mu B_0 - I \langle S^z \rangle) \cdot \prod_{\substack{j \neq l \\ j \neq 5}} (\Omega_{kl} - \Omega_{kj})} \end{aligned}$$

$$G_{n,n}^{9,9} = \sum_{l=1}^3 \left(\frac{c(\omega_{kl}^+)}{\omega - \omega_{kl}^+} + \frac{c(\omega_{kl}^-)}{\omega - \omega_{kl}^-} \right); \quad (5)$$

$$c(\omega_{kl}^\pm) = -\frac{4J_s^2 \langle S^z \rangle^2 + (\Omega_{kl} - \Omega_t)(JS + \Omega_{kl} + \Omega_t)}{(\omega_{kl}^\pm - \omega_{kj}^\mp)/(\omega_{kl}^\pm - g_e \mu H_0 - I \langle S^z \rangle) \cdot \prod_{\substack{l=1 \\ j \neq l}}^7 (\Omega_{kl} - \Omega_{kj})}$$

The poles of the Green functions occur at energies, which are the roots of the spin wave dispersion equation for the nanowires under consideration. Note that it was expected to receive in the considering system of the eighteen frequencies. But the expression for fourteen different frequencies are obtained, because of degenerate in four frequencies.

$$\omega_{kl}^\pm = 0.5 \left(\mu H_0 (g_e + g_i) + I(\langle S^z \rangle + \langle s^z \rangle) + \Omega_{kl} \pm \sqrt{(\mu H_0 (g_e - g_i) + I(\langle S^z \rangle - \langle s^z \rangle) - \Omega_{kl})^2 + 4I^2 \langle S^z \rangle \langle s^z \rangle} \right) \quad (6)$$

$$\begin{aligned} \Omega_{k1} &= -2r \cos(\varphi/3) + (J \langle S^z \rangle + 2\Omega_t + \Omega_b)/3, \\ \Omega_{k2} &= 2r \cos((\pi - \varphi)/3) + (J \langle S^z \rangle + 2\Omega_t + \Omega_b)/3, \\ \Omega_{k3} &= 2r \cos((\pi + \varphi)/3) + (J \langle S^z \rangle + 2\Omega_t + \Omega_b)/3, \\ \Omega_{k4} &= \Omega_t + J \langle S^z \rangle, \\ \Omega_{k5} &= \Omega_t, \\ \Omega_{k6} &= 0.5(J \langle S^z \rangle + 2\Omega_t) + 0.5 \langle S^z \rangle \sqrt{J^2 + 8J_s^2}, \\ \Omega_{k7} &= 0.5(J \langle S^z \rangle + 2\Omega_t) - 0.5 \langle S^z \rangle \sqrt{J^2 + 8J_s^2} \end{aligned}$$

where

$$\begin{aligned} r &= \sqrt{3\psi - (J \langle S^z \rangle + 2\Omega_t + \Omega_b)^2}/3, \quad \varphi = \arccos\left(\frac{q}{r^3}\right) \\ q &= (J \langle S^z \rangle + 2\Omega_t + \Omega_b)^3/27 - \psi(J \langle S^z \rangle + 2\Omega_t + \Omega_b)/6 - 2S^2(J_s^2 \Omega_b + J^2 \Omega_t) + \Omega_t \Omega_b (J \langle S^z \rangle + \Omega_t)/2 \\ \psi &= -4 \langle S^z \rangle^2 (J_s^2 + J^2) + J \langle S^z \rangle (\Omega_b + \Omega_t) + 2\Omega_t \Omega_b + \Omega_t^2 \\ \Omega_t &= 2J_s \langle S^z \rangle (2 - \cos ka), \quad \Omega_b = 2J \langle S^z \rangle (3 - \cos ka) \end{aligned}$$

Solving the average spin, we derive the correlation function $\langle S^- S^+ \rangle$ using the spectrum theorem [11,12]

$$\langle S^- S^+ \rangle = -\frac{2S}{N\pi} \sum_k \int_{-\infty}^{\infty} d\omega \frac{\text{Im}G(k, \omega + i\varepsilon)}{e^{\beta\omega} - 1} \quad (7)$$

Here $\beta = 1/k_B T$, k_B is the Boltzmann constant, T is the temperature. Using (5) and the relation $1/(x + i\varepsilon) = P(1/x) - i\pi\delta(x)$ to obtain the imaginary part of the Green functions, one finally obtains [11]

$$\begin{aligned} \langle S_{n,9}^- S_{n,9}^+ \rangle &= -\frac{2S}{N} \sum_k \sum_{l=1}^3 \left(\frac{c(\omega_{kl}^+)}{\exp(\beta\omega_{kl}^+) - 1} + \frac{c(\omega_{kl}^-)}{\exp(\beta\omega_{kl}^-) - 1} \right) \\ \langle S_{n,\tau}^- S_{n,\tau}^+ \rangle &= -\frac{2S}{N} \sum_k \sum_{\substack{l=1 \\ l \neq 4}}^7 \left(\frac{a(\omega_{kl}^+)}{\exp(\beta\omega_{kl}^+) - 1} + \frac{a(\omega_{kl}^-)}{\exp(\beta\omega_{kl}^-) - 1} \right) \quad \tau = 1, 3, 5, 7 \\ \langle S_{n,\tau}^- S_{n,\tau}^+ \rangle &= -\frac{2S}{N} \sum_k \sum_{\substack{l=1 \\ l \neq 5}}^7 \left(\frac{b(\omega_{kl}^+)}{\exp(\beta\omega_{kl}^+) - 1} + \frac{b(\omega_{kl}^-)}{\exp(\beta\omega_{kl}^-) - 1} \right) \quad \tau = 2, 4, 6, 8 \end{aligned} \quad (8)$$

A MICROSCOPIC THEORY OF LOCAL SPIN EXCITATIONS IN A RECTANGULARFERROMAGNETIC SEMICONDUCTOR...

According to the theory of Callen [13] the average spin can be calculated using the following equation

$$\langle S^z \rangle = \frac{(S+1+\Phi)\Phi^{2S+1} + (S-\Phi)(1+\Phi)^{2S+1}}{\Phi^{2S+1} - (1+\Phi)^{2S+1}} \quad (9)$$

where $\Phi = \frac{\langle S^- S^+ \rangle}{2\langle S^z \rangle}$.

Now the equation (8) and (9) can be solved self consistently to obtain the average spin at any given temperature.

If $S = 1/2$ $\langle S^z \rangle = \frac{1}{2} - \langle S^- S^+ \rangle$

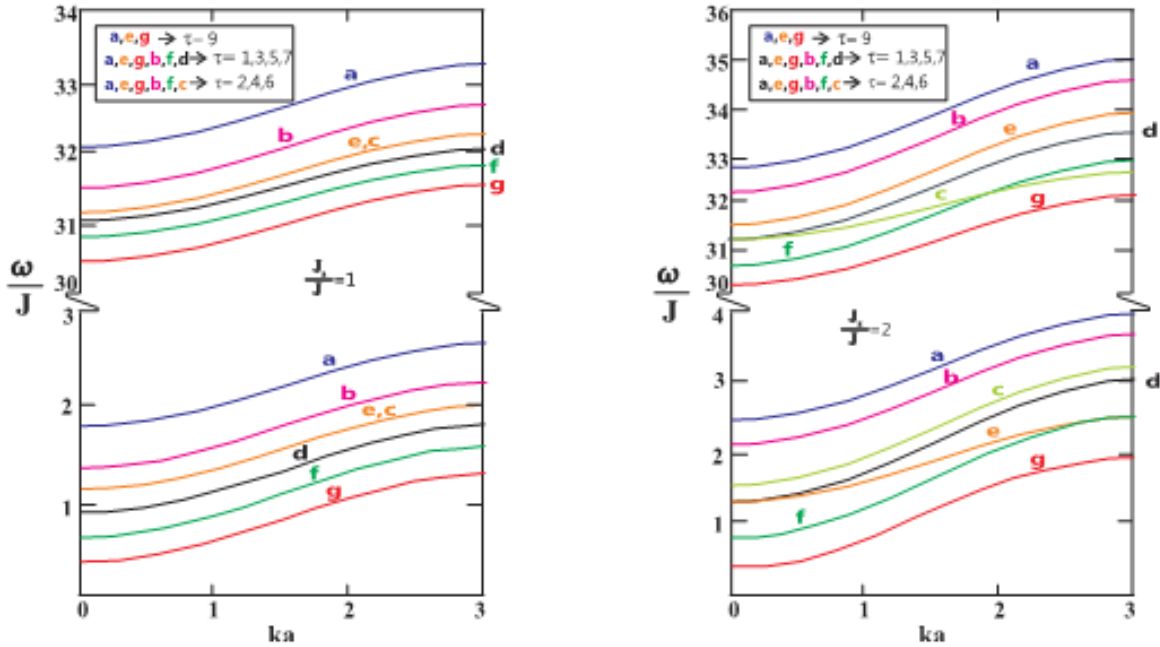


Fig.2. The frequencies of the spin-wave branches plotted versus ka for nanowires under consideration. The parameters are $g\mu_B H_0/J = 0.3$; $g_e\mu_B H_0/J = 0.2$ $\langle S^z \rangle = 0.5$ $\langle s^z \rangle = 0.5$; $I/J = 30$;

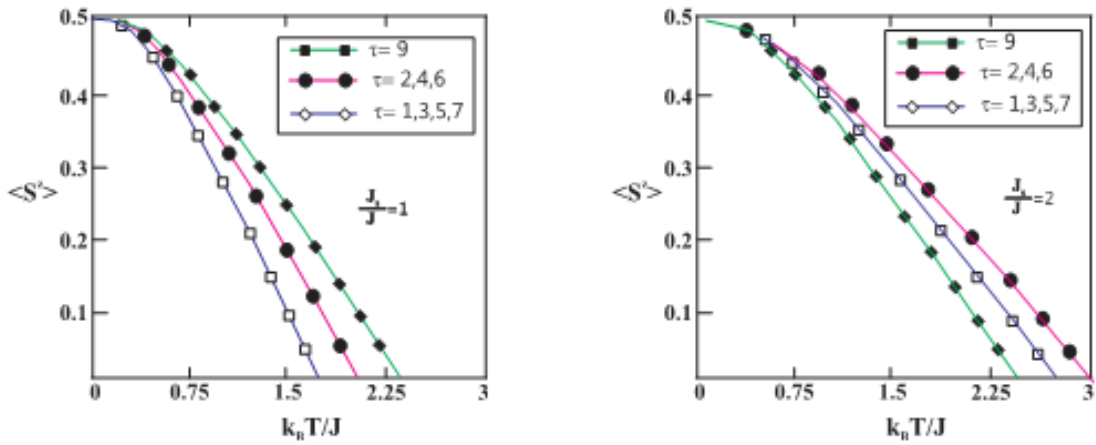


Fig. 3. The temperature dependence of magnetization in the nanowires under consideration. The spontaneous magnetization of the spins at zero temperature is $\langle S^z \rangle = 0.5$. The parameters are $g\mu_B H_0/J = 0.3$; $g_e\mu_B H_0/J = 0.2$ $\langle s^z \rangle = 0.5$; $I/J = 30$;

CONCLUSION

In this section, we present numerical calculations of the theoretical results. Fig. 2 shows the frequencies of the spin-wave branches plotted versus ka for nanowires under consideration. As shown, spin-wave branches appears in two ranges of low and high frequencies. Both the low and high frequencies are minimum at zero wave vector. The spin wave frequencies increase with increasing wave vectors, exchange coupling between between localized spins and also (sd) or (sf) exchange interaction of the spins of the conduction electrons.

The temperature dependence of magnetization in the nanowires under consideration is demonstrated in fig. 3.

The spontaneous magnetization of the spins at zero temperature is $\langle S^z \rangle = 0.5$. In the case $J_s = J$, magnetization of the surface spins labeled $\tau = 1, 3, 5, 7$ are smaller than that of the spins labeled $\tau = 2, 4, 6, 8$, and the bulk spin ($\tau = 9$) magnetization are stronger than that of surface spins. With the increase of the exchange interaction between surface localized spins magnetization are stronger than that of bulk localized spins. Besides the weakening sd (sf) interaction also decreases the local magnetization and tends to zero at lower temperatures.

-
- [1] *So Takei and Victor Galitski* Phys.Rev. B 86, 054521, 2012.
 - [2] *Tudor D. Stănescu, Roman M. Lutchyn, and S. Das Sarma* Phys.Rev. B 84, 144522, 2012.
 - [3] *V.S.Tkachenko, V.V. Kruglyak, A.N. Kuchko* Phys.Rev. B 81, 024425, 2010.
 - [4] *Z. K. Wang, M. H. Kuok, S. C. Ng, D. J. Lockwood, M. G. Cottam, K. Nielsch, R. B. Wehrspohn, and U. Gösele,* Phys. Rev. Lett. v.89, n.2, 027201, 2002.
 - [5] *O.A. Tretiakov and Ar. Abanov* Phys. Rev. Lett. 105, 157201, 2010.
 - [6] *H. Leblond, V. Veerakumar, M. Manna.* Physical Review B 75, 214413, (2007).
 - [7] *T.M. Nguyen and M.G.Cottam.* Phys.Rev. B 71, 094406, 2005.
 - [8] *T.M.Nguyen and M.G.Cottam.* Journal of Magnetism and Magnetic Materials 272-276, p.1672-1673, 2004.
 - [9] *J.M. Wesselinova, E.Kroumova, N. Teofilov, W. Nolting.* Phys. Rev. B57, 11, 1998.
 - [10] *V.A. Tanriverdiyev, V.S. Tagiyev, S.M. Seyid-Rzayeva*, FNT 12, 2003.
 - [11] *H.T. Diep* Phys.Lett. A 138, 69, 1989.
 - [12] *R. Schiller and W. Nolting.* Phys. Rev. B 60, 462–471, 1999.
 - [13] *H.B. Callen.* Phys. Rev. 130 890, 1963.

Received: 11.02.2014

THEORETICAL MODELS OF THE ISOBUTANOL MOLECULE CONFORMATIONS MICROWAVE SPECTRA

**G.I. ISMAILZADEH, I.Z. MOVSUMOV, M.R. MENZELEYEV, A.S. QASANOVA,
S.B. KAZIMOVA**

Institute of Physics of Azerbaijan Republic NSA

Az-1143, Baku, 33 H. Javid ave.

e-mail: mmenzeleyev@gmail.com

The modeling of microwave spectra of the isobutyl alcohol ($\text{CH}_3)_2\text{CHCH}_2\text{OH}$ molecule isomeric forms has been provided. The modeling results in the form of spectral lines list in the MW 10-80GHz frequency range for different conformations are presented.

Keywords: Isobutanol, microwave spectra

PACS: 32.30.Bv; 33.15.Bh

1. INTRODUCTION

Investigation of microwave (MW) absorption spectra of gas-core molecules allows to receive comprehensive and high precision information about such important components of their structure as the values of structural parameters (valence bond lengths, valence angles), dipole moments and its rectangular components along main axes, conformation properties, effects related with slackness of molecular skeleton, dynamics of different symmetry atomic groups intramolecular motion etc.

The study of MW spectra of sufficiently complex molecular structures, especially of complicated by many forms of hyperfine spectra structure, composition of different conformations spectrums and distribution of them for several vibration states always closed with necessity of univocal assignment of extremely big number of spectral lines. Therefore all works intended to reach of this assignment have special actuality and require authentic theoretical basis.

The ones from the numbers of each spectral line main features, determining its identity and allow to provide its identification with sufficient grade of probability, are the value of frequency of corresponding transition and it relative intensity. Thereupon modeling of MW spectra of investigated material on the base of preliminary theoretical calculation of corresponding spectral lines noted parameters is necessary stage of concerned task solution, which make possible to decrease in considerable proportion the number of possible assignments and thereby essentially simplify further experimental investigations.

2. RESULTS OF THEORETICAL RESEARCHES

Alongside with realization of eight possible stable isomeric form the feature of isobutanol molecule ($\text{CH}_3)_2\text{CHCH}_2\text{OH}$ is the number of intramolecular motion degrees of freedom related with presence of two symmetrical (methyl) atomic groups and inversion of asymmetric hydroxyl group. This certainly has to complicate total pattern of its MW spectra. The values of rotational constants (A,B &C) for the process of different isobutanol molecule conformations MW absorption spectra theoretical modeling have been calculated as for the rigid rotator model, i.e. taking into account corresponding spatial configurations and postulated

values of some particular atomic fragments molecular structure parameters [1-5].

The relative intensity of each spectral line determined by corresponding absorption ratio value calculated in accordance with following mathematical equation:

$$\alpha_{max} = 1.23 \cdot 10^{-21} \cdot \sqrt{A \cdot B \cdot C} \cdot v^2 \cdot \mu_g^2 \cdot S_{J_{ke}J_{mn}}^g$$

The v here is the value of rotational transition frequency value, μ_g is adequate (g=a; b; c) dipole moment component, $S_{J_{ke}J_{mn}}^g$ - the value proportional to rotational transition probability, the transition strength, tabulated for each of asymmetry parameter values $\chi=+1; +0.5; -0.5; 1$.

The values used in calculation for each of observed isomeric form of isobutanol molecule are presented in table 1 [6].

Theoretical models of isobutanol molecule different conformations microwave absorption spectra presented in tables 2-5. Taking into account extremely high saturation of conformations spectra and use of rigid rotator model the shown lines are selected only. The selection criteria were corresponding to greatest components of dipole moment and low quantum number value.

3. DISCUSSION

Calculated values of the frequency and intensity of rotational transitions of eight conformational forms of isobutyl alcohol form the basis of the successful identification of experimental studies obtained by swallowing spectra corresponding conformations of the molecule. Comparison of the frequencies of the theoretically predicted transitions with frequencies corresponding spectral lines that allow a high degree of reliability to judge the effects of being here slackness molecular skeleton and their nature. As for the future comparisons of the intensity values calculated from the intensities of the transitions experimentally derived lines, here the most interesting, in our view, is the possibility of obtaining more information interaction mechanism corrective conformational original picture.

This work has been supported by the Science Development Foundation under the President of the Republic of Azerbaijan -Grant № EIF-BGM-2-BRFTF-1-2012/2013-07/04/1.

Table 1

Rotational constants of isobutyl alcohol ($\text{CH}_3\text{CHCH}_2\text{OH}$) molecule isomeric forms

Nº	Conformer	A	B	C	Δ	χ
1	T-t	6242.624620	3983.956018	3171.755311	48.48698812	-0.4710288
2	T-g	6127.823330	4107.103513	3254.305320	50.24241774	-0.40644312
3	T-g'	6225.011060	3998.807669	3178.201711	48.56812657	-0.46133423
4	G-t	7647.817790	3488.776538	2638.033515	19.37166809	-0.6603674
5	G-g	7560.573110	3540.231101	2685.685045	21.42847912	-0.64940895
6	G-g'	7600.749230	3577.008260	2681.487695	19.31224439	-0.6359126
7	G-g''	7631.470217	3494.458987	2637.442032	19.23465968	-0.65678329
8	G-g'''	7642.824724	3494.363588	2648.317504	19.92731945	-0.66120939

Table 2

MW spectra of Trans-trans & Trans-gauche conformers

Tt				Tg													
Transition			Frequency MHz	Intensity cm^{-1}	Transition			Frequency MHz	Intensity cm^{-1}								
1			2	3	4			5	6								
1	1	0	-	0	0	0	10226.58	9.85E-08	2	1	1	-	1	1	0	15575.62	2.00E-07
2	1	1	-	1	0	1	18194.49	4.67E-07	2	1	2	-	1	1	1	13870.02	1.59E-07
2	2	0	-	1	1	0	22082.17	7.82E-07	2	2	0	-	1	0	1	24729.33	1.44E-08
2	0	2	-	1	1	0	11058.02	3.40E-08	2	2	1	-	2	0	2	10006.51	3.91E-09
2	2	1	-	1	1	1	22711.83	7.28E-07	2	0	2	-	1	0	1	14504.78	2.27E-07
3	3	0	-	3	2	2	13453.96	1.17E-07	2	1	2	-	1	0	1	15890.74	2.32E-07
3	3	0	-	2	2	0	34738.56	2.94E-06	2	2	0	-	1	1	1	22708.61	3.89E-07
3	3	0	-	2	0	2	45762.71	1.65E-08	2	0	2	-	1	1	1	12484.06	7.38E-08
3	1	2	-	2	2	0	15596.77	4.73E-08	2	2	1	-	1	1	0	21637.78	4.31E-07
3	1	2	-	2	0	2	26620.93	1.23E-06	3	3	0	-	3	1	3	22416.65	2.53E-09
3	3	1	-	3	2	1	12568.45	1.08E-07	3	3	0	-	2	1	1	40540.75	2.20E-08
3	3	1	-	3	0	3	24945.69	6.57E-09	3	3	1	-	3	1	2	17299.86	4.32E-09
3	3	1	-	2	2	1	34894.66	2.94E-06	3	1	2	-	2	1	1	23204.65	7.80E-07
3	2	1	-	3	1	3	11393.68	6.47E-08	3	3	1	-	2	1	2	43062.90	1.49E-08
3	1	3	-	2	2	1	10932.54	1.03E-08	3	1	3	-	2	1	2	20682.50	6.23E-07
3	2	1	-	2	1	1	29102.22	1.81E-06	3	2	1	-	2	2	0	22876.40	4.81E-07
3	0	3	-	2	1	1	16724.98	1.02E-07	3	2	1	-	2	0	2	33100.95	6.19E-08
3	2	2	-	2	1	2	30679.74	1.47E-06	3	2	2	-	3	0	3	10798.69	1.27E-08
4	4	1	-	4	3	1	18214.74	2.31E-07	3	0	3	-	2	2	0	11067.50	1.16E-09
4	3	1	-	4	2	3	14050.01	1.99E-07	3	0	3	-	2	0	2	21292.05	7.14E-07
4	3	1	-	3	2	1	41670.01	4.78E-06	3	2	2	-	2	2	1	22084.23	4.46E-07
1	2	3	4	5	6	3	54047.25	8.61E-08	3	3	0	-	3	2	1	11384.15	8.75E-08
4	4	1	-	4	1	3	36636.69	4.49E-09	3	3	0	-	3	0	3	23193.05	5.97E-09
4	1	3	-	3	2	1	23248.06	2.57E-07	3	3	0	-	2	2	1	34478.59	1.71E-06
4	1	3	-	3	0	3	35625.30	2.39E-06	3	1	2	-	2	2	1	17142.49	5.59E-08
4	4	0	-	4	3	2	18397.32	2.34E-07	3	3	1	-	3	2	2	12358.12	9.72E-08
4	3	2	-	4	2	2	11566.13	1.63E-07	3	3	1	-	2	2	0	34224.31	1.71E-06
4	3	2	-	4	0	4	26693.53	2.45E-08	3	3	1	-	2	0	2	44448.86	1.81E-08
4	3	2	-	3	2	2	42349.67	4.75E-06	3	2	2	-	3	1	3	10022.28	7.89E-08
4	4	0	-	4	1	4	44582.44	1.53E-09	3	1	3	-	2	2	0	11843.91	8.37E-09
4	2	2	-	4	1	4	14619.00	7.80E-08	3	1	3	-	2	0	2	22068.46	6.46E-07
4	1	4	-	3	2	2	16164.55	4.04E-08	3	2	1	-	2	1	2	31714.99	5.46E-07
4	4	0	-	3	3	0	47293.03	7.47E-06	3	0	3	-	2	1	2	19906.09	4.31E-07
4	4	0	-	3	1	2	66434.81	1.12E-08	3	2	2	-	2	1	1	28146.39	8.08E-07
4	2	2	-	3	3	0	17329.59	3.30E-08	4	3	1	-	4	1	4	25026.75	6.14E-09
4	2	2	-	3	1	2	36471.37	3.65E-06	4	3	1	-	3	3	0	30001.53	8.63E-07
4	0	4	-	3	1	2	21343.97	1.53E-07	4	3	1	-	3	1	2	47337.63	9.22E-08
4	4	1	-	3	3	1	47316.30	7.47E-06	4	3	2	-	4	1	3	16498.77	1.53E-08
4	4	1	-	3	1	3	71278.43	5.22E-09	4	1	3	-	3	3	0	13259.24	7.89E-10
4	2	3	-	3	3	1	15051.56	2.13E-08	4	1	3	-	3	1	2	30595.33	1.87E-06
4	2	3	-	3	1	3	39013.68	2.59E-06	4	3	2	-	3	3	1	29794.25	8.51E-07
5	5	0	-	5	4	2	23610.61	3.94E-07	4	3	2	-	3	1	3	52174.65	4.27E-08

THEORETICAL MODELS OF THE ISOBUTANOL MOLECULE CONFORMATIONS MICROWAVE SPECTRA

1					2	3	4				5	6					
5	5	0	-	5	2	4	56683.07	2.19E-09	4	1	4	-	3	1	3	27391.43	1.52E-06
5	5	0	-	4	4	0	59789.86	1.51E-05	4	4	0	-	4	2	3	29715.09	4.70E-09
5	4	2	-	5	3	2	17722.75	3.85E-07	4	4	0	-	3	2	1	57978.17	3.42E-08
5	3	2	-	5	2	4	15349.71	2.58E-07	4	4	0	-	3	0	3	69787.07	8.53E-10
5	3	2	-	4	4	0	18456.51	2.76E-08	4	4	1	-	4	2	2	27059.24	4.86E-09
5	3	2	-	4	2	2	48419.95	7.60E-06	4	2	2	-	3	2	1	30913.96	1.59E-06
5	3	2	-	4	0	4	63547.35	2.00E-07	4	2	2	-	3	0	3	42722.86	1.21E-07
5	4	2	-	5	1	4	36081.20	2.39E-08	4	4	1	-	4	0	4	41982.11	3.03E-10
5	1	4	-	4	2	2	30061.50	6.32E-07	4	2	3	-	4	0	4	12271.98	2.64E-08
5	1	4	-	4	0	4	45188.90	3.88E-06	4	0	4	-	3	2	1	15991.09	3.89E-09
5	5	1	-	5	4	1	23582.40	3.93E-07	4	0	4	-	3	0	3	27800.00	1.60E-06
5	5	1	-	5	2	3	52069.28	2.73E-09	4	4	1	-	3	2	2	58983.41	3.31E-08
5	5	1	-	5	0	5	71435.50	1.30E-10	4	2	3	-	3	2	2	29273.28	1.40E-06
5	5	1	-	4	4	1	59792.68	1.51E-05	4	4	0	-	4	3	1	16592.48	1.83E-07
5	4	1	-	5	3	3	18424.28	4.07E-07	4	3	1	-	4	2	2	10471.73	1.47E-07
5	3	3	-	5	2	3	10062.60	1.79E-07	4	3	1	-	4	0	4	25394.59	1.93E-08
5	3	3	-	5	0	5	29428.82	4.95E-08	4	3	1	-	3	2	2	42395.90	2.33E-06
5	3	3	-	4	4	1	17786.00	2.52E-08	4	4	0	-	4	1	3	33334.78	4.64E-09
5	3	3	-	4	2	3	50050.74	7.28E-06	4	1	3	-	3	2	2	25653.60	3.50E-07
5	4	1	-	5	1	5	47618.07	5.26E-09	4	4	1	-	4	3	2	16831.04	1.88E-07
5	2	3	-	5	1	5	19131.19	8.49E-08	4	3	2	-	4	2	3	12879.09	1.87E-07
4	4	1	-	5	1	5	11407.79	1.88E-11	4	3	2	-	3	2	1	41142.16	2.37E-06
5	1	5	-	4	2	3	20856.96	8.45E-08	4	3	2	-	3	0	3	52951.06	9.54E-08
5	4	1	-	4	3	1	54425.02	1.06E-05	4	4	1	-	4	1	4	41614.27	1.38E-09
5	4	1	-	4	1	3	72846.97	6.93E-08	4	2	3	-	4	1	4	11904.14	1.33E-07
5	2	3	-	4	3	1	25938.14	2.00E-07	4	1	4	-	3	2	1	16358.93	1.84E-08
5	2	3	-	4	1	3	44360.09	6.40E-06	4	1	4	-	3	0	3	28167.83	1.47E-06
5	0	5	-	4	1	3	24993.87	1.78E-07	4	4	0	-	3	3	1	46630.25	4.47E-06
5	4	2	-	4	3	2	54576.57	1.06E-05	4	4	0	-	3	1	3	69010.66	5.34E-09
5	2	4	-	4	3	2	21504.11	9.68E-08	4	2	2	-	3	3	1	19566.05	3.85E-08
5	2	4	-	4	1	4	47689.24	4.09E-06	4	2	2	-	3	1	3	41946.45	6.09E-07
6	6	1	-	6	5	1	28873.42	5.94E-07	4	0	4	-	3	1	3	27023.59	1.28E-06
6	5	1	-	6	4	3	23491.37	6.99E-07	4	4	1	-	3	3	0	46589.05	4.47E-06
6	5	1	-	6	2	5	57946.11	8.99E-09	4	4	1	-	3	1	2	63925.15	1.30E-08
6	5	1	-	5	4	1	66986.19	1.99E-05	4	2	3	-	3	3	0	16878.92	2.27E-08
6	6	1	-	6	3	3	69095.66	2.24E-09	4	2	3	-	3	1	2	34215.02	1.41E-06
6	4	3	-	6	3	3	16730.86	4.64E-07	5	5	0	-	5	3	3	38443.13	6.34E-09
6	3	3	-	6	2	5	17723.87	2.95E-07	5	5	0	-	5	1	5	66469.87	3.70E-11
6	3	3	-	5	4	1	26763.95	1.49E-07	5	5	0	-	4	3	1	75457.24	5.40E-08
6	3	3	-	5	2	3	55250.83	1.18E-05	5	5	1	-	5	3	2	37546.82	6.23E-09
6	3	3	-	5	0	5	74617.05	2.69E-07	5	3	2	-	5	1	5	28922.44	8.69E-09
6	4	3	-	6	1	5	36282.49	7.05E-08	5	3	2	-	4	3	1	37909.80	2.51E-06
6	1	5	-	5	2	3	35699.20	9.58E-07	5	3	2	-	4	1	3	54652.10	2.51E-07
6	1	5	-	5	0	5	55065.42	5.74E-06	5	5	1	-	5	1	4	54573.60	2.46E-10
6	6	0	-	6	5	2	28877.15	5.94E-07	5	3	3	-	5	1	4	16131.08	3.53E-08
6	5	2	-	6	4	2	23353.24	6.92E-07	5	1	4	-	5	1	5	11895.66	3.57E-08
6	5	2	-	6	2	4	50220.17	1.43E-08	5	1	4	-	4	3	1	20883.03	7.50E-09
6	5	2	-	6	0	6	75116.75	5.81E-10	5	1	4	-	4	1	3	37625.32	3.52E-06
6	5	2	-	5	4	2	67010.37	1.99E-05	5	5	1	-	4	3	2	75700.15	5.40E-08
6	6	0	-	6	3	4	70902.62	2.21E-09	5	3	3	-	4	3	2	37257.63	2.42E-06
6	4	2	-	6	3	4	18672.24	5.38E-07	5	3	3	-	4	1	4	62040.86	7.94E-08
6	3	4	-	6	0	6	33091.27	7.49E-08	5	1	5	-	4	1	4	34014.11	2.98E-06
6	3	4	-	5	4	2	24984.89	1.23E-07	5	4	1	-	5	2	4	30717.17	1.35E-08
6	3	4	-	5	2	4	58057.35	1.06E-05	5	4	1	-	4	4	0	37327.36	1.37E-06
6	4	2	-	6	1	6	51662.53	1.02E-08	5	4	1	-	4	2	2	64391.57	1.09E-07
6	2	4	-	6	1	6	24795.60	9.06E-08	5	4	1	-	4	0	4	79314.43	4.17E-09
6	1	6	-	5	2	4	25067.06	1.34E-07	5	4	2	-	5	2	3	25480.63	1.57E-08
6	6	0	-	5	5	0	72276.91	2.67E-05	5	2	3	-	4	4	0	11803.21	2.11E-10
6	4	2	-	5	5	0	20046.52	2.67E-08	5	2	3	-	4	2	2	38867.42	3.50E-06
6	4	2	-	5	3	2	61379.87	1.47E-05	5	2	3	-	4	0	4	53790.29	1.52E-07
6	4	2	-	5	1	4	79738.32	2.52E-07	5	4	2	-	5	0	5	45044.56	1.13E-09
6	2	4	-	5	3	2	34512.95	6.81E-07	5	2	4	-	5	0	5	14370.91	4.48E-08
6	2	4	-	5	1	4	52871.40	9.94E-06	5	0	5	-	4	2	2	19303.49	4.47E-09
5	5	0	-	6	0	6	31716.99	5.15E-12	5	0	5	-	4	0	4	34226.35	3.04E-06
6	0	6	-	5	1	4	27974.82	1.95E-07	5	4	2	-	4	4	1	37288.81	1.36E-06
6	6	1	-	5	5	1	72277.21	2.67E-05	5	4	2	-	4	2	3	66998.93	9.50E-08

1						2	3	4				5	6				
6	4	3	-	5	5	1	19912.42	2.63E-08	5	2	4	-	4	2	3	36325.28	2.97E-06
6	4	3	-	5	3	3	61919.10	1.47E-05	5	5	0	-	5	4	1	21537.40	3.10E-07
5	5	1	-	6	2	5	14542.32	2.82E-11	5	5	0	-	5	2	3	47061.54	2.85E-09
6	2	5	-	5	3	3	27464.36	2.36E-07	5	5	0	-	5	0	5	66625.48	1.29E-10
6	2	5	-	5	1	5	56658.15	5.95E-06	5	5	0	-	4	4	1	58869.72	9.18E-06
7	7	0	-	7	6	2	34149.51	8.30E-07	5	4	1	-	5	3	2	16010.04	3.23E-07
7	6	2	-	7	5	2	28721.61	1.07E-06	5	3	2	-	5	0	5	29078.04	3.07E-08
7	5	2	-	7	4	4	23378.00	9.35E-07	5	3	2	-	4	4	1	21322.29	3.32E-08
7	5	2	-	7	2	6	59932.41	2.16E-08	5	3	2	-	4	2	3	51032.41	2.79E-06
7	5	2	-	6	6	0	21891.44	2.69E-08	5	4	1	-	5	1	4	33036.81	2.39E-08
7	5	2	-	6	4	2	74121.83	2.58E-05	5	1	4	-	5	0	5	12051.27	1.61E-07
7	6	2	-	7	3	4	67216.42	1.02E-08	5	1	4	-	4	2	3	34005.64	1.20E-06
7	4	4	-	7	3	4	15116.81	4.72E-07	5	5	1	-	5	4	2	21580.30	3.11E-07
7	3	4	-	7	2	6	21437.60	3.13E-07	5	5	1	-	5	2	4	52253.95	2.10E-09
6	6	0	-	7	3	4	16603.37	2.59E-11	5	5	1	-	4	4	0	58864.14	9.18E-06
7	3	4	-	6	4	2	35627.01	4.85E-07	5	4	2	-	5	3	3	16862.21	3.50E-07
7	3	4	-	6	2	4	62493.94	1.77E-05	5	3	3	-	5	2	4	13811.44	2.87E-07
7	4	4	-	7	1	6	37541.39	1.43E-07	5	3	3	-	4	4	0	20421.63	2.95E-08
6	6	0	-	7	1	6	39027.96	5.78E-12	5	3	3	-	4	2	2	47485.83	3.15E-06
7	1	6	-	6	4	2	13202.43	2.53E-09	5	3	3	-	4	0	4	62408.70	2.39E-07
7	1	6	-	6	2	4	40069.36	1.09E-06	5	4	2	-	5	1	5	44888.96	4.54E-09
7	1	6	-	6	0	6	64965.93	8.00E-06	5	2	4	-	5	1	5	14215.31	2.05E-07
7	7	1	-	7	6	1	34149.07	8.30E-07	5	1	5	-	4	2	2	19459.09	1.80E-08
7	6	1	-	7	5	3	28743.65	1.07E-06	5	1	5	-	4	0	4	34381.95	2.88E-06
7	5	3	-	7	4	3	22892.32	9.04E-07	5	4	1	-	4	3	2	54163.37	5.72E-06
7	5	3	-	7	2	5	48450.48	4.73E-08	5	4	1	-	4	1	4	78946.59	1.92E-08
7	5	3	-	7	0	7	79841.89	1.37E-09	5	2	3	-	4	3	2	28639.22	2.25E-07
7	5	3	-	6	6	1	21869.87	2.68E-08	5	2	3	-	4	1	4	53422.45	6.10E-07
7	5	3	-	6	4	3	74234.67	2.59E-05	5	0	5	-	4	1	4	33858.51	2.75E-06
7	6	1	-	7	3	5	71034.10	9.64E-09	5	4	2	-	4	3	1	53876.32	5.70E-06
7	4	3	-	7	3	5	19398.13	6.35E-07	5	4	2	-	4	1	3	70618.62	8.16E-08
7	3	5	-	7	0	7	37551.44	9.77E-08	5	2	4	-	4	3	1	23202.67	8.31E-08
6	6	1	-	7	3	5	20420.58	3.31E-11	5	2	4	-	4	1	3	39944.96	2.39E-06
7	3	5	-	6	4	3	31944.22	3.35E-07	6	5	1	-	6	3	4	38537.52	1.90E-08
7	3	5	-	6	2	5	66398.96	1.46E-05	6	5	1	-	6	1	6	70624.43	1.45E-10
7	4	3	-	7	1	7	56908.26	1.42E-08	6	5	1	-	5	5	0	44733.97	1.98E-06
7	2	5	-	7	1	7	31350.10	9.90E-08	6	5	2	-	6	3	3	36206.02	1.85E-08
6	6	1	-	7	1	7	57930.71	6.23E-13	6	3	3	-	6	1	6	34411.80	8.84E-09
7	1	7	-	6	2	5	28888.83	1.83E-07	6	3	3	-	5	3	2	46068.77	5.20E-06
7	6	1	-	6	5	1	79486.95	3.34E-05	6	3	3	-	5	1	4	63095.54	4.75E-07
7	4	3	-	6	5	1	27850.98	1.33E-07	6	5	2	-	6	1	5	55040.55	1.48E-09
7	4	3	-	6	3	3	68073.22	2.00E-05	6	3	4	-	6	1	5	16509.65	6.51E-08
7	2	5	-	6	3	3	42515.05	1.60E-06	6	1	5	-	6	1	6	15577.27	6.06E-08
7	2	5	-	6	1	5	62066.68	1.41E-05	5	5	0	-	6	1	5	10313.20	2.59E-12
6	5	1	-	7	0	7	29098.60	1.65E-11	6	1	5	-	5	3	2	27234.24	2.31E-08
7	0	7	-	6	3	3	11123.64	9.27E-10	6	1	5	-	5	1	4	44261.01	5.77E-06
7	0	7	-	6	1	5	30675.27	2.18E-07	6	5	2	-	5	5	1	44727.97	1.98E-06
7	6	2	-	6	5	2	79490.19	3.34E-05	6	3	4	-	5	3	3	44639.58	4.83E-06
7	4	4	-	6	5	2	27390.58	1.28E-07	6	3	4	-	5	1	5	72666.33	1.18E-07
7	4	4	-	6	3	4	69416.06	2.00E-05	5	5	1	-	6	1	6	25889.85	9.74E-13
7	2	6	-	6	3	4	32861.65	4.18E-07	6	1	6	-	5	3	3	12552.67	4.02E-10
7	2	6	-	6	1	6	65851.94	8.18E-06	6	1	6	-	5	1	5	40579.41	5.12E-06
8	8	1	-	8	7	1	39420.96	1.10E-06	6	6	0	-	6	4	3	47843.24	7.83E-09
8	7	1	-	8	6	3	34025.89	1.52E-06	6	6	1	-	6	4	2	47635.73	7.79E-09
8	6	3	-	8	5	3	28467.81	1.45E-06	6	4	2	-	6	2	5	32512.56	2.46E-08
8	5	3	-	8	4	5	23370.60	1.11E-06	6	4	2	-	5	4	1	45024.56	3.66E-06
8	5	3	-	8	2	7	62829.03	3.86E-08	6	4	2	-	5	2	3	70548.70	2.66E-07
8	5	3	-	7	6	1	29482.37	1.28E-07	6	6	1	-	6	2	4	71624.57	1.09E-10
8	6	3	-	8	3	5	64776.19	3.04E-08	6	4	3	-	6	2	4	23781.40	3.53E-08
8	4	5	-	8	3	5	12937.78	4.27E-07	6	2	4	-	5	4	1	21035.73	3.10E-09
8	3	5	-	8	2	7	26520.65	3.22E-07	6	2	4	-	5	2	3	46559.87	6.26E-06
8	3	5	-	7	4	3	44809.96	1.25E-06	6	2	4	-	5	0	5	66123.80	1.63E-07
8	3	5	-	7	2	5	70368.12	2.48E-05	6	4	3	-	6	0	6	49231.44	2.23E-09
8	4	5	-	8	1	7	39943.94	2.25E-07	6	2	5	-	6	0	6	16926.31	6.83E-08
7	6	1	-	8	1	7	33832.17	2.57E-11	6	0	6	-	5	2	3	21109.83	3.34E-09
8	1	7	-	7	4	3	17803.80	7.04E-09	6	0	6	-	5	0	5	40673.77	5.15E-06

THEORETICAL MODELS OF THE ISOBUTANOL MOLECULE CONFORMATIONS MICROWAVE SPECTRA

1					2	3	4				5	6					
8	1	7	-	7	2	5	43361.96	1.09E-06	6	4	3	-	5	4	2	44860.65	3.63E-06
8	1	7	-	7	0	7	74753.37	1.06E-05	6	4	3	-	5	2	4	75534.30	1.89E-07
8	8	0	-	8	7	2	39421.01	1.10E-06	6	2	5	-	5	4	2	12555.52	4.36E-10
8	7	2	-	8	6	2	34022.81	1.52E-06	6	2	5	-	5	2	4	43229.17	5.28E-06
8	6	2	-	8	5	4	28560.89	1.45E-06	6	6	0	-	6	5	1	26388.99	4.65E-07
8	5	4	-	8	4	4	22017.54	1.02E-06	6	5	1	-	6	4	2	21246.81	5.69E-07
8	5	4	-	8	2	6	47180.06	1.21E-07	6	5	1	-	6	2	4	45235.64	1.52E-08
8	5	4	-	7	6	2	29392.78	1.27E-07	6	5	1	-	6	0	6	70685.68	5.31E-10
8	6	2	-	8	3	6	71536.89	2.55E-08	6	5	1	-	5	4	2	66314.89	1.12E-05
8	4	4	-	8	3	6	20958.46	7.01E-07	6	6	0	-	6	3	3	62601.63	2.25E-09
8	3	6	-	8	0	8	42656.32	1.18E-07	6	4	2	-	6	3	3	14965.83	4.20E-07
7	6	2	-	8	3	6	13583.22	7.10E-11	6	3	3	-	6	0	6	34473.04	3.26E-08
8	3	6	-	7	4	4	38516.39	6.75E-07	6	3	3	-	5	4	2	30102.25	1.68E-07
8	3	6	-	7	2	6	75070.80	1.94E-05	6	3	3	-	5	2	4	60775.90	2.91E-06
8	4	4	-	8	1	8	63598.46	1.53E-08	6	4	2	-	6	1	5	33800.36	6.37E-08
8	2	6	-	8	1	8	38435.93	1.12E-07	6	1	5	-	6	0	6	15638.51	2.62E-07
7	6	2	-	8	1	8	56223.22	2.57E-12	6	1	5	-	5	4	2	11267.72	8.32E-10
8	1	8	-	7	2	6	32430.81	2.32E-07	6	1	5	-	5	2	4	41941.37	2.96E-06
8	6	2	-	7	7	0	23804.15	2.74E-08	6	6	1	-	6	5	2	26395.54	4.65E-07
7	7	0	-	8	4	4	26774.27	3.27E-11	6	5	2	-	6	4	3	21447.63	5.78E-07
8	4	4	-	7	5	2	36096.85	3.96E-07	6	5	2	-	6	2	5	53752.76	8.38E-09
8	4	4	-	7	3	4	74591.66	2.71E-05	6	5	2	-	5	4	1	66264.75	1.12E-05
7	7	0	-	8	2	6	51936.79	2.87E-12	6	6	1	-	6	3	4	64926.44	2.19E-09
8	2	6	-	7	5	2	10934.33	8.21E-10	6	4	3	-	6	3	4	17083.28	5.07E-07
8	2	6	-	7	3	4	49429.14	2.68E-06	6	3	4	-	6	2	5	15221.85	4.08E-07
8	2	6	-	7	1	6	71853.72	1.87E-05	6	3	4	-	5	4	1	27733.85	1.29E-07
7	5	2	-	8	0	8	27517.93	2.98E-11	6	3	4	-	5	2	3	53258.00	4.18E-06
8	0	8	-	7	3	4	10976.88	5.75E-10	6	3	4	-	5	0	5	72821.93	4.02E-07
8	0	8	-	7	1	6	33401.47	2.50E-07	6	4	3	-	6	1	6	49170.19	8.57E-09
8	6	3	-	7	7	1	23801.12	2.74E-08	6	2	5	-	6	1	6	16865.06	2.97E-07
7	7	1	-	8	4	5	28037.29	3.51E-11	6	1	6	-	5	2	3	21171.08	1.28E-08
8	4	5	-	7	5	3	34855.42	3.62E-07	6	1	6	-	5	0	5	40735.01	5.02E-06
8	4	5	-	7	3	5	77145.87	2.64E-05	6	6	0	-	5	5	1	71123.58	1.63E-05
7	7	1	-	8	2	7	67495.73	8.86E-13	6	4	2	-	5	5	1	23487.77	3.30E-08
8	2	7	-	7	3	5	37687.44	6.12E-07	6	4	2	-	5	3	3	61930.29	6.94E-06
8	2	7	-	7	1	7	75197.57	1.07E-05	6	2	4	-	5	3	3	37941.46	7.87E-07
9	9	0	-	9	8	2	44691.40	1.40E-06	6	2	4	-	5	1	5	65968.20	6.08E-07
9	8	2	-	9	7	2	39307.17	2.03E-06	5	5	1	-	6	0	6	25951.09	3.58E-12
9	7	2	-	9	6	4	33851.34	2.08E-06	6	0	6	-	5	3	3	12491.42	1.45E-09
9	7	2	-	8	8	0	25734.75	2.80E-08	6	0	6	-	5	1	5	40518.17	4.96E-06
9	6	4	-	9	5	4	28034.94	1.72E-06	6	6	1	-	5	5	0	71122.89	1.63E-05
9	5	4	-	9	4	6	23656.64	1.24E-06	6	4	3	-	5	5	0	23279.73	3.23E-08
9	5	4	-	9	2	8	66835.84	5.52E-08	6	4	3	-	5	3	2	60827.17	6.93E-06
8	8	0	-	9	5	4	36151.53	3.47E-11	6	4	3	-	5	1	4	77853.94	2.96E-07
9	5	4	-	8	6	2	37292.29	3.65E-07	6	2	5	-	5	3	2	28522.04	1.43E-07
9	6	4	-	9	3	6	62081.02	7.58E-08	6	2	5	-	5	1	4	45548.81	3.99E-06
9	4	6	-	9	3	6	10389.44	3.47E-07	7	7	0	-	7	5	3	57458.55	9.26E-09
9	3	6	-	9	2	8	32789.76	3.34E-07	7	7	1	-	7	5	2	57420.15	9.26E-09
8	8	0	-	9	3	6	70197.61	1.09E-12	7	5	2	-	7	3	5	38993.87	3.75E-08
9	3	6	-	8	4	4	53824.63	2.72E-06	7	5	2	-	7	1	7	75859.45	3.08E-10
9	3	6	-	8	2	6	78987.16	3.28E-05	7	5	2	-	6	5	1	52348.01	5.03E-06
8	4	6	-	9	1	8	43402.47	3.02E-07	7	5	3	-	7	3	4	34231.82	3.76E-08
9	6	2	-	9	1	8	29766.83	5.74E-11	7	3	4	-	7	1	7	41589.24	7.47E-09
9	1	8	-	8	4	4	20811.59	1.02E-08	7	3	4	-	6	5	1	18077.80	9.72E-10
9	1	8	-	8	2	6	45974.12	1.09E-06	7	3	4	-	6	3	3	54290.44	9.17E-06
9	9	1	-	9	8	1	44691.40	1.40E-06	7	3	4	-	6	1	5	73124.96	6.37E-07
9	8	1	-	9	7	3	39307.56	2.03E-06	7	5	3	-	7	1	6	56704.78	4.30E-09
9	7	3	-	9	6	3	33836.20	2.08E-06	7	3	5	-	7	1	6	17749.29	1.04E-07
9	7	3	-	8	8	1	25734.36	2.80E-08	7	1	6	-	7	1	7	19116.29	9.20E-08
9	6	3	-	9	5	5	28347.09	1.75E-06	7	1	6	-	6	3	3	31817.48	3.29E-08
9	5	5	-	9	4	5	20527.58	1.02E-06	7	1	6	-	6	1	5	50652.01	8.75E-06
9	5	5	-	9	2	7	46838.50	2.48E-07	7	5	3	-	6	5	2	52316.23	5.03E-06
8	8	1	-	9	5	5	36448.93	3.51E-11	7	3	5	-	6	5	2	13360.75	4.10E-10
9	5	5	-	8	6	3	36997.92	3.58E-07	7	3	5	-	6	3	4	51891.65	8.18E-06
9	6	3	-	9	3	7	72606.97	5.18E-08	6	5	2	-	7	1	7	23504.83	2.74E-12
9	4	5	-	9	3	7	23732.30	7.35E-07	7	1	7	-	6	3	4	15026.07	6.03E-10

1			2	3	4			5	6
9	3	7	-	9 0 9	48248.16	1.36E-07	7 1 7 - 6 1 6	47112.99	8.05E-06
9	3	7	-	8 4 5	44576.46	1.11E-06	7 6 1 - 7 4 4	47567.89	2.35E-08
9	4	5	-	9 1 9	71974.18	1.33E-08	7 6 1 - 6 6 0	52159.82	2.70E-06
9	2	7	-	9 1 9	45663.25	1.29E-07	7 6 2 - 7 4 3	46866.11	2.31E-08
8	6	3	-	9 1 9	55503.83	5.81E-12	7 4 3 - 7 2 6	35445.72	3.37E-08
9	1	9	-	8 2 7	35793.01	2.80E-07	7 4 3 - 6 4 2	52928.60	7.09E-06
9	6	3	-	8 7 1	31319.12	1.26E-07	7 4 3 - 6 2 4	76917.43	5.73E-07
8	7	1	-	9 4 5	17555.55	7.51E-11	7 6 2 - 7 2 5	69903.77	8.16E-10
9	4	5	-	8 5 3	44938.16	9.39E-07	7 4 4 - 7 2 5	22336.79	6.71E-08
8	7	1	-	9 2 7	43866.47	1.86E-11	7 2 5 - 7 2 6	12408.06	6.94E-08
9	2	7	-	8 5 3	18627.23	6.06E-09	6 6 0 - 7 2 5	17744.86	2.19E-12
9	2	7	-	8 3 5	54935.61	3.36E-06	7 2 5 - 6 4 2	29890.94	1.79E-08
8	5	3	-	9 0 9	27042.30	4.04E-11	7 2 5 - 6 2 4	53879.77	9.84E-06
9	0	9	-	8 1 7	36272.24	2.89E-07	7 2 5 - 6 0 6	79329.81	1.72E-07
9	6	4	-	8 7 2	31304.42	1.26E-07	7 4 4 - 7 0 7	54515.35	3.22E-09
8	7	2	-	9 4 6	20387.16	9.45E-11	7 2 6 - 7 0 7	19770.50	9.71E-08
9	4	6	-	8 5 4	42196.53	7.78E-07	6 6 0 - 7 0 7	49923.42	1.32E-13
8	7	2	-	9 2 8	63566.35	4.53E-12	7 0 7 - 6 2 4	21701.22	2.19E-09
9	2	8	-	8 3 6	41993.34	7.93E-07	7 0 7 - 6 0 6	47151.25	8.07E-06
10	10	1	-	10 9 1	49961.01	1.73E-06	7 6 2 - 6 6 1	52158.98	2.70E-06
10	9	1	-	10 8 3	44585.66	2.60E-06	7 4 4 - 6 4 3	52435.17	6.95E-06
10	8	3	-	10 7 3	39148.80	2.81E-06	6 6 1 - 7 2 6	30152.85	1.47E-12
10	7	3	-	10 6 5	33619.49	2.54E-06	7 2 6 - 6 4 3	17690.31	1.53E-09
10	7	3	-	9 8 1	33214.55	1.25E-07	7 2 6 - 6 2 5	49995.44	8.40E-06
10	6	5	-	10 5 5	27285.94	1.87E-06	7 7 0 - 7 6 1	31219.36	6.47E-07
10	5	5	-	10 4 7	24529.17	1.33E-06	7 7 0 - 7 4 3	78086.38	2.10E-09
10	5	5	-	10 2 9	72185.51	6.51E-08	7 6 1 - 7 5 2	26200.81	8.67E-07
9	8	1	-	10 5 5	27690.88	1.05E-10	7 5 2 - 7 4 3	20666.21	7.78E-07
10	5	5	-	9 6 3	45452.89	8.18E-07	7 5 2 - 7 2 5	43703.88	5.04E-08
10	6	5	-	10 3 7	59548.31	1.69E-07	7 5 2 - 7 0 7	75882.43	1.15E-09
10	3	7	-	10 2 9	39923.14	3.58E-07	7 5 2 - 6 6 1	25959.08	3.42E-08
9	8	1	-	10 3 7	59953.25	8.34E-12	7 5 2 - 6 4 3	73802.25	1.33E-05
10	3	7	-	9 6 3	13190.52	1.13E-09	7 6 1 - 7 3 4	60471.02	1.05E-08
10	3	7	-	9 4 5	62065.19	4.87E-06	7 4 3 - 7 3 4	13603.99	4.82E-07
10	4	7	-	10 1 9	47754.16	3.68E-07	7 3 4 - 7 0 7	41612.22	2.80E-08
9	6	3	-	10 1 9	26830.45	8.97E-11	7 3 4 - 6 4 3	39532.04	5.28E-07
10	1	9	-	9 4 5	22044.23	9.01E-09	7 3 4 - 6 2 5	71837.17	2.77E-06
10	1	9	-	9 2 7	48355.15	1.12E-06	7 4 3 - 7 1 6	36076.95	1.09E-07
10	10	0	-	10 9 2	49961.01	1.73E-06	7 2 5 - 7 1 6	13039.29	3.82E-07
10	9	2	-	10 8 2	44585.62	2.60E-06	7 1 6 - 7 0 7	19139.27	3.88E-07
10	8	2	-	10 7 4	39151.00	2.81E-06	6 6 1 - 7 1 6	30784.08	4.69E-12
10	7	4	-	10 6 4	33560.67	2.54E-06	7 1 6 - 6 4 3	17059.08	4.35E-09
10	7	4	-	9 8 2	33212.40	1.25E-07	7 1 6 - 6 2 5	49364.21	5.73E-06
10	6	4	-	10 5 6	28161.82	1.98E-06	7 7 1 - 7 6 2	31220.26	6.47E-07
10	5	6	-	10 4 6	18329.55	9.23E-07	7 7 1 - 7 4 4	78787.24	2.11E-09
10	5	6	-	10 2 8	47719.45	4.13E-07	7 6 2 - 7 5 3	26238.28	8.69E-07
9	8	2	-	10 5 6	28510.09	1.10E-10	7 5 3 - 7 4 4	21328.69	8.20E-07
10	5	6	-	9 6 4	44648.42	7.82E-07	7 5 3 - 7 2 6	56073.55	1.94E-08
10	6	4	-	10 3 8	74451.82	8.74E-08	7 5 3 - 6 6 0	25920.63	3.41E-08
10	4	6	-	10 3 8	27960.46	7.45E-07	7 5 3 - 6 4 2	73556.43	1.32E-05
10	3	8	-	10 0 10	54179.30	1.53E-07	7 6 2 - 7 3 5	65193.77	9.42E-09
9	8	2	-	10 3 8	74800.09	4.33E-12	7 4 4 - 7 3 5	17626.79	6.73E-07
10	3	8	-	9 4 6	50050.00	1.58E-06	7 3 5 - 7 2 6	17118.06	5.61E-07
10	2	8	-	10 1 10	52747.48	1.48E-07	6 6 0 - 7 3 5	13034.86	1.57E-11
9	6	4	-	10 1 10	55818.50	9.61E-12	7 3 5 - 6 4 2	34600.94	3.03E-07
10	1	10	-	9 2 8	39052.27	3.29E-07	7 3 5 - 6 2 4	58589.77	5.69E-06
10	8	2	-	9 9 0	27672.00	2.86E-08	7 4 4 - 7 1 7	54492.37	1.22E-08
9	9	0	-	10 6 4	45039.67	3.40E-11	7 2 6 - 7 1 7	19747.52	4.10E-07
10	6	4	-	9 7 2	38958.90	3.51E-07	6 6 0 - 7 1 7	49900.44	4.99E-13
10	4	6	-	9 5 4	54353.81	1.98E-06	7 1 7 - 6 2 4	21724.20	8.26E-09
9	7	2	-	10 2 8	36922.37	5.73E-11	7 1 7 - 6 0 6	47174.23	8.05E-06
10	2	8	-	9 5 4	24963.91	1.95E-08	7 6 1 - 6 5 2	78555.43	1.92E-05
10	2	8	-	9 3 6	59009.99	3.47E-06	7 4 3 - 6 5 2	31688.41	1.53E-07
9	5	4	-	10 0 10	27785.94	4.63E-11	7 4 3 - 6 3 4	70219.31	7.85E-06
10	0	10	-	9 1 8	39273.18	3.33E-07	7 2 5 - 6 3 4	47181.65	2.14E-06
10	8	3	-	9 9 1	27671.95	2.86E-08	7 2 5 - 6 1 6	79268.56	6.33E-07

THEORETICAL MODELS OF THE ISOBUTANOL MOLECULE CONFORMATIONS MICROWAVE SPECTRA

Table 3

MW spectra of Trans- gauche' & Gauche-trans conformers

Tg'						Gt											
Transition			Frequency MHz	Intensity cm ⁻¹		Transition			Frequency MHz	Intensity cm ⁻¹							
1			2	3		4			5	6							
1	1	0	-	0	0	0	10223.82	9.86E-08	1	1	1	-	0	0	0	10285.85	6.97E-08
2	1	1	-	1	0	1	18221.43	4.69E-07	1	1	0	-	0	0	0	11136.59	3.43E-08
2	2	0	-	1	1	0	22041.44	7.82E-07	2	2	0	-	2	1	1	12594.78	1.12E-07
2	0	2	-	1	1	0	11119.01	3.40E-08	2	2	1	-	2	1	2	15029.35	1.24E-07
2	2	1	-	1	1	1	22673.84	7.26E-07	2	1	2	-	1	0	1	15561.92	2.39E-07
3	3	0	-	3	2	2	13317.10	1.14E-07	2	2	0	-	1	1	1	26549.88	6.29E-07
3	3	0	-	2	2	0	34659.93	2.93E-06	2	2	1	-	1	1	0	25581.49	6.46E-07
3	3	0	-	2	0	2	45582.36	1.69E-08	2	2	1	-	2	1	1	12477.12	3.58E-08
3	1	2	-	2	2	0	15760.55	4.85E-08	2	1	1	-	1	0	1	18114.15	1.36E-07
3	1	2	-	2	0	2	26682.98	1.24E-06	2	2	0	-	2	1	2	15147.00	3.89E-08
3	3	1	-	3	2	1	12405.52	1.05E-07	2	2	0	-	1	1	0	25699.14	2.97E-07
3	3	1	-	3	0	3	24719.02	6.62E-09	2	2	1	-	1	1	1	26432.23	2.89E-07
3	3	1	-	2	2	1	34820.29	2.93E-06	3	3	0	-	3	2	1	22427.36	3.24E-07
3	2	1	-	3	1	3	11361.80	6.29E-08	3	3	0	-	3	0	3	41913.13	7.68E-09
3	1	3	-	2	2	1	11052.96	1.04E-08	3	3	0	-	2	2	1	41381.85	2.73E-06
3	2	1	-	2	1	1	29093.38	1.82E-06	3	2	1	-	3	1	2	11854.42	1.97E-07
3	0	3	-	2	1	1	16779.88	1.01E-07	3	3	1	-	3	2	2	22991.13	3.35E-07
3	2	2	-	2	1	2	30671.46	1.47E-06	3	3	1	-	2	2	0	41253.91	2.72E-06
4	4	1	-	4	3	1	18000.95	2.25E-07	3	3	1	-	2	0	2	59826.86	1.00E-08
4	3	1	-	4	2	3	13933.72	1.94E-07	3	2	2	-	3	1	3	16374.53	2.39E-07
4	3	1	-	3	2	1	41609.72	4.79E-06	3	1	3	-	2	0	2	20461.20	5.75E-07
4	3	1	-	3	0	3	53923.22	8.76E-08	3	2	1	-	2	1	2	33983.84	9.18E-07
4	4	1	-	4	1	3	36195.75	4.60E-09	3	0	3	-	2	1	2	14498.07	2.01E-07
4	1	3	-	3	2	1	23414.92	2.60E-07	3	2	2	-	2	1	1	30857.55	1.04E-06
4	1	3	-	3	0	3	35728.42	2.40E-06	3	3	0	-	3	2	2	23001.42	1.11E-07
4	4	0	-	4	3	2	18193.09	2.29E-07	3	3	0	-	2	2	0	41264.20	1.20E-06
4	3	2	-	4	2	2	11382.16	1.58E-07	3	3	0	-	2	0	2	59837.15	3.49E-09
4	3	2	-	4	0	4	26508.92	2.44E-08	3	2	2	-	3	1	2	11280.36	5.47E-08
4	3	2	-	3	2	2	42304.72	4.75E-06	3	1	2	-	2	0	2	25555.37	3.44E-07
4	4	0	-	4	1	4	44216.47	1.54E-09	3	3	1	-	3	2	1	22417.07	1.08E-07
4	2	2	-	4	1	4	14641.21	7.56E-08	3	3	1	-	3	0	3	41902.84	2.68E-09
4	1	4	-	3	2	2	16281.34	4.03E-08	3	3	1	-	2	2	1	41371.56	1.20E-06
4	4	0	-	3	3	0	47180.70	7.45E-06	3	2	1	-	3	1	3	16948.59	6.49E-08
4	4	0	-	3	1	2	66080.08	1.17E-08	3	2	1	-	2	1	1	31431.61	5.67E-07
4	2	2	-	3	3	0	17605.45	3.41E-08	3	0	3	-	2	1	1	11945.84	2.29E-08
4	2	2	-	3	1	2	36504.83	3.67E-06	3	2	2	-	2	1	2	33409.78	5.13E-07
4	0	4	-	3	1	2	21378.07	1.49E-07	4	4	0	-	4	3	1	31835.71	6.58E-07
4	4	1	-	3	3	1	47205.15	7.45E-06	4	3	1	-	4	2	2	21726.47	5.69E-07
4	4	1	-	3	1	3	70972.47	5.32E-09	4	3	1	-	4	0	4	43243.72	3.42E-08
4	2	3	-	3	3	1	15270.48	2.18E-08	4	3	1	-	3	2	2	47777.17	3.58E-06
4	2	3	-	3	1	3	39037.81	2.59E-06	4	4	0	-	4	1	3	64953.02	3.86E-09
5	5	0	-	5	4	2	23344.88	3.84E-07	4	2	2	-	4	1	3	11390.84	2.81E-07
5	5	0	-	5	2	4	56112.16	2.22E-09	4	1	3	-	4	0	4	10126.40	1.87E-07
5	5	0	-	4	4	0	59642.84	1.51E-05	4	1	3	-	3	2	2	14659.85	8.44E-08
5	4	2	-	5	3	2	17489.12	3.74E-07	4	4	1	-	4	3	2	31906.19	6.61E-07
5	3	2	-	5	2	4	15278.15	2.51E-07	4	3	2	-	4	2	3	23290.65	6.22E-07
5	3	2	-	4	4	0	18808.83	2.86E-08	4	3	2	-	3	2	1	47131.89	3.55E-06
5	3	2	-	4	2	2	48384.08	7.64E-06	4	3	2	-	3	0	3	66617.66	5.81E-08
5	3	2	-	4	0	4	63510.84	1.99E-07	4	4	1	-	4	1	4	73388.49	1.98E-09
5	4	2	-	5	1	4	35669.60	2.44E-08	4	2	3	-	4	1	4	18191.66	3.75E-07
5	1	4	-	4	2	2	30203.61	6.30E-07	4	1	4	-	3	0	3	25135.35	1.17E-06
5	1	4	-	4	0	4	45330.36	3.89E-06	4	4	0	-	3	3	1	56621.75	7.18E-06
5	5	1	-	5	4	1	23314.55	3.83E-07	4	2	2	-	3	1	3	42425.23	1.17E-06
5	5	1	-	5	2	3	51397.32	2.80E-09	4	3	1	-	4	0	4	18457.68	5.06E-10
5	5	1	-	5	0	5	70837.64	1.33E-10	4	0	4	-	3	1	3	20907.98	6.95E-07
5	5	1	-	4	4	1	59645.86	1.51E-05	4	4	1	-	3	3	0	56610.72	7.18E-06
5	4	1	-	5	3	3	18225.74	3.97E-07	4	2	3	-	3	1	2	35695.66	1.61E-06
5	3	3	-	5	0	5	29297.36	4.89E-08	4	4	1	-	4	3	1	31834.97	2.22E-07
5	3	3	-	4	4	1	18105.58	2.60E-08	4	3	1	-	4	2	3	23361.87	1.94E-07
5	3	3	-	4	2	3	50040.25	7.29E-06	4	3	1	-	3	2	1	47203.11	1.72E-06

1						2	3	4				5	6				
5	4	1	-	5	1	5	47301.63	5.23E-09	4	3	1	-	3	0	3	66688.88	2.00E-08
5	2	3	-	5	1	5	19218.86	8.21E-08	4	4	1	-	4	1	3	64952.28	1.34E-09
4	4	1	-	5	1	5	10970.31	1.75E-11	4	1	3	-	3	2	1	14085.79	2.72E-08
5	1	5	-	4	2	3	20964.35	8.37E-08	4	1	3	-	3	0	3	33571.57	6.73E-07
5	4	1	-	4	3	1	54332.27	1.06E-05	4	4	0	-	4	3	2	31906.93	2.23E-07
5	4	1	-	4	1	3	72527.06	7.21E-08	4	3	2	-	4	2	2	21655.25	1.77E-07
5	2	3	-	4	3	1	26249.49	2.06E-07	4	3	2	-	4	0	4	43172.50	1.21E-08
5	2	3	-	4	1	3	44444.29	6.44E-06	4	3	2	-	3	2	2	47705.95	1.73E-06
5	0	5	-	4	1	3	25003.97	1.72E-07	4	4	0	-	4	1	4	73389.23	6.88E-10
5	4	2	-	4	3	2	54491.05	1.06E-05	4	2	2	-	4	1	4	19827.05	8.35E-08
5	2	4	-	4	3	2	21723.77	9.80E-08	4	4	0	-	3	3	0	56611.46	3.11E-06
5	2	4	-	4	1	4	47747.14	4.10E-06	4	2	2	-	3	1	2	37331.06	1.03E-06
6	6	1	-	6	5	1	28548.33	5.79E-07	3	3	0	-	4	0	4	18467.97	1.76E-10
6	5	1	-	6	4	3	23223.86	6.81E-07	4	0	4	-	3	1	2	15813.81	4.43E-08
6	5	1	-	6	2	5	57413.88	9.06E-09	4	4	1	-	3	3	1	56621.00	3.11E-06
6	5	1	-	5	4	1	66861.32	1.99E-05	4	2	3	-	3	1	3	40789.83	8.40E-07
6	6	1	-	6	3	3	68234.30	2.28E-09	5	5	0	-	5	4	1	41011.39	1.10E-06
6	4	3	-	6	3	3	16462.11	4.48E-07	5	5	0	-	4	4	1	71913.11	1.48E-05
6	3	3	-	6	2	5	17727.91	2.86E-07	5	4	1	-	5	3	2	31587.21	1.20E-06
6	3	3	-	5	4	1	27175.34	1.54E-07	5	3	2	-	5	2	3	20626.90	7.61E-07
6	3	3	-	5	2	3	55258.11	1.19E-05	5	3	2	-	5	0	5	45641.05	8.15E-08
6	3	3	-	5	0	5	74698.44	2.63E-07	5	3	2	-	4	2	3	54511.34	4.51E-06
6	4	3	-	6	1	5	35929.85	7.14E-08	5	4	1	-	5	1	4	63719.79	2.09E-08
6	1	5	-	5	2	3	35790.37	9.40E-07	5	2	3	-	5	1	4	11505.68	3.79E-07
6	1	5	-	5	0	5	55230.70	5.76E-06	5	1	4	-	5	0	5	13508.48	3.20E-07
6	6	0	-	6	5	2	28552.42	5.79E-07	4	4	1	-	5	1	4	32818.07	3.39E-10
6	5	2	-	6	4	2	23075.50	6.74E-07	5	1	4	-	4	2	3	22378.76	3.63E-07
6	5	2	-	6	2	4	49542.31	1.47E-08	5	5	1	-	5	4	2	41017.99	1.10E-06
6	5	2	-	6	0	6	74585.74	5.85E-10	5	5	1	-	4	4	0	71912.31	1.48E-05
6	5	2	-	5	4	2	66887.23	1.99E-05	5	4	2	-	5	3	3	31859.19	1.22E-06
6	6	0	-	6	3	4	70120.83	2.25E-09	5	3	3	-	5	2	4	23859.68	9.06E-07
6	4	2	-	6	3	4	18492.91	5.23E-07	5	3	3	-	4	2	2	52597.32	4.47E-06
6	3	4	-	6	0	6	33017.33	7.36E-08	5	3	3	-	4	0	4	74114.56	1.82E-07
6	3	4	-	5	4	2	25318.82	1.26E-07	5	4	2	-	5	1	5	76195.61	7.88E-09
6	3	4	-	5	2	4	58086.09	1.06E-05	5	2	4	-	5	1	5	20476.75	5.43E-07
6	4	2	-	6	1	6	51416.35	1.01E-08	4	4	0	-	5	1	5	45301.29	1.70E-10
6	2	4	-	6	1	6	24949.53	8.78E-08	5	1	5	-	4	0	4	29778.14	2.14E-06
6	1	6	-	5	2	4	25162.66	1.32E-07	5	4	1	-	4	3	2	62807.90	8.74E-06
6	6	0	-	5	5	0	72094.76	2.66E-05	5	2	3	-	4	3	2	10593.79	2.51E-08
6	4	2	-	5	5	0	20466.84	2.78E-08	5	2	3	-	4	1	4	52076.09	1.31E-06
6	4	2	-	5	3	2	61300.85	1.47E-05	4	3	2	-	5	0	5	14420.36	1.18E-09
6	4	2	-	5	1	4	79481.33	2.60E-07	5	0	5	-	4	1	4	27061.94	1.67E-06
6	2	4	-	5	3	2	34834.04	6.98E-07	5	4	2	-	4	3	1	62730.03	8.73E-06
6	2	4	-	5	1	4	53014.52	9.99E-06	5	2	4	-	4	1	3	40128.48	2.39E-06
5	5	0	-	6	0	6	31043.40	5.04E-12	5	5	0	-	5	4	2	41018.04	3.74E-07
6	0	6	-	5	1	4	27971.08	1.89E-07	5	5	0	-	4	4	0	71912.36	6.37E-06
6	6	1	-	5	5	1	72095.10	2.66E-05	5	4	2	-	5	3	2	31580.56	3.91E-07
6	4	3	-	5	5	1	20322.91	2.73E-08	5	3	2	-	5	2	4	24138.30	2.60E-07
6	4	3	-	5	3	3	61863.19	1.48E-05	5	3	2	-	4	2	2	52875.94	2.43E-06
5	5	1	-	6	2	5	13867.11	2.63E-11	5	3	2	-	4	0	4	74393.19	6.01E-08
6	2	5	-	5	3	3	27673.17	2.37E-07	5	4	2	-	5	1	4	63713.14	7.30E-09
6	2	5	-	5	1	5	56749.06	5.97E-06	4	4	0	-	5	1	4	32818.82	1.18E-10
7	7	0	-	7	6	2	33766.34	8.10E-07	5	1	4	-	4	2	2	20743.37	1.01E-07
7	6	2	-	7	5	2	28390.92	1.04E-06	5	1	4	-	4	0	4	42260.61	1.11E-06
7	5	2	-	7	4	4	23112.90	9.10E-07	5	5	1	-	5	4	1	41011.34	3.74E-07
7	5	2	-	7	2	6	59459.20	2.17E-08	5	5	1	-	4	4	1	71913.06	6.37E-06
7	5	2	-	6	6	0	22387.95	2.81E-08	5	4	1	-	5	3	3	31865.84	3.96E-07
7	5	2	-	6	4	2	74015.87	2.58E-05	5	3	3	-	5	2	3	20348.28	2.16E-07
7	6	2	-	7	3	4	66308.79	1.04E-08	5	3	3	-	5	0	5	45362.43	2.99E-08
7	4	4	-	7	3	4	14804.97	4.53E-07	5	3	3	-	4	2	3	54232.71	2.45E-06
7	3	4	-	7	2	6	21541.33	3.03E-07	5	4	1	-	5	1	5	76202.26	2.74E-09
6	6	0	-	7	3	4	15529.92	2.38E-11	5	2	3	-	5	1	5	23988.15	9.58E-08
7	3	4	-	6	4	2	36098.00	5.01E-07	4	4	1	-	5	1	5	45300.54	5.92E-11
7	3	4	-	6	2	4	62564.81	1.78E-05	5	4	1	-	4	3	1	62736.68	4.03E-06
7	4	4	-	7	1	6	37272.18	1.43E-07	5	2	3	-	4	3	1	10522.57	8.99E-09
6	6	0	-	7	1	6	37997.13	5.81E-12	5	2	3	-	4	1	3	43639.88	1.73E-06

THEORETICAL MODELS OF THE ISOBUTANOL MOLECULE CONFORMATIONS MICROWAVE SPECTRA

1		2	3	4				5	6		
7	1	6	-	6	4	2	13630.79	2.73E-09	4 3 1 - 5 0 5	14491.58	4.08E-10
7	1	6	-	6	2	4	40097.60	1.05E-06	5 0 5 - 4 1 3	18625.73	5.80E-08
7	1	6	-	6	0	6	65141.03	8.03E-06	5 4 2 - 4 3 2	62801.25	4.03E-06
7	7	1	-	7	6	1	33765.84	8.10E-07	5 2 4 - 4 1 4	48564.69	1.28E-06
7	6	1	-	7	5	3	28415.12	1.04E-06	6 6 0 - 6 5 1	50150.76	1.64E-06
7	5	3	-	7	4	3	22592.50	8.77E-07	6 5 1 - 6 4 2	40890.32	2.04E-06
7	5	3	-	7	2	5	47793.67	4.88E-08	6 5 1 - 5 4 2	78075.94	1.73E-05
7	5	3	-	7	0	7	79390.51	1.37E-09	6 4 2 - 6 3 3	31080.03	1.67E-06
7	5	3	-	6	6	1	22364.29	2.80E-08	6 3 3 - 6 2 4	19297.81	9.18E-07
7	5	3	-	6	4	3	74136.48	2.59E-05	6 3 3 - 6 0 6	49369.37	1.34E-07
7	6	1	-	7	3	5	70271.34	9.79E-09	6 3 3 - 5 2 4	61824.45	5.37E-06
7	4	3	-	7	3	5	19263.72	6.17E-07	6 4 2 - 6 1 5	62808.00	6.84E-08
7	3	5	-	7	0	7	37534.29	9.56E-08	6 2 4 - 6 1 5	12430.16	5.18E-07
6	6	1	-	7	3	5	19491.93	3.13E-11	6 1 5 - 6 0 6	17641.40	5.13E-07
7	3	5	-	6	4	3	32280.26	3.41E-07	5 4 2 - 6 1 5	25622.38	1.25E-09
7	3	5	-	6	2	5	66470.28	1.47E-05	6 1 5 - 5 2 4	30096.48	1.06E-06
7	4	3	-	7	1	7	56760.10	1.38E-08	6 6 1 - 6 5 2	50151.29	1.64E-06
7	2	5	-	7	1	7	31558.93	9.62E-08	6 5 2 - 6 4 3	40922.63	2.04E-06
6	6	1	-	7	1	7	56988.30	6.20E-13	6 5 2 - 5 4 1	78068.76	1.73E-05
7	1	7	-	6	2	5	28973.91	1.80E-07	6 4 3 - 6 3 4	31850.30	1.73E-06
7	6	1	-	6	5	1	79327.73	3.33E-05	6 3 4 - 6 2 5	24782.92	1.21E-06
7	4	3	-	6	5	1	28320.12	1.37E-07	6 3 4 - 5 2 3	57509.93	5.47E-06
7	4	3	-	6	3	3	68006.10	2.01E-05	6 4 3 - 6 1 6	79837.11	1.85E-08
7	2	5	-	6	3	3	42804.93	1.62E-06	6 2 5 - 6 1 6	23203.88	7.51E-07
7	2	5	-	6	1	5	62272.67	1.41E-05	5 4 1 - 6 1 6	42690.98	5.75E-10
6	5	1	-	7	0	7	28477.89	1.60E-11	6 1 6 - 5 0 5	34537.28	3.61E-06
7	0	7	-	6	3	3	11208.09	8.93E-10	6 4 2 - 5 3 3	69044.81	1.05E-05
7	0	7	-	6	1	5	30675.82	2.12E-07	5 5 1 - 6 2 4	54210.21	2.08E-10
7	6	2	-	6	5	2	79331.29	3.33E-05	6 2 4 - 5 3 3	18666.96	1.37E-07
7	4	4	-	6	5	2	27827.47	1.32E-07	6 2 4 - 5 1 5	63003.39	1.36E-06
7	4	4	-	6	3	4	69395.88	2.00E-05	5 3 3 - 6 0 6	11404.59	1.50E-09
7	2	6	-	6	3	4	33049.59	4.16E-07	6 0 6 - 5 1 5	32931.83	3.21E-06
7	2	6	-	6	1	6	65973.02	8.20E-06	6 4 3 - 5 3 2	68733.34	1.04E-05
8	8	1	-	8	7	1	38979.39	1.07E-06	5 5 0 - 6 2 5	60498.49	1.95E-10
8	7	1	-	8	6	3	33638.80	1.48E-06	6 2 5 - 5 3 2	12100.11	4.18E-08
8	6	3	-	8	5	3	28126.28	1.41E-06	6 2 5 - 5 1 4	44232.69	3.48E-06
8	5	3	-	8	4	5	23119.59	1.08E-06	6 6 1 - 6 5 1	50150.75	5.60E-07
8	5	3	-	8	2	7	62439.57	3.83E-08	6 5 1 - 6 4 3	40923.17	6.76E-07
8	5	3	-	7	6	1	30016.78	1.33E-07	6 5 1 - 5 4 1	78069.29	7.77E-06
8	6	3	-	8	3	5	63834.63	3.13E-08	6 4 3 - 6 3 3	31047.18	5.15E-07
8	4	5	-	8	3	5	12588.76	4.06E-07	6 3 3 - 6 2 5	25586.04	3.12E-07
8	3	5	-	8	2	7	26731.21	3.11E-07	6 3 3 - 5 2 3	58313.05	3.40E-06
8	3	5	-	7	4	3	45316.04	1.29E-06	6 4 3 - 6 1 5	62775.15	2.39E-08
8	3	5	-	7	2	5	70517.21	2.50E-05	5 4 1 - 6 1 5	25629.03	4.33E-10
8	4	5	-	8	1	7	39768.87	2.23E-07	6 1 5 - 5 2 3	26585.08	2.23E-07
7	6	1	-	8	1	7	32871.69	2.53E-11	6 1 5 - 5 0 5	51599.23	1.66E-06
8	1	7	-	7	4	3	18135.92	7.23E-09	6 6 0 - 6 5 2	50151.29	5.60E-07
8	1	7	-	7	2	5	43337.09	1.05E-06	6 5 2 - 6 4 2	40889.79	6.75E-07
8	1	7	-	7	0	7	74933.93	1.07E-05	6 5 2 - 5 4 2	78075.41	7.77E-06
8	8	0	-	8	7	2	38979.44	1.07E-06	6 4 2 - 6 3 4	31883.15	5.36E-07
8	7	2	-	8	6	2	33635.34	1.48E-06	6 3 4 - 6 2 4	18494.69	2.30E-07
8	6	2	-	8	5	4	28228.30	1.42E-06	6 3 4 - 6 0 6	48566.25	5.35E-08
8	5	4	-	8	4	4	21675.69	9.80E-07	6 3 4 - 5 2 4	61021.33	3.37E-06
8	5	4	-	8	2	6	46584.04	1.24E-07	6 4 2 - 6 1 6	79869.95	6.42E-09
8	5	4	-	7	6	2	29918.66	1.32E-07	6 2 4 - 6 1 6	29492.11	1.03E-07
8	6	2	-	8	3	6	70811.53	2.58E-08	5 4 2 - 6 1 6	42684.33	2.01E-10
8	4	4	-	8	3	6	20907.55	6.79E-07	6 1 6 - 5 2 4	13034.53	1.71E-08
8	3	6	-	8	0	8	42691.06	1.15E-07	6 4 2 - 5 3 2	68766.18	5.17E-06
7	6	2	-	8	3	6	12664.57	6.38E-11	5 5 0 - 6 2 4	54210.26	7.26E-11
8	3	6	-	7	4	4	38839.25	6.81E-07	6 2 4 - 5 3 2	18388.34	4.97E-08
8	3	6	-	7	2	6	75185.54	1.95E-05	6 2 4 - 5 1 4	50520.92	2.70E-06
8	4	4	-	8	1	8	63583.82	1.46E-08	5 3 2 - 6 0 6	11683.22	5.13E-10
8	2	6	-	8	1	8	38675.46	1.09E-07	6 0 6 - 5 1 4	20449.36	6.25E-08
7	6	2	-	8	1	8	55340.84	2.53E-12	6 4 3 - 5 3 3	69011.96	5.19E-06
8	1	8	-	7	2	6	32509.27	2.27E-07	5 5 1 - 6 2 5	60498.44	6.78E-11
8	6	2	-	7	7	0	24380.62	2.87E-08	6 2 5 - 5 3 3	12378.73	1.74E-08

1				2	3	4				5	6		
7	7	0	-	8 4 4	25523.36	3.11E-11	6	2	5	-	5 1 5	56715.16	1.83E-06
8	4	4	-	7 5 2	36633.89	4.08E-07	7	7	0	-	7 6 1	59284.45	2.27E-06
8	4	4	-	7 3 4	74551.76	2.73E-05	7	6	1	-	7 5 2	50059.99	3.07E-06
7	7	0	-	8 2 6	50431.72	2.98E-12	7	5	2	-	7 4 3	40674.35	2.88E-06
8	2	6	-	7 5 2	11725.54	9.94E-10	7	4	3	-	7 3 4	30184.04	2.04E-06
8	2	6	-	7 3 4	49643.41	2.67E-06	7	3	4	-	7 2 5	18067.05	1.06E-06
8	2	6	-	7 1 6	72110.62	1.88E-05	7	3	4	-	7 0 7	54641.77	1.71E-07
7	5	2	-	8 0 8	26964.71	2.84E-11	6	6	1	-	7 3 4	77698.35	1.67E-10
8	0	8	-	7 3 4	10953.15	5.33E-10	7	3	4	-	6 4 3	13375.57	5.33E-08
8	0	8	-	7 1 6	33420.37	2.44E-07	7	3	4	-	6 2 5	70008.80	5.98E-06
8	6	3	-	7 7 1	24377.22	2.87E-08	7	4	3	-	7 1 6	62577.71	1.66E-07
7	7	1	-	8 4 5	26868.65	3.36E-11	7	2	5	-	7 1 6	14326.61	7.29E-07
8	4	5	-	7 5 3	35312.30	3.70E-07	7	1	6	-	7 0 7	22248.11	7.79E-07
8	4	5	-	7 3 5	77168.52	2.64E-05	6	4	3	-	7 1 6	19018.09	2.31E-09
7	7	1	-	8 2 7	66188.63	8.98E-13	7	1	6	-	6 2 5	37615.14	2.45E-06
8	2	7	-	7 3 5	37848.55	6.05E-07	7	7	1	-	7 6 2	59284.49	2.27E-06
8	2	7	-	7 1 7	75344.92	1.08E-05	7	6	2	-	7 5 3	50063.11	3.07E-06
9	9	0	-	9 8 2	44191.41	1.37E-06	7	5	3	-	7 4 4	40789.16	2.90E-06
9	8	2	-	9 7 2	38861.88	1.98E-06	7	4	4	-	7 3 5	31946.17	2.23E-06
9	7	2	-	9 6 4	33458.96	2.03E-06	7	3	5	-	7 2 6	26127.32	1.56E-06
9	7	2	-	8 8 0	26392.23	2.94E-08	6	6	0	-	7 3 5	79578.46	1.70E-10
9	6	4	-	9 5 4	27671.70	1.67E-06	7	3	5	-	6 4 2	11462.62	3.78E-08
9	5	4	-	9 4 6	23443.58	1.21E-06	7	3	5	-	6 2 4	61840.46	6.63E-06
9	5	4	-	9 2 8	66560.90	5.41E-08	7	2	6	-	7 1 7	26323.77	1.01E-06
8	8	0	-	9 5 4	34738.43	3.34E-11	6	4	2	-	7 1 7	40988.46	1.14E-09
9	5	4	-	8 6 2	37876.36	3.76E-07	7	1	7	-	6 0 6	39460.94	5.70E-06
9	6	4	-	9 3 6	61135.90	7.83E-08	7	4	3	-	6 3 4	75409.92	1.23E-05
9	4	6	-	9 3 6	10020.62	3.27E-07	6	5	2	-	7 2 5	45614.11	8.77E-10
9	3	6	-	9 2 8	33096.70	3.23E-07	7	2	5	-	6 3 4	27158.82	4.50E-07
8	8	0	-	9 3 6	68202.63	1.14E-12	7	2	5	-	6 1 6	75145.63	1.36E-06
9	3	6	-	8 4 4	54316.14	2.80E-06	7	0	7	-	6 1 6	38570.91	5.40E-06
9	3	6	-	8 2 6	79224.49	3.30E-05	7	4	4	-	6 3 3	74488.82	1.22E-05
8	4	6	-	9 1 8	43320.89	2.97E-07	6	5	1	-	7 2 6	55555.02	7.79E-10
9	6	2	-	9 1 8	28888.12	5.53E-11	7	2	6	-	6 3 3	16415.33	9.06E-08
9	1	8	-	8 4 4	21015.87	9.98E-09	7	2	6	-	6 1 5	48143.30	5.02E-06
9	1	8	-	8 2 6	45924.22	1.05E-06	7	7	0	-	7 6 2	59284.49	7.80E-07
9	9	1	-	9 8 1	44191.41	1.37E-06	7	6	2	-	7 5 2	50059.95	1.03E-06
9	8	1	-	9 7 3	38862.33	1.98E-06	7	5	2	-	7 4 4	40792.33	9.27E-07
9	7	3	-	9 6 3	33441.99	2.03E-06	7	4	4	-	7 3 4	30066.07	5.93E-07
9	7	3	-	8 8 1	26391.78	2.94E-08	7	3	4	-	7 2 6	28007.43	3.52E-07
9	6	3	-	9 5 5	28013.05	1.70E-06	6	6	0	-	7 3 4	77698.35	5.83E-11
9	5	5	-	9 4 5	20123.41	9.74E-07	7	3	4	-	6 4 2	13342.73	1.94E-08
9	5	5	-	9 2 7	46346.67	2.52E-07	7	3	4	-	6 2 4	63720.57	4.74E-06
8	8	1	-	9 5 5	35063.26	3.39E-11	7	4	4	-	7 1 6	62459.73	5.87E-08
9	5	5	-	8 6 3	37554.93	3.69E-07	6	4	2	-	7 1 6	19050.93	8.02E-10
9	6	3	-	9 3 7	71943.00	5.22E-08	7	1	6	-	6 2 4	31326.91	3.50E-07
9	4	5	-	9 3 7	23806.53	7.10E-07	7	1	6	-	6 0 6	61398.47	2.32E-06
9	3	7	-	9 0 9	48326.74	1.33E-07	7	7	1	-	7 6 1	59284.45	7.80E-07
8	8	1	-	9 3 7	78993.20	7.40E-13	7	6	1	-	7 5 3	50063.15	1.03E-06
9	3	7	-	8 4 5	44870.86	1.11E-06	7	5	3	-	7 4 3	40671.18	9.22E-07
9	4	5	-	9 1 9	72127.65	1.25E-08	7	4	3	-	7 3 5	32064.15	6.50E-07
9	2	7	-	9 1 9	45904.40	1.26E-07	7	3	5	-	7 2 5	16186.95	2.22E-07
8	6	3	-	9 1 9	54696.13	5.65E-12	7	3	5	-	7 0 7	52761.66	7.86E-08
9	1	9	-	8 2 7	35869.71	2.74E-07	6	6	1	-	7 3 5	79578.45	5.92E-11
9	6	3	-	8 7 1	31929.18	1.31E-07	7	3	5	-	6 4 3	11495.47	1.40E-08
8	7	1	-	9 4 5	16207.28	6.71E-11	7	3	5	-	6 2 5	68128.69	4.52E-06
9	4	5	-	8 5 3	45557.80	9.68E-07	7	2	5	-	7 1 7	36264.14	1.09E-07
8	7	1	-	9 2 7	42430.53	1.89E-11	6	4	3	-	7 1 7	40955.62	3.99E-10
9	2	7	-	8 5 3	19334.55	6.77E-09	7	1	7	-	6 2 5	15677.61	2.69E-08
9	2	7	-	8 3 5	55042.90	3.28E-06	7	4	3	-	6 3 3	74606.80	6.57E-06
8	5	3	-	9 0 9	26575.48	3.81E-11	6	5	1	-	7 2 5	45614.64	3.06E-10
9	0	9	-	8 1 7	36312.99	2.82E-07	7	2	5	-	6 3 3	26355.71	1.62E-07
9	6	4	-	8 7 2	31912.72	1.31E-07	7	2	5	-	6 1 5	58083.68	3.91E-06
8	7	2	-	9 4 6	19202.56	8.74E-11	6	3	3	-	7 0 7	10219.01	5.13E-10
9	4	6	-	8 5 4	42661.07	7.93E-07	7	0	7	-	6 1 5	21508.96	6.23E-08
8	7	2	-	9 2 8	62319.88	4.53E-12	7	4	4	-	6 3 4	75291.94	6.62E-06

THEORETICAL MODELS OF THE ISOBUTANOL MOLECULE CONFORMATIONS MICROWAVE SPECTRA

1						2	3	4						5	6		
9	2	8	-	8	3	6	42126.99	7.80E-07	6	5	2	-	7	2	6	55554.49	2.72E-10
10	10	1	-	10	9	1	49402.58	1.69E-06	7	2	6	-	6	3	4	17218.45	4.52E-08
10	9	1	-	10	8	3	44082.26	2.54E-06	7	2	6	-	6	1	6	65205.25	2.50E-06
10	8	3	-	10	7	3	38698.20	2.74E-06	8	8	0	-	8	7	1	68416.49	3.00E-06
10	7	3	-	10	6	5	33220.92	2.47E-06	8	7	1	-	8	6	2	59205.61	4.29E-06
10	7	3	-	9	8	1	33903.98	1.30E-07	8	6	2	-	8	5	3	49920.21	4.36E-06
10	6	5	-	10	5	5	26881.03	1.81E-06	8	5	3	-	8	4	4	40299.48	3.63E-06
10	5	5	-	10	4	7	24393.92	1.29E-06	8	4	4	-	8	3	5	28826.32	2.32E-06
10	5	5	-	10	2	9	72064.51	6.29E-08	8	3	5	-	8	2	6	17317.27	1.21E-06
9	8	1	-	10	5	5	26197.97	9.80E-11	8	3	5	-	8	0	8	61612.76	1.80E-07
10	5	5	-	9	6	3	46106.35	8.41E-07	7	6	2	-	8	3	5	69583.42	7.14E-10
10	6	5	-	10	3	7	58646.34	1.75E-07	8	3	5	-	7	4	4	21268.86	1.96E-07
10	3	7	-	10	2	9	40299.21	3.48E-07	8	3	5	-	7	2	6	79342.35	6.23E-06
9	8	1	-	10	3	7	57963.27	8.71E-12	8	4	4	-	8	1	7	63414.99	3.19E-07
10	3	7	-	9	6	3	14341.05	1.43E-09	8	2	6	-	8	1	7	17271.39	1.04E-06
10	3	7	-	9	4	5	62477.52	4.94E-06	8	1	7	-	8	0	8	27024.09	1.12E-06
10	4	7	-	10	1	9	47758.58	3.61E-07	7	4	4	-	8	1	7	13319.81	2.65E-09
9	6	3	-	10	1	9	26046.14	8.51E-11	8	1	7	-	7	2	6	44753.69	4.77E-06
10	1	9	-	9	4	5	22090.32	8.50E-09	8	8	1	-	8	7	2	68416.50	3.00E-06
10	1	9	-	9	2	7	48313.57	1.08E-06	8	7	2	-	8	6	3	59205.88	4.29E-06
10	10	0	-	10	9	2	49402.58	1.69E-06	8	6	3	-	8	5	4	49933.48	4.37E-06
10	9	2	-	10	8	2	44082.20	2.54E-06	8	5	4	-	8	4	5	40628.76	3.68E-06
10	8	2	-	10	7	4	38700.72	2.74E-06	8	4	5	-	8	3	6	32232.94	2.73E-06
10	7	4	-	10	6	4	33155.12	2.47E-06	8	3	6	-	8	2	7	27933.68	1.96E-06
10	7	4	-	10	4	6	78847.75	5.67E-08	7	6	1	-	8	3	6	73332.90	7.34E-10
10	7	4	-	9	8	2	33901.52	1.30E-07	8	3	6	-	7	4	3	17401.44	1.21E-07
10	6	4	-	10	5	6	27835.17	1.92E-06	8	3	6	-	7	2	5	65652.54	8.07E-06
10	5	6	-	10	4	6	17857.47	8.76E-07	8	2	7	-	8	1	8	29769.31	1.31E-06
10	5	6	-	10	2	8	47361.43	4.15E-07	7	4	3	-	8	1	8	40301.55	1.72E-09
9	8	2	-	10	5	6	27088.77	1.04E-10	8	1	8	-	7	0	7	44524.26	8.50E-06
10	5	6	-	9	6	4	45232.07	8.02E-07	7	5	3	-	8	2	6	36837.58	2.11E-09
10	6	4	-	10	3	8	73878.27	8.75E-08	8	2	6	-	7	3	5	35897.76	1.16E-06
10	4	6	-	10	3	8	28185.64	7.18E-07	8	0	8	-	7	1	7	44053.36	8.30E-06
10	3	8	-	10	0	10	54292.13	1.49E-07	8	4	5	-	7	3	4	79818.43	1.39E-05
9	8	2	-	10	3	8	73131.87	4.41E-12	7	5	2	-	8	2	7	51206.59	1.81E-09
10	3	8	-	9	4	6	50304.25	1.57E-06	8	2	7	-	7	3	4	19651.80	1.29E-07
10	2	8	-	10	1	10	52971.71	1.45E-07	8	2	7	-	7	1	6	52045.47	7.18E-06
9	6	4	-	10	1	10	55101.07	9.25E-12	8	8	1	-	8	7	1	68416.49	1.03E-06
10	1	10	-	9	2	8	39131.53	3.22E-07	8	7	1	-	8	6	3	59205.88	1.45E-06
10	8	2	-	9	9	0	28410.82	3.01E-08	8	6	3	-	8	5	3	49919.94	1.42E-06
9	9	0	-	10	6	4	43445.01	3.30E-11	8	5	3	-	8	4	5	40642.30	1.13E-06
10	6	4	-	9	7	2	39608.28	3.62E-07	8	4	5	-	8	3	5	28483.51	6.21E-07
10	4	6	-	9	5	4	55046.31	2.05E-06	8	3	5	-	8	2	7	31683.12	3.77E-07
9	7	2	-	10	2	8	35588.31	5.67E-11	7	6	1	-	8	3	5	69583.46	2.49E-10
10	2	8	-	9	5	4	25542.35	2.07E-08	8	3	5	-	7	4	3	21150.88	7.32E-08
10	2	8	-	9	3	6	59006.55	3.35E-06	8	3	5	-	7	2	5	69401.98	6.51E-06
9	5	4	-	10	0	10	27431.46	4.34E-11	8	4	5	-	8	1	7	63072.17	1.15E-07
10	0	10	-	9	1	8	39333.01	3.25E-07	7	4	3	-	8	1	7	13437.78	9.22E-10
10	8	3	-	9	9	1	28410.77	3.01E-08	8	1	7	-	7	2	5	34813.31	4.29E-07

Table 4

Spectra of Gauche- gauche & Gauche-gauch' conformers

Gg			Gg'				
Transition		Frequency MHz	Intensity cm ⁻¹	Transition		Frequency MHz	Intensity cm ⁻¹
1		2	3	4		5	6
2	1	1	-	1	1	0	11100.80
2	1	2	-	1	1	1	13306.38
2	2	0	-	1	0	1	11597.29
2	2	1	-	2	0	2	30364.59
2	0	2	-	1	0	1	17912.76
3	3	0	-	3	1	3	12329.53
3	3	0	-	2	1	1	12061.03
3	3	1	-	3	1	2	18181.27
3	1	2	-	2	1	1	14746.97

1		2	3	4				5	6
3	3	1	-	2	1	2	55968.82	1.54E-08	2 2 0 - 1 1 0
3	1	3	-	2	1	2	17354.17	7.32E-07	2 2 1 - 1 1 1
3	2	1	-	2	2	0	19290.98	5.66E-07	3 3 0 - 3 1 3
3	2	1	-	2	0	2	37444.01	5.57E-08	3 3 0 - 2 1 1
3	2	2	-	3	0	3	18535.01	2.47E-08	3 3 1 - 3 1 2
3	0	3	-	2	0	2	18260.00	8.98E-07	3 1 2 - 2 1 1
3	2	2	-	2	2	1	18775.49	5.35E-07	3 3 1 - 2 1 2
4	3	1	-	4	1	4	40959.55	1.53E-08	3 1 3 - 2 1 2
4	3	1	-	3	3	0	25341.87	1.02E-06	3 2 1 - 2 2 0
4	3	1	-	3	1	2	58608.62	6.74E-08	3 2 2 - 3 0 3
4	3	2	-	4	1	3	32004.35	2.53E-08	3 2 2 - 3 0 3
4	1	3	-	3	1	2	26517.14	2.38E-06	3 0 3 - 2 0 2
4	3	2	-	3	3	1	25267.35	1.01E-06	3 2 2 - 2 2 1
4	3	2	-	3	1	3	63882.00	4.47E-08	3 3 0 - 3 2 2
4	3	1	-	4	1	4	15605.07	1.81E-10	3 3 0 - 2 2 0
4	1	4	-	3	1	3	23009.58	1.80E-06	3 3 0 - 2 0 2
4	4	0	-	4	2	3	53867.83	8.97E-09	3 2 2 - 3 1 2
4	4	0	-	3	2	1	78148.39	3.29E-08	3 1 2 - 2 0 2
4	4	1	-	4	2	2	52030.95	8.94E-09	3 3 1 - 3 2 1
4	2	2	-	3	2	1	26116.46	1.86E-06	3 3 1 - 3 0 3
4	2	2	-	3	0	3	45300.47	1.37E-07	3 3 1 - 2 2 1
4	4	1	-	4	0	4	73485.32	3.17E-10	3 2 1 - 3 1 3
4	2	3	-	4	0	4	19618.47	5.40E-08	3 2 1 - 2 1 1
4	0	4	-	3	0	3	23846.11	2.02E-06	3 0 3 - 2 1 1
4	4	1	-	3	2	2	78796.42	3.28E-08	3 2 2 - 2 1 2
4	2	3	-	3	2	2	24929.57	1.69E-06	4 3 1 - 4 1 4
5	5	0	-	5	3	3	71017.03	1.18E-08	4 3 1 - 3 3 0
5	5	1	-	5	3	2	70677.38	1.17E-08	4 3 1 - 3 1 2
5	3	2	-	5	1	5	44261.32	2.72E-08	4 3 2 - 4 1 3
5	3	2	-	4	3	1	31886.99	2.94E-06	4 1 3 - 3 1 2
5	3	2	-	4	1	3	63978.47	1.75E-07	4 3 2 - 3 3 1
5	3	3	-	5	1	4	30828.58	5.89E-08	4 3 2 - 3 1 3
5	1	4	-	5	1	5	13093.16	6.25E-08	3 3 1 - 4 1 4
5	1	4	-	4	1	3	32810.30	4.62E-06	4 1 4 - 3 1 3
5	3	3	-	4	3	2	31634.54	2.89E-06	4 4 0 - 4 2 3
5	3	3	-	4	1	4	72506.96	8.84E-08	4 4 0 - 3 2 1
4	3	2	-	5	1	5	12287.20	3.12E-10	4 4 1 - 4 2 2
5	1	5	-	4	1	4	28585.22	3.54E-06	4 2 2 - 3 2 1
5	4	1	-	5	2	4	54467.90	2.74E-08	4 2 2 - 3 0 3
5	4	1	-	4	4	0	31596.42	1.62E-06	4 4 1 - 4 0 4
5	4	2	-	5	2	3	50553.76	2.78E-08	4 2 3 - 4 0 4
4	4	0	-	5	2	3	18966.14	2.39E-10	4 0 4 - 3 0 3
5	2	3	-	4	2	2	33065.80	4.18E-06	4 4 1 - 3 2 2
5	2	3	-	4	0	4	54520.16	2.27E-07	4 2 3 - 3 2 2
5	4	2	-	5	0	5	75858.70	1.62E-09	4 4 1 - 4 3 1
5	2	4	-	5	0	5	21399.59	9.46E-08	4 3 1 - 4 2 3
4	4	0	-	5	0	5	44271.08	3.36E-11	4 3 1 - 3 2 1
5	0	5	-	4	0	4	29215.23	3.76E-06	4 3 1 - 3 0 3
5	4	2	-	4	4	1	31588.61	1.62E-06	4 4 1 - 4 1 3
4	4	1	-	5	2	4	22870.50	2.96E-10	4 1 3 - 3 2 1
5	2	4	-	4	2	3	30996.35	3.64E-06	4 1 3 - 3 0 3
6	5	1	-	6	3	4	70917.65	3.60E-08	4 4 0 - 4 3 2
6	5	1	-	5	5	0	37888.64	2.34E-06	4 3 2 - 4 2 2
6	5	2	-	6	3	3	69944.90	3.56E-08	4 3 2 - 4 0 4
6	3	3	-	6	1	6	48791.34	3.76E-08	4 3 2 - 3 2 2
5	5	0	-	6	3	3	32057.03	3.68E-10	4 4 0 - 4 1 4
6	3	3	-	5	3	2	38620.42	6.03E-06	4 2 2 - 4 1 4
6	3	3	-	5	1	4	69788.58	3.76E-07	4 4 0 - 3 3 0
6	3	4	-	6	1	5	29986.17	1.13E-07	4 2 2 - 3 1 2
6	1	5	-	6	1	6	17833.19	1.07E-07	3 3 0 - 4 0 4
5	5	0	-	6	1	5	63015.18	1.81E-11	4 0 4 - 3 1 2
6	1	5	-	5	1	4	38830.43	7.75E-06	4 4 1 - 3 3 1
6	5	2	-	5	5	1	37887.94	2.34E-06	4 2 3 - 3 1 3

THEORETICAL MODELS OF THE ISOBUTANOL MOLECULE CONFORMATIONS MICROWAVE SPECTRA

1		2	3	4				5	6								
5	5	1	-	6	3	4	33028.94	3.85E-10	5	5	0	-	5	3	3	70673.96	7.05E-09
6	3	4	-	5	3	3	37988.01	5.83E-06	5	5	1	-	5	3	2	70374.66	7.02E-09
6	1	6	-	5	1	5	34090.41	6.07E-06	5	3	2	-	5	1	5	43612.23	1.67E-08
6	4	2	-	6	2	5	55537.37	5.49E-08	5	3	2	-	4	3	1	31669.31	1.90E-06
6	4	2	-	5	4	1	38028.81	4.31E-06	5	3	2	-	4	1	3	63703.80	1.04E-07
6	4	3	-	6	2	4	48568.18	5.90E-08	5	3	3	-	5	1	4	30794.10	3.50E-08
5	4	1	-	6	2	4	10582.70	3.07E-10	5	1	4	-	5	1	5	12518.89	3.73E-08
6	2	4	-	5	2	3	39979.86	7.72E-06	5	1	4	-	4	1	3	32610.46	3.00E-06
6	2	4	-	5	0	5	65284.79	2.88E-07	5	3	3	-	4	3	2	31446.69	1.88E-06
6	4	3	-	6	0	6	79357.06	4.29E-09	5	3	3	-	4	1	4	71873.40	5.37E-08
6	2	5	-	6	0	6	23863.02	1.46E-07	4	3	2	-	5	1	5	11866.30	1.82E-10
5	4	1	-	6	0	6	41371.58	1.27E-10	5	1	5	-	4	1	4	28560.41	2.32E-06
6	0	6	-	5	0	5	34495.91	6.26E-06	5	4	1	-	5	2	4	54112.60	1.64E-08
6	4	3	-	5	4	2	37994.28	4.30E-06	5	4	1	-	4	4	0	31407.46	1.05E-06
5	4	2	-	6	2	5	17499.77	6.01E-10	5	4	2	-	5	2	3	50487.57	1.66E-08
6	2	5	-	5	2	4	36959.33	6.51E-06	4	4	0	-	5	2	3	19087.52	1.45E-10
7	5	2	-	7	3	5	70913.12	7.34E-08	5	2	3	-	4	2	2	32783.99	2.69E-06
7	5	2	-	6	5	1	44290.85	5.94E-06	5	2	3	-	4	0	4	53863.49	1.42E-07
7	5	3	-	7	3	4	68658.38	7.17E-08	5	4	2	-	5	0	5	75153.78	9.31E-10
7	3	4	-	7	1	7	54823.78	4.27E-08	5	2	4	-	5	0	5	21048.59	5.71E-08
6	5	1	-	7	3	4	24372.05	8.13E-10	4	4	0	-	5	0	5	43753.73	1.93E-11
7	3	4	-	6	3	3	45573.62	1.06E-05	5	0	5	-	4	0	4	29197.29	2.47E-06
7	3	4	-	6	1	5	76531.77	6.76E-07	5	4	2	-	4	4	1	31400.88	1.05E-06
7	3	5	-	7	1	6	29753.72	1.89E-07	4	4	1	-	5	2	4	22704.31	1.77E-10
7	1	6	-	7	1	7	22819.84	1.68E-07	5	2	4	-	4	2	3	30858.28	2.37E-06
6	5	1	-	7	1	6	56375.99	1.05E-10	5	5	0	-	5	4	2	39777.39	6.43E-07
7	1	6	-	6	3	3	13569.68	7.24E-09	5	5	0	-	4	4	0	71177.43	1.15E-05
7	1	6	-	6	1	5	44527.82	1.18E-05	5	4	2	-	5	3	2	30597.33	6.70E-07
7	5	3	-	6	5	2	44287.10	5.94E-06	5	3	2	-	5	2	4	23507.86	4.45E-07
6	5	2	-	7	3	5	26621.51	9.32E-10	5	3	2	-	4	2	2	52674.23	4.45E-06
7	3	5	-	6	3	4	44295.38	9.99E-06	5	3	2	-	4	0	4	73753.74	1.13E-07
6	5	2	-	7	1	7	79195.07	1.96E-11	5	4	2	-	5	1	4	61690.67	1.36E-08
7	1	7	-	6	1	6	39541.17	9.54E-06	4	4	0	-	5	1	4	30290.62	2.00E-10
7	6	1	-	6	6	0	44187.20	3.18E-06	5	1	4	-	4	2	2	21580.89	2.00E-07
7	4	3	-	7	2	6	57273.10	8.92E-08	5	1	4	-	4	0	4	42660.40	2.07E-06
6	6	0	-	7	4	3	44146.84	4.51E-10	5	5	1	-	5	4	1	39769.92	6.43E-07
7	4	3	-	6	4	2	44544.37	8.31E-06	5	5	1	-	4	4	1	71178.21	1.15E-05
7	4	4	-	7	2	5	46269.62	1.07E-07	5	4	1	-	5	3	3	30903.98	6.81E-07
7	2	5	-	7	2	6	10848.42	8.69E-08	5	3	3	-	5	2	3	19591.00	3.67E-07
7	2	5	-	6	2	4	46731.19	1.26E-05	5	3	3	-	5	0	5	44257.21	5.36E-08
7	2	5	-	6	0	6	77520.07	3.17E-07	5	3	3	-	4	2	3	54066.90	4.47E-06
7	2	6	-	7	0	7	26896.53	2.09E-07	5	4	1	-	5	1	5	74216.97	4.95E-09
6	4	2	-	7	0	7	39625.26	2.60E-10	5	2	3	-	5	1	5	23721.99	1.63E-07
7	0	7	-	6	0	6	39775.13	9.68E-06	4	4	1	-	5	1	5	42808.68	1.01E-10
7	6	2	-	6	6	1	44187.15	3.18E-06	5	1	5	-	4	2	3	10753.91	1.78E-08
6	6	1	-	7	4	4	44301.89	4.54E-10	5	4	1	-	4	3	1	62274.05	7.29E-06
7	4	4	-	6	4	3	44432.63	8.27E-06	5	2	3	-	4	3	1	11779.07	2.07E-08
6	4	3	-	7	2	6	12685.41	6.69E-10	5	2	3	-	4	1	3	43813.56	3.22E-06
7	2	6	-	6	2	5	42808.64	1.04E-05	4	3	1	-	5	0	5	12887.14	6.06E-10
8	7	1	-	7	7	0	50487.59	4.12E-06	5	0	5	-	4	1	3	19147.35	1.08E-07
8	5	3	-	8	3	6	71126.64	1.24E-07	5	4	2	-	4	3	2	62343.26	7.30E-06
7	7	0	-	8	5	3	55802.97	5.03E-10	5	2	4	-	4	1	4	48664.78	2.36E-06
8	5	3	-	7	5	2	50737.99	1.10E-05	6	5	1	-	6	3	4	70573.67	2.16E-08
8	5	4	-	8	3	5	66686.42	1.20E-07	6	5	1	-	5	5	0	37664.50	1.52E-06
8	3	5	-	8	1	8	62564.51	4.18E-08	6	5	2	-	6	3	3	69713.14	2.13E-08
7	5	2	-	8	3	5	15967.69	8.62E-10	6	3	3	-	6	1	6	47863.57	2.34E-08
8	3	5	-	7	3	4	52695.21	1.70E-05	5	5	0	-	6	3	3	32049.25	2.22E-10
8	3	6	-	8	1	7	30345.02	2.88E-07	6	3	3	-	5	3	2	38325.46	3.90E-06
8	1	7	-	8	1	8	27798.52	2.48E-07	6	3	3	-	5	1	4	69418.80	2.24E-07
7	5	2	-	8	1	7	50733.68	3.14E-10	6	3	4	-	6	1	5	29918.72	6.69E-08
8	1	7	-	7	3	4	17929.22	1.67E-08	6	1	5	-	6	1	6	17084.93	6.34E-08
8	1	7	-	7	1	6	49933.16	1.68E-05	5	5	0	-	6	1	5	62827.89	9.87E-12
8	7	2	-	7	7	1	50487.59	4.12E-06	6	1	5	-	5	1	4	38640.17	5.05E-06

1						2	3	4					5	6			
7	7	1	-	8	5	4	55822.23	5.04E-10	6	5	2	-	5	5	1	37663.94	1.52E-06
8	5	4	-	7	5	3	50723.25	1.10E-05	5	5	1	-	6	3	4	32909.12	2.31E-10
7	5	3	-	8	3	6	20384.14	1.27E-09	6	3	4	-	5	3	3	37764.79	3.78E-06
8	3	6	-	7	3	5	50524.46	1.55E-05	5	5	1	-	6	1	6	79912.77	2.53E-12
7	5	3	-	8	1	8	78527.68	4.86E-11	6	1	6	-	5	1	5	34074.12	3.99E-06
8	1	8	-	7	1	7	44954.49	1.41E-05	6	4	2	-	6	2	5	55091.17	3.30E-08
8	6	2	-	7	6	1	50577.30	7.79E-06	6	4	2	-	5	4	1	37791.47	2.80E-06
8	4	4	-	8	2	7	59913.27	1.26E-07	6	4	3	-	6	2	4	48604.63	3.52E-08
7	6	1	-	8	4	4	37150.33	1.21E-09	5	4	1	-	6	2	4	10849.73	1.92E-10
8	4	4	-	7	4	3	51183.70	1.39E-05	6	2	4	-	5	2	3	39645.25	4.99E-06
8	4	5	-	8	2	6	43922.20	1.78E-07	6	2	4	-	5	0	5	64311.46	1.83E-07
8	2	6	-	8	2	7	15543.09	1.55E-07	6	4	3	-	6	0	6	78422.10	2.52E-09
8	2	6	-	7	2	5	53238.20	1.89E-05	6	2	5	-	6	0	6	23367.51	8.83E-08
8	2	7	-	8	0	8	30360.03	2.83E-07	5	4	1	-	6	0	6	40667.20	7.37E-11
7	4	3	-	8	0	8	39089.60	3.95E-10	6	0	6	-	5	0	5	34493.99	4.11E-06
8	0	8	-	7	0	7	45080.02	1.42E-05	6	4	3	-	5	4	2	37762.31	2.79E-06
8	6	3	-	7	6	2	50576.95	7.79E-06	5	4	2	-	6	2	5	17292.28	3.58E-10
7	6	2	-	8	4	5	37598.26	1.24E-09	6	2	5	-	5	2	4	36812.90	4.25E-06
8	4	5	-	7	4	4	50890.78	1.37E-05	6	6	1	-	6	5	1	48634.78	9.64E-07
8	2	7	-	7	2	6	48543.53	1.55E-05	6	5	1	-	6	4	3	39679.57	1.16E-06
9	7	2	-	8	7	1	56870.49	9.84E-06	6	5	1	-	5	4	1	77434.47	1.41E-05
9	5	4	-	9	3	7	71722.25	1.86E-07	6	4	3	-	6	3	3	30034.18	8.80E-07
8	7	1	-	9	5	4	49046.38	1.47E-09	6	3	3	-	6	2	5	25020.42	5.34E-07
9	5	4	-	8	5	3	57244.18	1.77E-05	6	3	3	-	5	2	3	58215.70	6.28E-06
9	5	5	-	9	3	6	64041.59	1.84E-07	6	4	3	-	6	1	5	60812.82	4.45E-08
9	3	6	-	9	1	9	72062.49	3.72E-08	5	4	1	-	6	1	5	23057.92	6.95E-10
9	3	6	-	8	3	5	59842.44	2.53E-05	6	1	5	-	5	2	3	27437.07	4.31E-07
9	3	7	-	9	1	8	31829.93	4.07E-07	6	1	5	-	5	0	5	52103.27	3.08E-06
9	1	8	-	9	1	9	32617.72	3.44E-07	6	6	0	-	6	5	2	48635.40	9.64E-07
8	5	3	-	9	1	8	46308.00	6.39E-10	6	5	2	-	6	4	2	39642.39	1.16E-06
9	1	8	-	8	3	5	20397.68	2.18E-08	6	5	2	-	5	4	2	77441.27	1.41E-05
9	1	8	-	8	1	7	55163.66	2.28E-05	6	4	2	-	6	3	4	30930.67	9.20E-07
9	7	3	-	8	7	2	56870.46	9.84E-06	6	3	4	-	6	2	4	17710.53	3.87E-07
8	7	2	-	9	5	5	49112.21	1.48E-09	6	3	4	-	6	0	6	47528.00	9.46E-08
9	5	5	-	8	5	4	57197.60	1.77E-05	6	3	4	-	5	2	4	60973.40	6.19E-06
8	5	4	-	9	3	7	14458.82	1.18E-09	6	4	2	-	6	1	6	77934.32	1.15E-08
9	3	7	-	8	3	6	56648.57	2.24E-05	6	2	4	-	6	1	6	29293.12	1.76E-07
8	5	4	-	9	1	9	78906.47	8.86E-11	5	4	2	-	6	1	6	40135.44	3.34E-10
9	1	9	-	8	1	8	50344.46	1.98E-05	6	1	6	-	5	2	4	13969.75	3.51E-08
9	8	1	-	8	8	0	56788.87	5.16E-06	6	4	2	-	5	3	2	68396.21	9.42E-06
8	8	0	-	9	6	3	67359.72	5.38E-10	5	5	0	-	6	2	4	50619.70	1.26E-10
9	6	3	-	8	6	2	56999.56	1.40E-05	6	2	4	-	5	3	2	19755.01	1.06E-07
9	4	5	-	9	2	8	63738.46	1.56E-07	6	2	4	-	5	1	4	50848.35	5.02E-06
8	6	2	-	9	4	5	29729.34	1.86E-09	5	3	2	-	6	0	6	10062.46	6.97E-10
9	4	5	-	8	4	4	57998.30	2.13E-05	6	0	6	-	5	1	4	21030.88	1.16E-07
9	4	6	-	9	2	7	41831.16	2.78E-07	6	4	3	-	5	3	3	68658.88	9.46E-06
9	2	7	-	9	2	8	20806.96	2.54E-07	5	5	1	-	6	2	5	57069.61	1.17E-10
8	6	2	-	9	2	7	72660.83	1.61E-10	6	2	5	-	5	3	3	13604.29	3.82E-08
9	2	7	-	8	4	4	15066.80	7.40E-09	6	2	5	-	5	1	5	56917.28	3.38E-06
9	2	7	-	8	2	6	59436.99	2.64E-05	7	5	2	-	7	3	5	70551.87	4.40E-08
9	2	8	-	9	0	9	34124.54	3.69E-07	7	5	2	-	6	5	1	44021.74	3.86E-06
8	4	4	-	9	0	9	39864.70	5.00E-10	7	5	3	-	7	3	4	68544.96	4.30E-08
9	0	9	-	8	0	8	50408.61	1.98E-05	7	3	4	-	7	1	7	53515.38	2.71E-08
9	8	2	-	8	8	1	56788.87	5.16E-06	6	5	1	-	7	3	4	24526.87	4.96E-10
8	8	1	-	9	6	4	67361.77	5.38E-10	7	3	4	-	6	3	3	45186.89	6.84E-06
9	6	4	-	8	6	3	56997.93	1.40E-05	7	3	4	-	6	1	5	75965.52	4.07E-07
8	6	3	-	9	4	6	30829.26	1.98E-09	7	3	5	-	7	1	6	29591.75	1.13E-07
9	4	6	-	8	4	5	57345.94	2.08E-05	7	1	6	-	7	1	7	21920.37	1.00E-07
9	2	8	-	8	2	7	54173.11	2.18E-05	6	5	1	-	7	1	6	56121.88	5.79E-11
10	9	1	-	9	9	0	63090.70	6.27E-06	7	1	6	-	6	3	3	13591.88	4.46E-09
9	9	0	-	10	7	3	78889.64	5.60E-10	7	1	6	-	6	1	5	44370.51	7.71E-06
10	7	3	-	9	7	2	63279.23	1.73E-05	7	5	3	-	6	5	2	44018.70	3.86E-06
10	5	5	-	10	3	8	72904.22	2.57E-07	6	5	2	-	7	3	5	26529.52	5.60E-10

THEORETICAL MODELS OF THE ISOBUTANOL MOLECULE CONFORMATIONS MICROWAVE SPECTRA

1					2	3	4				5	6					
9	5	2	-	10	5	5	42085.04	2.60E-09	7	3	5	-	6	3	4	44043.54	6.49E-06
10	5	5	-	9	5	4	63831.83	2.63E-05	6	5	2	-	7	1	7	78041.63	1.13E-11
10	5	6	-	10	3	7	60896.72	2.67E-07	7	1	7	-	6	1	6	39535.08	6.27E-06
10	3	7	-	10	3	8	11816.38	1.43E-07	7	6	1	-	6	6	0	43927.13	2.06E-06
10	3	7	-	9	3	6	66851.40	3.57E-05	7	4	3	-	7	2	6	56678.71	5.41E-08
10	3	8	-	10	1	9	34130.56	5.46E-07	6	6	0	-	7	4	3	44028.15	2.71E-10
10	1	9	-	10	1	10	37245.94	4.51E-07	7	4	3	-	6	4	2	44249.64	5.39E-06
9	5	4	-	10	1	9	43202.95	1.00E-09	7	4	4	-	7	2	5	46393.85	6.36E-08
10	1	9	-	9	3	6	20904.47	1.90E-08	7	2	5	-	7	2	6	10153.72	5.02E-08
10	1	9	-	9	1	8	60349.23	3.02E-05	7	2	5	-	6	2	4	46365.84	8.16E-06
10	9	2	-	9	9	1	63090.70	6.27E-06	7	2	5	-	6	0	6	76183.31	2.03E-07
9	9	1	-	10	7	4	78889.84	5.60E-10	7	2	6	-	7	0	7	26246.55	1.26E-07
10	7	4	-	9	7	3	63279.07	1.73E-05	6	4	2	-	7	0	7	38675.63	1.53E-10
9	7	3	-	10	5	6	42276.12	2.62E-09	7	0	7	-	6	0	6	39783.04	6.36E-06
10	5	6	-	9	5	5	63706.54	2.62E-05	7	6	2	-	6	6	1	43927.09	2.06E-06
10	3	8	-	9	3	7	62649.86	3.08E-05	6	6	1	-	7	4	4	44159.30	2.72E-10
10	1	10	-	9	1	9	55721.02	2.67E-05	7	4	4	-	6	4	3	44155.06	5.37E-06
10	8	2	-	9	8	1	63166.75	1.21E-05	6	4	3	-	7	2	6	12392.51	3.93E-10
9	8	1	-	10	6	4	60688.80	1.66E-09	7	2	6	-	6	2	5	42662.09	6.81E-06
10	6	4	-	9	6	3	63459.79	2.21E-05	7	7	0	-	7	6	2	57493.55	1.34E-06
10	4	6	-	10	2	9	69053.28	1.72E-07	7	6	2	-	7	5	2	48540.13	1.77E-06
9	6	3	-	10	4	6	21699.62	1.92E-09	7	5	2	-	7	4	4	39546.26	1.59E-06
10	4	6	-	9	4	5	65029.27	3.08E-05	7	4	4	-	7	3	4	29002.35	1.01E-06
10	4	7	-	10	2	8	40319.71	4.11E-07	7	3	4	-	7	2	6	27545.22	6.00E-07
10	2	8	-	10	2	9	26371.58	3.91E-07	6	6	0	-	7	3	4	73161.65	1.02E-10
9	6	3	-	10	2	8	64381.32	4.34E-10	7	3	4	-	6	4	2	15116.14	4.57E-08
10	2	8	-	9	4	5	22347.57	2.70E-08	7	3	4	-	6	2	4	63757.34	8.80E-06
10	2	8	-	9	2	7	65279.06	3.50E-05	7	4	4	-	7	1	6	60597.36	1.08E-07
10	2	9	-	10	0	10	38086.30	4.68E-07	6	4	2	-	7	1	6	16478.87	1.18E-09
9	4	5	-	10	0	10	42110.31	5.56E-10	7	1	6	-	6	2	4	32162.33	6.59E-07
10	0	10	-	9	0	9	55752.69	2.68E-05	7	1	6	-	6	0	6	61979.80	4.30E-06
10	8	3	-	9	8	2	63166.74	1.21E-05	7	7	1	-	7	6	1	57493.50	1.34E-06
9	8	2	-	10	6	5	60696.84	1.66E-09	7	6	1	-	7	5	3	48543.83	1.77E-06
10	6	5	-	9	6	4	63453.80	2.21E-05	7	5	3	-	7	4	3	39411.46	1.58E-06
9	6	4	-	10	4	7	24059.57	2.30E-09	7	4	3	-	7	3	5	31136.76	1.11E-06
10	4	7	-	9	4	6	63767.61	2.96E-05	7	3	5	-	7	2	5	15388.23	3.71E-07
10	2	9	-	9	2	8	59714.45	2.94E-05	7	3	5	-	7	0	7	51788.50	1.38E-07
11	9	2	-	10	9	1	69464.84	1.44E-05	6	6	1	-	7	3	5	75164.91	1.04E-10
10	9	1	-	11	7	4	72263.06	1.79E-09	7	3	5	-	6	4	3	13149.44	3.34E-08
11	7	4	-	10	7	3	69717.28	2.67E-05	7	3	5	-	6	2	5	68204.04	8.32E-06
11	5	6	-	11	3	9	74918.31	3.27E-07	7	2	5	-	7	1	7	36123.88	1.85E-07
10	7	3	-	11	5	6	34829.06	3.42E-09	6	4	3	-	7	1	7	38362.67	6.49E-10
11	5	6	-	10	5	5	70535.21	3.70E-05	7	1	7	-	6	2	5	16691.92	5.42E-08
11	5	7	-	11	3	8	57534.16	3.78E-07	7	4	3	-	6	3	3	74320.39	1.20E-05
11	3	8	-	11	3	9	16897.2	2.53E-07	6	5	1	-	7	2	5	41918.36	5.17E-10
11	3	8	-	10	5	5	12514.1	3.70E-09	7	2	5	-	6	3	3	27795.39	3.34E-07
11	3	8	-	10	3	7	73601.94	4.77E-05	7	2	5	-	6	1	5	58574.03	7.27E-06
11	3	9	-	11	1	10	37087.9	7.06E-07	6	5	1	-	7	0	7	78318.63	4.21E-11
11	1	10	-	11	1	11	41719.34	5.68E-07	7	0	7	-	6	1	5	22173.76	1.16E-07
10	5	5	-	11	1	10	41471	1.33E-09	7	4	4	-	6	3	4	75049.16	1.21E-05
11	1	10	-	10	3	7	19616.85	1.25E-08	6	5	2	-	7	2	6	52071.47	4.61E-10
11	1	10	-	10	1	9	65563.78	3.89E-05	7	2	6	-	6	3	4	18501.59	9.44E-08
11	9	3	-	10	9	2	69464.83	1.44E-05	7	2	6	-	6	1	6	65505.24	4.61E-06
10	9	2	-	11	7	5	72263.93	1.79E-09	8	7	1	-	7	7	0	50191.40	2.68E-06
11	7	5	-	10	7	4	69716.61	2.67E-05	8	5	3	-	8	3	6	70718.25	7.44E-08
10	7	4	-	11	5	7	35315.82	3.51E-09	7	7	0	-	8	5	3	55614.11	3.02E-10
11	5	7	-	10	5	6	70239.38	3.67E-05	8	5	3	-	7	5	2	50419.56	7.14E-06
11	3	9	-	10	3	8	68521.13	4.07E-05	8	5	4	-	8	3	5	66733.99	7.23E-08
10	3	8	-	11	1	11	10286.11	4.63E-10	8	3	5	-	8	1	8	60775.03	2.71E-08
11	1	11	-	10	1	10	61090.38	3.51E-05	7	5	2	-	8	3	5	16330.03	5.39E-10
11	10	1	-	10	10	0	69392.89	7.44E-06	8	3	5	-	7	3	4	52218.58	1.09E-05
11	8	3	-	10	8	2	69566.38	2.08E-05	8	3	6	-	8	1	7	30026.98	1.72E-07
10	8	2	-	11	6	5	53889.48	3.13E-09	8	1	7	-	8	1	8	26779.40	1.48E-07

1						2	3	4						5	6		
11	6	5	-	10	6	4	69966.07	3.20E-05	7	5	2	-	8	1	7	50325.66	1.76E-10
11	4	7	-	11	2	10	76126.95	1.70E-07	8	1	7	-	7	3	4	18222.95	1.10E-08
10	6	4	-	11	4	7	12897.27	1.18E-09	8	1	7	-	7	1	6	49817.96	1.10E-05
11	4	7	-	10	4	6	72262.14	4.29E-05	8	7	2	-	7	7	1	50191.40	2.68E-06
11	4	8	-	11	2	9	39674.23	5.76E-07	7	7	1	-	8	5	4	55629.71	3.02E-10
11	2	9	-	11	2	10	31950.74	5.68E-07	8	5	4	-	7	5	3	50407.62	7.14E-06
10	6	4	-	11	2	9	57073.48	9.04E-10	7	5	3	-	8	3	6	20295.03	7.65E-10
11	2	9	-	10	4	6	28085.94	5.80E-08	8	3	6	-	7	3	5	50253.19	1.01E-05
11	2	9	-	10	2	8	70767.64	4.46E-05	7	5	3	-	8	1	8	77101.41	2.84E-11
11	2	10	-	11	0	11	42169.15	5.78E-07	8	1	8	-	7	1	7	44958.93	9.24E-06
10	4	6	-	11	0	11	46033.96	5.59E-10	8	6	2	-	7	6	1	50273.45	5.06E-06
11	0	11	-	10	0	10	61105.62	3.51E-05	8	4	4	-	8	2	7	59092.19	7.68E-08
11	10	2	-	10	10	1	69392.89	7.44E-06	7	6	1	-	8	4	4	37137.81	7.30E-10
11	8	4	-	10	8	3	69566.37	2.08E-05	8	4	4	-	7	4	3	50817.47	8.98E-06
10	8	3	-	11	6	6	53916.2	3.13E-09	8	4	5	-	8	2	6	44095.25	1.05E-07
11	6	6	-	10	6	5	69947.38	3.20E-05	8	2	6	-	8	2	7	14616.81	8.99E-08
10	6	5	-	11	4	8	17391.21	2.01E-09	8	2	6	-	7	2	5	52867.09	1.22E-05
11	4	8	-	10	4	7	70122.16	4.02E-05	8	2	7	-	8	0	8	29555.57	1.71E-07
11	2	10	-	10	2	9	65188.47	3.84E-05	7	4	3	-	8	0	8	37830.29	2.34E-10
12	11	1	-	11	11	0	75695.33	8.66E-06	8	0	8	-	7	0	7	45094.98	9.31E-06
12	9	3	-	11	9	2	75857.77	2.45E-05	8	6	3	-	7	6	2	50273.17	5.06E-06
11	9	2	-	12	7	5	65539.26	3.52E-09	7	6	2	-	8	4	5	37517.90	7.42E-10
12	7	5	-	11	7	4	76188.64	3.81E-05	8	4	5	-	7	4	4	50568.49	8.89E-06
12	5	7	-	12	3	10	78052.72	3.86E-07	8	2	7	-	7	2	6	48404.00	1.01E-05
11	7	4	-	12	5	7	27145.69	3.53E-09	8	8	1	-	8	7	1	66350.48	1.77E-06
12	5	7	-	11	5	6	77400.65	5.01E-05	8	7	1	-	8	6	3	57411.77	2.48E-06
12	5	8	-	12	3	9	54293.57	5.25E-07	8	6	3	-	8	5	3	48393.74	2.44E-06
12	3	9	-	12	3	10	22648.43	4.10E-07	8	5	3	-	8	4	5	39397.33	1.94E-06
12	3	9	-	11	5	6	21996.36	1.95E-08	8	4	5	-	8	3	5	27352.26	1.05E-06
12	3	10	-	12	1	11	40529.16	8.88E-07	8	3	5	-	8	2	7	31359.80	6.41E-07
12	1	11	-	12	1	12	46088.22	6.93E-07	7	6	1	-	8	3	5	64870.20	4.27E-10

Table 5

Spectra of Gauche- gauche'' & Gauche-gauch''' conformers

Gg''						Gg'''											
Transition			Frequency MHz	Intensity cm ⁻¹	Transition	Transition			Frequency MHz	Intensity cm ⁻¹							
1			2	3	4	4			5	6							
1	1	1	-	0	0	0	10291.14	7.00E-08	1	1	1	-	0	0	0	10268.91	6.95E-08
1	1	0	-	0	0	0	11137.19	3.44E-08	1	1	0	-	0	0	0	11125.93	3.42E-08
2	2	0	-	2	1	1	12562.07	1.11E-07	2	2	0	-	2	1	1	12530.90	1.11E-07
2	2	1	-	2	1	2	14983.52	1.23E-07	2	2	1	-	2	1	2	14982.08	1.23E-07
2	1	2	-	1	0	1	15587.78	2.41E-07	2	1	2	-	1	0	1	15543.80	2.39E-07
2	2	0	-	1	1	1	26539.53	6.30E-07	2	2	0	-	1	1	1	26508.74	6.26E-07
2	2	1	-	1	1	0	25576.79	6.47E-07	2	2	1	-	1	1	0	25531.85	6.43E-07
2	2	1	-	2	1	1	12445.38	3.57E-08	2	2	1	-	2	1	1	12411.03	3.54E-08
2	1	1	-	1	0	1	18125.92	1.37E-07	2	1	1	-	1	0	1	18114.85	1.36E-07
2	2	0	-	2	1	2	15100.21	3.88E-08	2	2	0	-	2	1	2	15101.95	3.85E-08
2	2	0	-	1	1	0	25693.48	2.98E-07	2	2	0	-	1	1	0	25651.72	2.97E-07
2	2	1	-	1	1	1	26422.84	2.90E-07	2	2	1	-	1	1	1	26388.87	2.88E-07
3	3	0	-	3	2	1	22366.67	3.23E-07	3	3	0	-	3	2	1	22323.96	3.21E-07
3	3	0	-	3	0	3	41791.48	7.61E-09	3	3	0	-	3	0	3	41755.17	7.78E-09
3	3	0	-	2	2	1	41364.15	2.73E-06	3	3	0	-	2	2	1	41304.23	2.72E-06
3	2	1	-	3	1	2	11824.44	1.97E-07	3	2	1	-	3	1	2	11791.01	1.96E-07
3	3	1	-	3	2	2	22925.93	3.34E-07	3	3	1	-	3	2	2	22897.92	3.33E-07
3	3	1	-	2	2	0	41237.29	2.73E-06	3	3	1	-	2	2	0	41173.76	2.71E-06
3	3	1	-	2	0	2	59756.60	9.98E-09	3	3	1	-	2	0	2	59675.57	1.02E-08
3	2	2	-	3	1	3	16321.10	2.38E-07	3	2	2	-	3	1	3	16337.93	2.38E-07
3	1	3	-	2	0	2	20509.57	5.79E-07	3	1	3	-	2	0	2	20439.72	5.74E-07
3	2	1	-	2	1	2	33981.00	9.21E-07	3	2	1	-	2	1	2	33962.36	9.13E-07
3	0	3	-	2	1	2	14556.19	2.03E-07	3	0	3	-	2	1	2	14531.14	2.03E-07
3	2	2	-	2	1	1	30873.43	1.05E-06	3	2	2	-	2	1	1	30806.74	1.04E-06
3	3	0	-	3	2	2	22936.11	1.11E-07	3	3	0	-	3	2	2	22908.53	1.10E-07

THEORETICAL MODELS OF THE ISOBUTANOL MOLECULE CONFORMATIONS MICROWAVE SPECTRA

1		2	3	4			5	6
3	3	0	-	2	2	0	41247.46	1.20E-06
3	3	0	-	2	0	2	59766.78	3.47E-09
3	2	2	-	3	1	2	11255.00	5.46E-08
3	1	2	-	2	0	2	25575.67	3.45E-07
3	3	1	-	3	2	1	22356.50	1.08E-07
3	3	1	-	3	0	3	41781.31	2.66E-09
3	3	1	-	2	2	1	41353.98	1.20E-06
3	2	1	-	3	1	3	16890.54	6.47E-08
3	2	1	-	2	1	1	31442.86	5.69E-07
3	0	3	-	2	1	1	12018.05	2.33E-08
3	2	2	-	2	1	2	33411.56	5.14E-07
4	4	0	-	4	3	1	31747.40	6.56E-07
4	3	1	-	4	2	2	21670.91	5.67E-07
4	3	1	-	4	0	4	43111.60	3.40E-08
4	3	1	-	3	2	2	47773.05	3.59E-06
4	4	0	-	4	1	3	64778.86	3.82E-09
4	2	2	-	4	1	3	11360.55	2.80E-07
4	1	3	-	4	0	4	10080.15	1.86E-07
4	1	3	-	3	2	2	14741.60	8.54E-08
4	4	1	-	4	3	2	31817.12	6.58E-07
4	3	2	-	4	2	3	23223.06	6.20E-07
4	3	2	-	3	2	1	47133.17	3.56E-06
4	3	2	-	3	0	3	66557.97	5.79E-08
4	4	1	-	4	1	4	73168.14	1.96E-09
4	2	3	-	4	1	4	18127.95	3.74E-07
4	1	4	-	3	0	3	25206.96	1.18E-06
4	4	0	-	3	3	1	56594.52	7.19E-06
4	2	2	-	3	1	3	42423.25	1.17E-06
3	3	1	-	4	0	4	18264.49	4.95E-10
4	0	4	-	3	1	3	20982.55	7.01E-07
4	4	1	-	3	3	0	56583.61	7.19E-06
4	2	3	-	3	1	2	35734.54	1.61E-06
4	4	1	-	4	3	1	31746.67	2.22E-07
4	3	1	-	4	2	3	23293.51	1.93E-07
4	3	1	-	3	2	1	47203.62	1.72E-06
4	3	1	-	3	0	3	66628.42	1.99E-08
4	4	1	-	4	1	3	64778.12	1.33E-09
4	1	3	-	3	2	1	14172.16	2.75E-08
4	1	3	-	3	0	3	33596.97	6.76E-07
4	4	0	-	4	3	2	31817.85	2.23E-07
4	3	2	-	4	2	2	21600.46	1.77E-07
4	3	2	-	4	0	4	43041.15	1.20E-08
4	3	2	-	3	2	2	47702.60	1.73E-06
4	4	0	-	4	1	4	73168.87	6.83E-10
4	2	2	-	4	1	4	19750.56	8.33E-08
4	4	0	-	3	3	0	56584.35	3.11E-06
4	2	2	-	3	1	2	37357.15	1.03E-06
3	3	0	-	4	0	4	18274.66	1.72E-10
4	0	4	-	3	1	2	15916.45	4.51E-08
4	4	1	-	3	3	1	56593.79	3.11E-06
4	2	3	-	3	1	3	40800.64	8.43E-07
5	5	0	-	5	4	1	40897.09	1.09E-06
5	5	0	-	4	4	1	71875.94	1.48E-05
5	4	1	-	5	3	2	31501.20	1.20E-06
5	3	2	-	5	2	3	20578.25	7.59E-07
5	3	2	-	5	0	5	45490.79	8.10E-08
5	3	2	-	4	2	3	54517.83	4.52E-06
5	4	1	-	5	1	4	63549.73	2.07E-08
5	2	3	-	5	1	4	11470.28	3.77E-07
5	1	4	-	5	0	5	13442.26	3.18E-07
4	4	1	-	5	1	4	32570.88	3.33E-10
5	1	4	-	4	2	3	22469.30	3.67E-07
5	5	1	-	5	4	2	40903.61	1.09E-06

G.I. ISMAILZADEH, I.Z. MOVSUMOV, M.R. MENZELEYEV, A.S. QASANOVA, S.B. KAZIMOVA

1						2	3	4						5	6		
5	5	1	-	4	4	0	71875.16	1.48E-05	5	5	1	-	4	4	0	71768.07	1.48E-05
5	4	2	-	5	3	3	31770.28	1.22E-06	5	4	2	-	5	3	3	31723.89	1.21E-06
5	3	3	-	5	2	4	23787.67	9.02E-07	5	3	3	-	5	2	4	23781.56	9.00E-07
5	3	3	-	4	2	2	52619.59	4.48E-06	5	3	3	-	4	2	2	52511.50	4.45E-06
5	3	3	-	4	0	4	74060.28	1.81E-07	5	3	3	-	4	0	4	74007.96	1.84E-07
5	4	2	-	5	1	5	75958.17	7.82E-09	5	4	2	-	5	1	5	75977.74	7.94E-09
5	2	4	-	5	1	5	20400.23	5.41E-07	5	2	4	-	5	1	5	20472.29	5.41E-07
4	4	0	-	5	1	5	44986.62	1.67E-10	4	4	0	-	5	1	5	45053.09	1.70E-10
5	1	5	-	4	0	4	29872.39	2.16E-06	5	1	5	-	4	0	4	29754.11	2.14E-06
5	4	1	-	4	3	2	62795.97	8.76E-06	5	4	1	-	4	3	2	62703.16	8.70E-06
5	2	3	-	4	3	2	10716.52	2.57E-08	5	2	3	-	4	3	2	10757.96	2.59E-08
5	2	3	-	4	1	4	52067.53	1.31E-06	5	2	3	-	4	1	4	52130.25	1.30E-06
4	3	2	-	5	0	5	14196.03	1.15E-09	4	3	2	-	5	0	5	14285.82	1.17E-09
5	0	5	-	4	1	4	27154.99	1.68E-06	5	0	5	-	4	1	4	27086.47	1.67E-06
5	4	2	-	4	3	1	62718.96	8.75E-06	5	4	2	-	4	3	1	62622.84	8.69E-06
5	2	4	-	4	1	3	40192.47	2.40E-06	5	2	4	-	4	1	3	40066.28	2.38E-06
5	5	0	-	5	4	2	40903.66	3.73E-07	5	5	0	-	5	4	2	40843.47	3.70E-07
5	5	0	-	4	4	0	71875.21	6.38E-06	5	5	0	-	4	4	0	71768.13	6.34E-06
5	4	2	-	5	3	2	31494.64	3.90E-07	5	4	2	-	5	3	2	31436.93	3.86E-07
5	3	2	-	5	2	4	24063.31	2.59E-07	5	3	2	-	5	2	4	24068.52	2.57E-07
5	3	2	-	4	2	2	52895.23	2.44E-06	5	3	2	-	4	2	2	52798.46	2.43E-06
5	3	2	-	4	0	4	74335.92	6.00E-08	5	3	2	-	4	0	4	74294.92	6.07E-08
5	4	2	-	5	1	4	63543.17	7.23E-09	5	4	2	-	5	1	4	63409.49	7.42E-09
4	4	0	-	5	1	4	32571.62	1.16E-10	4	4	0	-	5	1	4	32484.84	1.19E-10
5	1	4	-	4	2	2	20846.69	1.02E-07	5	1	4	-	4	2	2	20825.90	1.01E-07
5	1	4	-	4	0	4	42287.39	1.12E-06	5	1	4	-	4	0	4	42322.35	1.11E-06
5	5	1	-	5	4	1	40897.05	3.73E-07	5	5	1	-	5	4	1	40836.48	3.70E-07
5	5	1	-	4	4	1	71875.90	6.38E-06	5	5	1	-	4	4	1	71768.85	6.34E-06
5	4	1	-	5	3	3	31776.84	3.95E-07	5	4	1	-	5	3	3	31730.83	3.92E-07
5	3	3	-	5	2	3	20302.61	2.16E-07	5	3	3	-	5	2	3	20214.38	2.13E-07
5	3	3	-	5	0	5	45215.15	2.98E-08	5	3	3	-	5	0	5	45258.16	3.00E-08
5	3	3	-	4	2	3	54242.19	2.45E-06	5	3	3	-	4	2	3	54175.14	2.44E-06
5	4	1	-	5	1	5	75964.73	2.72E-09	5	4	1	-	5	1	5	75984.68	2.76E-09
5	2	3	-	5	1	5	23885.28	9.55E-08	5	2	3	-	5	1	5	24039.47	9.45E-08
4	4	1	-	5	1	5	44985.88	5.84E-11	4	4	1	-	5	1	5	45052.31	5.93E-11
5	1	5	-	4	2	3	10054.30	8.69E-09	5	4	1	-	4	3	1	62629.77	4.01E-06
5	4	1	-	4	3	1	62725.52	4.03E-06	5	2	3	-	4	3	1	10684.57	9.27E-09
5	2	3	-	4	3	1	10646.07	9.22E-09	5	2	3	-	4	1	3	43633.47	1.73E-06
5	2	3	-	4	1	3	43677.52	1.74E-06	4	3	1	-	5	0	5	14359.21	4.04E-10
4	3	1	-	5	0	5	14266.48	3.96E-10	5	0	5	-	4	1	3	18589.69	5.70E-08
5	0	5	-	4	1	3	18764.98	5.92E-08	5	4	2	-	4	3	2	62696.23	4.02E-06
5	4	2	-	4	3	2	62789.40	4.04E-06	5	2	4	-	4	1	4	48563.06	1.28E-06
5	2	4	-	4	1	4	48582.48	1.28E-06	6	6	0	-	6	5	1	49937.63	1.63E-06
6	6	0	-	6	5	1	50010.83	1.63E-06	6	5	1	-	6	4	2	40712.83	2.02E-06
6	5	1	-	6	4	2	40777.09	2.03E-06	6	5	1	-	5	4	2	77937.59	1.72E-05
6	5	1	-	5	4	2	78054.34	1.73E-05	6	4	2	-	6	3	3	30924.92	1.65E-06
6	4	2	-	6	3	3	30998.67	1.66E-06	6	3	3	-	6	2	4	19167.13	9.09E-07
6	3	3	-	6	2	4	19255.46	9.15E-07	6	3	3	-	6	0	6	49329.48	1.34E-07
6	3	3	-	6	0	6	49191.88	1.34E-07	6	3	3	-	5	2	4	61805.29	5.33E-06
6	3	3	-	5	2	4	61836.51	5.39E-06	6	4	2	-	6	1	5	62519.87	6.96E-08
6	4	2	-	6	1	5	62637.90	6.77E-08	6	2	4	-	6	1	5	12427.81	5.17E-07
6	2	4	-	6	1	5	12383.77	5.16E-07	6	1	5	-	6	0	6	17734.54	5.15E-07
6	1	5	-	6	0	6	17552.66	5.10E-07	5	4	2	-	6	1	5	25295.11	1.25E-09
5	4	2	-	6	1	5	25360.66	1.21E-09	6	1	5	-	5	2	4	30210.35	1.08E-06
6	1	5	-	5	2	4	30197.29	1.07E-06	6	6	1	-	6	5	2	49938.19	1.63E-06
6	6	1	-	6	5	2	50011.35	1.63E-06	6	5	2	-	6	4	3	40746.50	2.03E-06
6	5	2	-	6	4	3	40808.97	2.04E-06	6	5	2	-	5	4	1	77930.09	1.72E-05
6	5	2	-	5	4	1	78047.25	1.73E-05	6	4	3	-	6	3	4	31717.02	1.72E-06
6	4	3	-	6	3	4	31760.97	1.73E-06	6	3	4	-	6	2	5	24719.70	1.20E-06
6	3	4	-	6	2	5	24703.94	1.21E-06	6	3	4	-	5	2	3	57411.78	5.45E-06
6	3	4	-	5	2	3	57556.76	5.50E-06	6	4	3	-	6	1	6	79656.10	1.86E-08
6	4	3	-	6	1	6	79577.24	1.84E-08	6	2	5	-	6	1	6	23219.39	7.49E-07
6	2	5	-	6	1	6	23112.33	7.48E-07	5	4	1	-	6	1	6	42472.51	5.75E-10

THEORETICAL MODELS OF THE ISOBUTANOL MOLECULE CONFORMATIONS MICROWAVE SPECTRA

1						2	3	4					5	6
5	4	1	-	6	1	6	42338.96	5.66E-10					34516.47	3.61E-06
6	1	6	-	5	0	5	34653.03	3.64E-06					68948.65	1.04E-05
6	4	2	-	5	3	3	69047.52	1.05E-05					53710.72	2.10E-10
5	5	1	-	6	2	4	53880.50	2.05E-10					18856.59	1.40E-07
6	2	4	-	5	3	3	18793.39	1.39E-07					63110.44	1.34E-06
6	2	4	-	5	1	5	62981.28	1.37E-06					11305.75	1.48E-09
5	3	3	-	6	0	6	11143.03	1.44E-09					32948.10	3.22E-06
6	0	6	-	5	1	5	33044.86	3.24E-06					68627.46	1.04E-05
6	4	3	-	5	3	2	68739.47	1.05E-05					60089.66	1.96E-10
5	5	0	-	6	2	5	60123.73	1.92E-10					12190.74	4.22E-08
6	2	5	-	5	3	2	12274.57	4.31E-08					44163.31	3.48E-06
6	2	5	-	5	1	4	44323.10	3.50E-06					49937.62	5.55E-07
6	6	1	-	6	5	1	50010.83	5.59E-07					40747.06	6.69E-07
6	5	1	-	6	4	3	40809.50	6.74E-07					77930.65	7.75E-06
6	5	1	-	5	4	1	78047.77	7.79E-06					30890.69	5.09E-07
6	4	3	-	6	3	3	30966.27	5.14E-07					25546.02	3.09E-07
6	3	3	-	6	2	5	25498.64	3.11E-07					58238.10	3.40E-06
6	3	3	-	5	2	3	58351.46	3.42E-06					62485.63	2.43E-08
6	4	3	-	6	1	5	62605.49	2.37E-08					25302.04	4.33E-10
5	4	1	-	6	1	5	25367.22	4.23E-10					26643.16	2.23E-07
6	1	5	-	5	2	3	26712.23	2.26E-07					51686.94	1.66E-06
6	1	5	-	5	0	5	51624.78	1.67E-06					49938.19	5.55E-07
6	6	0	-	6	5	2	50011.35	5.59E-07					40712.27	6.68E-07
6	5	2	-	6	4	2	40776.57	6.73E-07					77937.03	7.75E-06
6	5	2	-	5	4	2	78053.81	7.79E-06					31751.25	5.30E-07
6	4	2	-	6	3	4	31793.37	5.35E-07					18340.80	2.26E-07
6	3	4	-	6	2	4	18460.76	2.29E-07					48503.15	5.35E-08
6	3	4	-	6	0	6	48397.18	5.32E-08					60978.96	3.37E-06
6	3	4	-	5	2	4	61041.81	3.38E-06					79690.33	6.44E-09
6	4	2	-	6	1	6	79609.64	6.38E-09					29598.28	1.02E-07
6	2	4	-	6	1	6	29355.51	1.03E-07					42465.58	2.00E-10
5	4	2	-	6	1	6	42332.40	1.98E-10					13039.88	1.70E-08
6	1	6	-	5	2	4	13225.54	1.77E-08					68661.69	5.16E-06
6	4	2	-	5	3	2	68771.88	5.18E-06					53710.77	7.31E-11
5	5	0	-	6	2	4	53880.55	7.14E-11					18569.63	5.08E-08
6	2	4	-	5	3	2	18517.75	5.05E-08					50542.20	2.70E-06
6	2	4	-	5	1	4	50566.28	2.71E-06					11592.71	5.05E-10
5	3	2	-	6	0	6	11418.67	4.92E-10					20379.85	6.12E-08
6	0	6	-	5	1	4	20629.86	6.40E-08					68914.41	5.18E-06
6	4	3	-	5	3	3	69015.12	5.21E-06					60089.61	6.82E-11
5	5	1	-	6	2	5	60123.68	6.68E-11					12477.70	1.76E-08
6	2	5	-	5	3	3	12550.21	1.80E-08					56731.55	1.83E-06
6	2	5	-	5	1	5	56738.10	1.84E-06					59032.87	2.26E-06
7	7	0	-	7	6	1	59118.95	2.27E-06					49845.07	3.05E-06
7	6	1	-	7	5	2	49920.82	3.06E-06					40491.72	2.86E-06
7	5	2	-	7	4	3	40563.14	2.87E-06					30010.04	2.02E-06
7	4	3	-	7	3	4	30110.49	2.04E-06					17945.77	1.05E-06
7	3	4	-	7	2	5	18027.26	1.06E-06					54676.43	1.69E-07
7	3	4	-	7	0	7	54426.86	1.70E-07					77084.81	1.69E-10
6	6	1	-	7	3	4	77266.05	1.65E-10					13599.88	5.52E-08
7	3	4	-	6	4	3	13554.28	5.48E-08					70036.59	5.93E-06
7	3	4	-	6	2	5	70019.18	6.01E-06					62324.04	1.69E-07
7	4	3	-	7	1	6	62400.49	1.65E-07					14368.23	7.30E-07
7	2	5	-	7	1	6	14262.75	7.25E-07					22362.43	7.81E-07
7	1	6	-	7	0	7	22136.86	7.74E-07					18714.13	2.29E-09
6	4	3	-	7	1	6	18735.73	2.23E-09					37722.59	2.48E-06
7	1	6	-	6	2	5	37729.18	2.47E-06					59032.91	2.26E-06
7	7	1	-	7	6	2	59118.99	2.27E-06					49848.36	3.05E-06
7	6	2	-	7	5	3	49923.90	3.06E-06					40611.27	2.87E-06
7	5	3	-	7	4	4	40676.42	2.89E-06					31818.53	2.21E-06
7	4	4	-	7	3	5	31855.17	2.22E-06					26084.27	1.55E-06
7	3	5	-	7	2	6	26038.52	1.55E-06					79016.20	1.72E-10
6	6	0	-	7	3	5	79127.14	1.68E-10					11634.26	3.90E-08

G.I. ISMAILZADEH, I.Z. MOVSUMOV, M.R. MENZELEYEV, A.S. QASANOVA, S.B. KAZIMOVA

1						2	3	4					5	6			
7	3	5	-	6	4	2	11660.79	3.92E-08	7	3	5	-	6	2	4	61726.31	6.60E-06
7	3	5	-	6	2	4	61914.92	6.66E-06	7	2	6	-	7	1	7	26360.10	1.00E-06
7	2	6	-	7	1	7	26215.49	1.00E-06	6	4	2	-	7	1	7	40810.11	1.14E-09
6	4	2	-	7	1	7	40593.22	1.12E-09	7	1	7	-	6	0	6	39444.29	5.70E-06
7	1	7	-	6	0	6	39597.33	5.75E-06	7	4	3	-	6	3	4	75326.93	1.23E-05
7	4	3	-	6	3	4	75425.74	1.24E-05	6	5	2	-	7	2	5	45092.40	8.84E-10
6	5	2	-	7	2	5	45281.96	8.60E-10	7	2	5	-	6	3	4	27371.12	4.60E-07
7	2	5	-	6	3	4	27287.99	4.54E-07	7	2	5	-	6	1	6	75310.20	1.35E-06
7	2	5	-	6	1	6	75104.26	1.37E-06	7	0	7	-	6	1	6	38579.55	5.41E-06
7	0	7	-	6	1	6	38704.65	5.45E-06	7	4	4	-	6	3	3	74377.71	1.21E-05
7	4	4	-	6	3	3	74514.63	1.22E-05	6	5	1	-	7	2	6	55162.84	7.83E-10
6	5	1	-	7	2	6	55154.83	7.66E-10	7	2	6	-	6	3	3	16474.91	9.06E-08
7	2	6	-	6	3	3	16620.94	9.33E-08	7	2	6	-	6	1	5	48069.86	5.02E-06
7	2	6	-	6	1	5	48260.17	5.06E-06	7	7	0	-	7	6	2	59032.91	7.73E-07
7	7	0	-	7	6	2	59118.99	7.78E-07	7	6	2	-	7	5	2	49845.02	1.02E-06
7	6	2	-	7	5	2	49920.78	1.03E-06	7	5	2	-	7	4	4	40614.61	9.17E-07
7	5	2	-	7	4	4	40679.54	9.24E-07	7	4	4	-	7	3	4	29887.14	5.84E-07
7	4	4	-	7	3	4	29994.09	5.91E-07	7	3	4	-	7	2	6	28015.65	3.47E-07
7	3	4	-	7	2	6	27899.60	3.51E-07	6	6	0	-	7	3	4	77084.82	5.87E-11
6	6	0	-	7	3	4	77266.05	5.75E-11	7	3	4	-	6	4	2	13565.64	2.00E-08
7	3	4	-	6	4	2	13521.87	2.00E-08	7	3	4	-	6	2	4	63657.70	4.74E-06
7	3	4	-	6	2	4	63776.00	4.75E-06	7	4	4	-	7	1	6	62201.14	5.95E-08
7	4	4	-	7	1	6	62284.09	5.82E-08	6	4	2	-	7	1	6	18748.36	7.93E-10
6	4	2	-	7	1	6	18768.13	7.76E-10	7	1	6	-	6	2	4	31343.70	3.47E-07
7	1	6	-	6	2	4	31486.00	3.55E-07	7	1	6	-	6	0	6	61506.04	2.32E-06
7	1	6	-	6	0	6	61422.42	2.33E-06	7	7	1	-	7	6	1	59032.87	7.73E-07
7	7	1	-	7	6	1	59118.95	7.78E-07	7	6	1	-	7	5	3	49848.41	1.02E-06
7	6	1	-	7	5	3	49923.94	1.03E-06	7	5	3	-	7	4	3	40488.38	9.12E-07
7	5	3	-	7	4	3	40560.02	9.20E-07	7	4	3	-	7	3	5	31941.42	6.43E-07
7	4	3	-	7	3	5	31971.57	6.48E-07	7	3	5	-	7	2	5	16014.39	2.18E-07
7	3	5	-	7	2	5	16166.18	2.22E-07	7	3	5	-	7	0	7	52745.05	7.83E-08
7	3	5	-	7	0	7	52565.78	7.83E-08	6	6	1	-	7	3	5	79016.20	5.97E-11
6	6	1	-	7	3	5	79127.13	5.84E-11	7	3	5	-	6	4	3	11668.49	1.44E-08
7	3	5	-	6	4	3	11693.19	1.45E-08	7	3	5	-	6	2	5	68105.20	4.51E-06
7	3	5	-	6	2	5	68158.10	4.53E-06	7	2	5	-	7	1	7	36429.98	1.08E-07
7	2	5	-	7	1	7	36087.84	1.09E-07	6	4	3	-	7	1	7	40775.88	3.97E-10
6	4	3	-	7	1	7	40560.82	3.92E-10	7	1	7	-	6	2	5	15660.84	2.65E-08
7	1	7	-	6	2	5	15904.09	2.78E-08	7	4	3	-	6	3	3	74500.61	6.55E-06
7	4	3	-	6	3	3	74631.04	6.58E-06	6	5	1	-	7	2	5	45092.96	3.07E-10
6	5	1	-	7	2	5	45282.48	3.00E-10	7	2	5	-	6	3	3	26544.80	1.65E-07
7	2	5	-	6	3	3	26493.29	1.64E-07	7	2	5	-	6	1	5	58139.74	3.91E-06
7	2	5	-	6	1	5	58132.51	3.92E-06	6	3	3	-	7	0	7	10185.86	5.05E-10
7	0	7	-	6	1	5	21732.91	6.40E-08	7	0	7	-	6	1	5	21409.08	6.08E-08
7	4	4	-	6	3	4	75309.33	6.64E-06	7	4	4	-	6	3	4	75204.04	6.61E-06
6	5	2	-	7	2	6	55154.30	2.67E-10	6	5	2	-	7	2	6	55162.28	2.72E-10
7	2	6	-	6	3	4	17415.64	4.64E-08	7	2	6	-	6	3	4	17301.24	4.54E-08
7	2	6	-	6	1	6	65231.91	2.51E-06	7	2	6	-	6	1	6	65240.32	2.50E-06
8	8	0	-	8	7	1	68225.44	2.99E-06	8	8	0	-	8	7	1	68126.43	2.97E-06
8	7	1	-	8	6	2	59040.76	4.27E-06	8	7	1	-	8	6	2	58952.52	4.25E-06
8	6	2	-	8	5	3	49782.25	4.35E-06	8	6	2	-	8	5	3	49702.40	4.33E-06
8	5	3	-	8	4	4	40191.93	3.62E-06	8	5	3	-	8	4	4	40107.16	3.60E-06
8	4	4	-	8	3	5	28763.24	2.31E-06	8	4	4	-	8	3	5	28629.70	2.30E-06
8	3	5	-	8	2	6	17273.71	1.21E-06	8	3	5	-	8	2	6	17224.63	1.21E-06
8	3	5	-	8	0	8	61349.93	1.79E-07	8	3	5	-	8	0	8	61739.18	1.77E-07
7	6	2	-	8	3	5	69151.54	7.02E-10	7	6	2	-	8	3	5	68927.38	7.19E-10
8	3	5	-	7	4	4	21448.78	2.00E-07	8	3	5	-	7	4	4	21532.25	2.01E-07
8	3	5	-	7	2	6	79342.47	6.26E-06	8	3	5	-	7	2	6	79435.05	6.16E-06
8	4	4	-	8	1	7	63221.06	3.17E-07	8	4	4	-	8	1	7	63219.58	3.22E-07
8	2	6	-	8	1	7	17184.11	1.04E-06	8	2	6	-	8	1	7	17365.25	1.05E-06
8	1	7	-	8	0	8	26892.11	1.11E-06	8	1	7	-	8	0	8	27149.30	1.12E-06
7	4	4	-	8	1	7	13009.04	2.52E-09	7	4	4	-	8	1	7	13057.63	2.59E-09
8	1	7	-	7	2	6	44884.65	4.80E-06	8	1	7	-	7	2	6	44845.17	4.82E-06
8	8	1	-	8	7	2	68225.45	2.99E-06	8	8	1	-	8	7	2	68126.44	2.97E-06

THEORETICAL MODELS OF THE ISOBUTANOL MOLECULE CONFORMATIONS MICROWAVE SPECTRA

1						2	3	4						5	6		
8	7	2	-	8	6	3	59041.03	4.27E-06	8	7	2	-	8	6	3	58952.80	4.25E-06
8	6	3	-	8	5	4	49795.30	4.35E-06	8	6	3	-	8	5	4	49716.38	4.33E-06
8	5	4	-	8	4	5	40516.91	3.67E-06	8	5	4	-	8	4	5	40449.71	3.66E-06
8	4	5	-	8	3	6	32138.31	2.72E-06	8	4	5	-	8	3	6	32116.29	2.71E-06
8	3	6	-	8	2	7	27832.21	1.96E-06	8	3	6	-	8	2	7	27915.49	1.96E-06
7	6	1	-	8	3	6	72864.95	7.22E-10	7	6	1	-	8	3	6	72770.84	7.40E-10
8	3	6	-	7	4	3	17619.01	1.24E-07	8	3	6	-	7	4	3	17565.94	1.23E-07
8	3	6	-	7	2	5	65756.76	8.11E-06	8	3	6	-	7	2	5	65521.75	8.04E-06
8	2	7	-	8	1	8	29643.20	1.30E-06	8	2	7	-	8	1	8	29825.90	1.31E-06
7	4	3	-	8	1	8	39856.41	1.69E-09	7	4	3	-	8	1	8	40175.45	1.71E-09
8	1	8	-	7	0	7	44680.94	8.58E-06	8	1	8	-	7	0	7	44511.02	8.50E-06
7	5	3	-	8	2	6	36501.36	2.06E-09	7	5	3	-	8	2	6	36303.65	2.12E-09
8	2	6	-	7	3	5	36030.24	1.17E-06	8	2	6	-	7	3	5	36126.15	1.18E-06
8	0	8	-	7	1	7	44208.03	8.37E-06	8	0	8	-	7	1	7	44055.97	8.31E-06
8	4	5	-	7	3	4	79867.81	1.39E-05	8	4	5	-	7	3	4	79692.28	1.38E-05
7	5	2	-	8	2	7	50776.34	1.78E-09	7	5	2	-	8	2	7	50841.26	1.82E-09
8	2	7	-	7	3	4	19897.29	1.33E-07	8	2	7	-	7	3	4	19660.50	1.27E-07
8	2	7	-	7	1	6	52187.29	7.23E-06	8	2	7	-	7	1	6	51974.50	7.19E-06
8	8	1	-	8	7	1	68225.44	1.03E-06	8	8	1	-	8	7	1	68126.43	1.02E-06
8	7	1	-	8	6	3	59041.03	1.44E-06	8	7	1	-	8	6	3	58952.80	1.43E-06
8	6	3	-	8	5	3	49781.98	1.42E-06	8	6	3	-	8	5	3	49702.11	1.41E-06

-
- [1] *A Maeda A., De Lucia F.C., and E. Herbst.* The Astrophysical Journal Supplement Series. 2006, 162, C .428-435.
- [2] *J.C. Pearson, Sastry K.V.L.N., E. Herbst and F.C. De Lucia.* Journal of Molecular Spectroscopy.- 1996.-175, Issue 2.- pp 246-261.
- [3] *Ch.O. Qajar, S.A. Musayev, E.Yu. Salayev.* J. of Applied Spectroscopy. 1983, vol. 39, p.793.
- [4] *O.I. Baskakov, M.A. Pashaev.* J. of Molecular Spectroscopy. 1992.-Vol.151, Issue 2, pp. 282-291.
- [5] *O.N. Ulenikov, A.B. Malikova, Ch.O. Qajar, S.A. Musaev, A.A. Adilov & M.I. Mehtiev.* J. of Molecular Spectroscopy. 1991, Vol.145.- Issue 2, pp. 262-269.
- [6] *G.I. İsmayılpənahov, İ.Z. Məvsumov, M.R. Menzəleyev.* MEA “Fizika” jurnalı, cild XVIII, №1, 2012, pp.31-36.

Received: 12.02.2014

INFLUENCE OF GAMMA RADIATION ON MONO-CRYSTALLINE SILICON SOLAR CELLS

DAVUD MOSTAFA TOBNAGHI^{1*} AND RAHIM MADATOV²

¹*Department of Electrical Engineering, Parsabad Moghan Branch,*

Islamic Azad University, Parsabad Moghan, Iran

²*Institute of Radiation Problems, Azerbaijan National Academy of Science, Baku, Azerbaijan*

**Corresponding Authors Email: d.mostafa.t@gmail.com*

In this experimental work, the change in output parameters of the mono-crystalline silicon solar cells was investigated under gamma irradiation. Experimental results showed that the main parameters of solar cells such as efficiency, open circuit voltage, short circuit current etc. changed to different extent with increasing the gamma radiation doses from 100 to 2000 krad. The parameters of I_{sc} and η decrease proportionally to the increase of the gamma radiation doses whereas V_{oc} is only slightly decreased. Large amount of radiation induced defects in the high dose have been formed. Obtained results could lead to new designs of silicon solar to increasing their applications in radiation environments.

Keywords: silicon solar cell, gamma radiation, current-voltage characteristics, short circuit current, open circuit voltage.

PACS: 61.82.-d, 61.82.Fk

1. INTRODUCTION

Mono-crystalline silicon solar cells are still the basic elements for photovoltaic conversion of solar energy. Regardless of the very high standards in the production of mono-crystalline silicon solar cells, it has been proved that silicon solar cells are extremely sensitive to electromagnetic radiation with substantially short wavelengths, such as x-rays and gamma rays.

During their operating lifetime, solar cells are exposed to radiation environments in which they are used, such as military and civil nuclear environments, etc. Studying radiation resistance of solar cells is interesting not only for the purpose of predicting lifespan of solar cells, but also to improve design of solar cells used in high radiation environments.

This is especially important for solar cells used in PV systems located near nuclear power plants [1-4].

When silicon solar cells irradiated with gamma rays, two types of radiation damage occur within it: displacement damage and ionization effects. Displacement damage is the movement of atoms from their initial location in the crystal lattice to another placement that results a defect in the crystal lattice of solar cells.

Ionization effect is the generation of electron-hole pairs in the bulk of solar cell that results radiation effects.

These defects mostly act as recombination points that decreased the diffusion length and life time of minority carrier as well as increased internal parameters of cells.

Output parameters of solar cell such as maximum output power, fill factor, efficiency, short circuit current, and open circuit voltage- P_{mp} , ff , η , I_{sc} , V_{oc} respectively strongly depend on internal parameters of solar cells such as series resistance, R_s , saturation current, I_0 and ideal factor, n . It has been proved that increasing each of above internal parameters of solar cell causes that the output characteristics of solar cells decreased [5-8].

Hence the changes in the electrical parameters of Mono-crystalline silicon solar cells samples under various doses of gamma radiation are presented in this paper.

2. EXPERIMENTAL METHODS

In this paper, the four samples of the commercially silicon solar cells having same characteristics are used for experimental measurements. The specifications of samples are shown in Table 1. The solar cells were fabricated mono-crystalline structure using phosphorus diffusion into a p-type silicon wafer. All four samples were irradiated with ^{60}Co gamma source with the energy of 1.23 MeV. The samples 1, 2, ..., 4 were irradiated with dose 100, 500, 1000, 2000 Krad respectively. Irradiation of cells was carried out in laboratory at the Institute of Radiation Problems of Azerbaijan National Academy of science.

Voltage-current (I-V) characteristics of all samples before and after irradiation were measured. To obtain of solar cells I-V characteristics samples were illuminated by reflective lamp with Light intensity equal to 1000 W/m^2 (corresponding to AM1.5).

The measurements were performed at room temperature with highly accurate measuring equipment.

Table 1
Properties of four samples of the experimental solar cells
(before irradiation)

Cells type	V_{oc} [mV]	I_{sc} [mA/cm ²]	P_{mmp} [mW/cm ²]	FF	η [%]
Si-monocrystalline	570	34	14	0.72	13.9

Notes: Condition for measurement: 1000 W/m^2 , AM 1.5, 25°C.

3. RESULTS AND DISCUSSION

Voltage-current characteristics of four solar cell samples before and after various doses of gamma radiation at under AM 1.5 illumination condition have been showed in figure 1. As can be seen, I-V characteristics of cells deteriorated with increasing gamma irradiation. From figure 1, fundamental parameters of solar cells like open circuit voltage (V_{oc}),

INFLUENCE OF GAMMA RADIATION ON MONO-CRYSTALLINE SILICON SOLAR CELLS

short circuit current (I_{sc}), fill factor (ff) and efficiency (η) could be extracted.

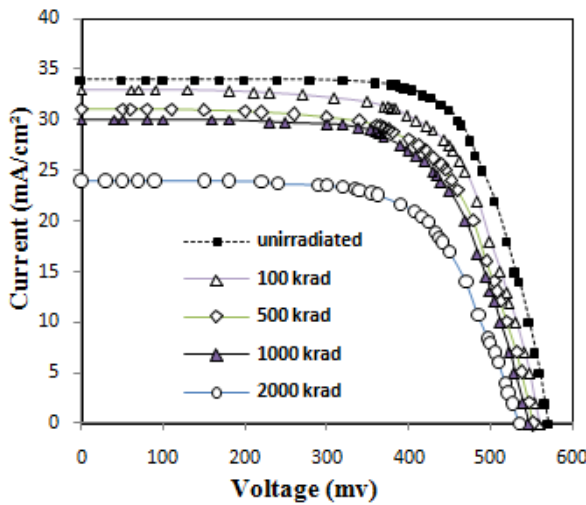


Fig. 1. The I - V characteristics of silicon solar cell irradiated with various doses of gamma radiation.

The fill factor (FF) parameter for solar cells can be expressed as

$$FF = \frac{V_{mp} I_{mp}}{V_{oc} I_{sc}} \quad (1)$$

Where V_{oc} and I_{sc} are the open circuit voltage and short circuit current, V_{mp} and I_{mp} are the voltage and the current at a maximum power point respectively.

The efficiency (η) for a solar cell is given by

$$\eta = \frac{V_{oc} I_{sc} FF}{P_{in}} \quad (2)$$

Where, P_{in} is the incident light power [14].

Figure 2 shows the changes in solar cells parameters as a function of gamma dose. The parameters are normalized to the values obtained before samples irradiated. It was found that the degradation of the solar cell parameters is dependent on the gamma radiation dose and the irradiation has affected the solar cell parameters to a certain extent. There is no substantial variation in the fill factor, which in some cases showed increased or relatively steady values. According to the results, the gamma radiation causes a significant Reduction in the short circuit current and efficiency while the open circuit voltage is slightly reduced. The decrease in the efficiency and short circuit current of solar cells under gamma radiation could be related to the minority carrier life time. The minority carrier life time is sensitive to the radiation induced defects and the decrease in the minority carrier life time reduced the electric properties of solar cells. According to results a large amount of radiation induced defects in the high dose have been formed [9-12]. The detail of solar cells parameters degraded under gamma radiation doses are shown in table 2.

Degradation of solar cell parameters under gamma radiation doses.

solar cell Sample	γ doses [Krad]	V_{OC} [mV]	I_{SC} [$\frac{mA}{cm^2}$]	V_{mp} [mV]	I_{mp} [$\frac{mA}{cm^2}$]	FF	η [%]
Mono-crystalline silicon	0	570	34	450	31	0.72	13.95
	100	560	33	440	29	0.674	12.47
	500	552	31	420	27	0.662	11.34
	1000	547	30	420	25.9	0.663	10.87
	2000	535	24	407	21	0.665	8.54

The short circuit current is because of the generation and collection of light-generated carriers. It was determined as:

$$I_{sc} = q \cdot G \cdot P \quad (3)$$

Where q is electron charge, G is number of carriers generated in the solar cell, and P is the collection probability of carriers. Since the amount of G remains approximately constant [13], decrease in the I_{sc} essentially relevant to the collection probability. The collection probability of carriers depends on the surface passivation and the minority carrier diffusion length in the base. Gamma radiation causes the activation of solar cell surface and also increases defects near the upper surface. Ultimately recombination is increased in the solar cell so P is decreased. In the base layer, irradiation of γ ray reduces the lifetime of minority carrier and the diffusion

length of minority carriers much smaller than the base thickness, $L_n \ll d_b$, the P value can be determined as:

$$P = \frac{\alpha L_n}{\alpha L_n + 1} \quad (4)$$

Where α is light absorption coefficient,

$L_n = \sqrt{D_n \tau_n}$, and D_n is the electron diffusion coefficient and τ_n is the minority carrier lifetime.

The open circuit voltage can be obtained using the following equation:

$$V_{oc} = \frac{n k T}{q} \ln \frac{I_{sc}}{I_0} \quad (5)$$

According to Eq. (5) V_{oc} does not change significantly with increasing n and I_0 and decreasing I_{sc} [13].

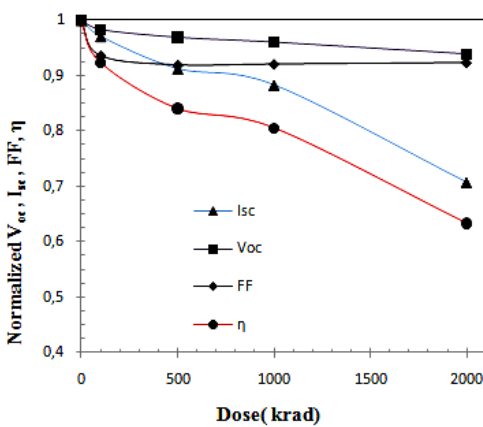


Fig. 2. Normalized solar cell parameters as a function of gamma radiation dose.

4. CONCLUSIONS

A deterioration of the electric properties of solar cells was observed when the gamma dose was increased (100-2000 krad). Except the fill factor, which in some cases showed increased or relatively steady values, gamma radiation causes a significant Reduction in the I_{sc} and η while the V_{oc} is slightly reduced. The decrease in short circuit current and other fundamental parameters is mainly related to the minority carrier life time. The life time of minority carriers is sensitive to the radiation induced defects that mostly act as recombination points, and the decrease in the minority carrier life time reduced the solar cells parameters.

- [1] T.M. Razikov, C.S. Ferekides, D. Morel, E. Stefanakos, and H.S. Ullal, Solar photovoltaic electricity: Current status and future prospects, *Solar Energy*, vol. 85, no. 8, pp. 1580–1608, 2011.
- [2] H.M. Diab, A. Ibrahim, and R. ElMallawany. Silicon Solar Cells as a Gamma Ray Dosimeter, *Measurement*, Vol. 46, no. 9, pp. 3635–3639, 2013
- [3] M. Alurraldea, M.J.L. Tamasi, and C.J. Bruno. Experimental and theoretical radiation damage studies on crystalline silicon solar cells, *Solar Energy Materials & Solar Cells*, vol. 82, no. 4, pp. 531–542, 2004
- [4] Vasić, M. Vujisić, B. Lončar, and P. Osmokrović. Aging of solar cells under working conditions, *Journal of optoelectronics and advanced materials*, Vol. 9, No. 6, pp. 1843 – 1846, 2007
- [5] A.Vasic, M. Vujisic, K. Stankovic and B. Jovanovic. Ambiguous Influence of Radiation Effects in Solar Cells, *Proceedings of Progressin Electromagnetics Research Symposium Proceedings*, pp. 1199–1203, 2010.
- [6] Dejan Nikolic, Koviljka Stankovic, Ljubinko Timotijevi. Comparative Study of Gamma Radiation Effects on Solar Cells, and Phototransistors, Article ID 843174, 2013
- [7] Jayashree, Student Member, IEEE, Ramani, M. C. Radhakrishna, Anil Agrawal, Saif Ahmad Khan, and A. Meulenberg. The Influence of High-Energy Lithium Ion Irradiation on Electrical Characteristics of Silicon and GaAs Solar Cells, *IEEE Transactions on nuclear science*, vol. 53, no. 6, pp. 3779-3785, 2006.
- [8] A.M. Saad. Effect of cobalt 60 and 1 MeV electron irradiation on silicon photodiodes solar cells, *Canadian Journal of Physics*, vol. 80, no. 12, pp. 1591-1599, 2002
- [9] S.M. Sze. *Physics of Semiconductor Devices*, 2nd edition, Wiley Interscience, NewYork, 1981.
- [10] Khuram Ali, Sohail A. Khan, and M.Z. MatJafri. ^{60}Co γ -irradiation Effects on Electrical Characteristics of Monocrystalline Silicon Solar Cell, *International Journal of Electrochemical Science*, vol.8, pp. 7831 – 7841, 2013
- [11] M. Alurralde, M.J.L. Tamasi, and C.J. Bruno. Experimental and theoretical radiation damage studies on crystalline silicon solar cells, *Solar Energy Materials & Solar Cells*, vol. 82, no. 4, pp. 531–542, 2004.
- [12] M. Imaizumi, S. J. Taylor, T.Hisamatsu, S.Matsuda, O.Kawasaki. Analysis of the spectral response of silicon solar cells, *Proceedings of the 26th PVSC Proceedings, IEEE*, pp.3–6, 1997.
- [13] N.A. Guseynov, Ya.M. Olikh, and Sh.G. Askerov. Ultrasonic treatment restores the photoelectric parameters of silicon solar cells degraded under the action of ^{60}Co gamma radiation, *Technical Physics Letters*, Vol. 33, no. 1, pp. 18–21, 2007
- [14] P. Sathyaranayana Bhat, A. Rao, H. Krishnan, and G. Sanjeev. A study on the variation of c-Si solar cell parameters under 8Me electron irradiation, *Solar EnergyMaterials&SolarCells*, vol. 120A, PP 191-196, 2014.

Received: 15.01.2014

ULTRA DISPERSE STATE OF POLYMER PHASE AS STABILIZER IN NANOSIZED BaTiO₃ AND POLAR AND NONPOLAR POLYMER COMPOSITES

**M.A. KURBANOV, A.A. BAYRAMOV, F.N. TATARLAR, F.F. YAHYAYEV,
A.A. NURALIYEV, Z.A. DADASHOV, B.Kh. KhUDAYAROV**

*H.Abdullayev Institute of Physics of Azerbaijan National Academy of Sciences,
Baku, AZ-1143, H. Javid Avenue, 33*

There have been described the new technology of uniform distribution of nanoparticles in polymer materials. Two factors are basis for offered technology:

- 1) creation functional oxygenic groups stabilizing nanoparticles along macromolecule chain;
- 2) use stabilizing state of polymer macromolecule segments under the action of electric gas discharge.

It was shown that creation of polymer macromolecule segments under the action of electric gas discharge and high mobility of segments prevent nanoparticles mobilization in polymer solution.

Keywords: ultra disperse state, polymer phase, nanoparticle.

PACS: 77.84.Lf

INTRODUCTION

At present, there have been widely investigated electret, pyro- and piezoelectric composites based on the polar and nonpolar polymer dispersed by ferropiezoceramic particles [1–3]. Various power and low capacity acoustoelectric and electroacoustic transducers based on these composites have been developed. It should be noted when we use piezoelectric transducers in various conditions we reveal its disadvantages. For example, transducers based on the polymer piezoelectric composites have a high piezosensitivity $g_{ij} = d_{ij} / \varepsilon \epsilon_0$ in regime of receiving acoustic waves (mechanical excitation): here, d_{ij} is a piezomodulus, ε is a dielectric permittivity, ϵ_0 is a dielectric constant. But in regime of radiation of elastic waves these transducers are less effective, because their electromechanical properties [electromechanical coupling coefficient K_{ij} , specific acoustic power $(d_{ij} Y)^2$, mechanic Q_m and piezoelectric quality coefficient $K_{ij}^2 / tg\delta$ and high mechanical elasticity S_{11}^2] [4] are small. For piezocomposite transducers a frequency range of amplitude-frequency characteristic isn't wide and for $f \geq 7$ kHz a value of output signal decreases appreciably [3–5].

There is a very important application of piezocomposite elements as sources of elastic waves intensive radiation [6]. But low electromechanical parameters of piezocomposite element is a reason for decreasing efficiency of antenna based on these composites in radiation regime. From Physics of polymer materials we know that physical-mechanical and electromechanical properties of matrix composites are depended on mobility of molecules and interphase interaction, therefore by variation of above mentioned factors we can regulate piezoelectric and electromechanical properties of composites and use as high powerful acoustic waves generator. We can assume that nanotechnology can create both powerful and low-power piezoelectric transducers. In this case the main component of piezoelectric nanocomposites should be various structure nanosized piezoelectric particles. But now there

aren't considerable results of possibility obtaining nanosized particles which are more effective than multicomponent piezoceramic PZT materials. As we know, piezoceramic PZT materials have stable structure and therefore they are based on these materials more effective obtaining transducers, acoustic transceiver antennas and various sensors [1,3,5,7,8]. Nanophase composites are strongly differed from ordinary microsized active phase materials [7]. In this way nanoparticles immobilization in polymer phase isn't solved problem up to now. Theoretical and experimental analysis show that there are differed each from other technology methods: obtaining polydispersed colloidal particles, particle immobilization in polymer matrix under the action of ultradispersed waves, chemical method - nanoparticles penetration into polymer during polycondensation, polymerization and copolymerization processes.

Application of these methods will allow us to fulfil nanoparticles immobilization in polymer phase. But the first method is more difficult. Second method has more complex structure and is used under the action of acoustic transducers and is connected with cavitation effect. Therefore, immobilization process is depended on distribution of cavitation centers. During cavitation usually released energy isn't sufficient for immobilization and there isn't possible increasing and controlling energy in this process. Using corona discharge it is difficult to increase the rate of immobilization process, there aren't possible by increase applied voltage in discharge canals to change energy.

The main goal of this work is a development of technology use ultradispersed state of polymer macromolecules in nanocomposites as stabilizer.

For solving this problem below tasks had been solved:

- Development of technology of polar and nonpolar polymers dissolution technology under the actions of plasma of electric discharge, temperature and organic solvents;
- Development of technology of using ultradispersed state of polymer macromolecules in nanocomposites as stabilizer;

- Development of disperse technology of (SiO_2 , BaTiO_3) nanoparticles in PE and PVDF;
- Choice and calculation of special construction of cells for creation of active centers with oxygen in nano- and microsized piezophase hybrid composites;
- Choice of barrier type electric gas discharge for use of ultradispersed state of nanoparticles in polymer composites as stabilizer; and development cells for carry out this process.

EXPERIMENTS

We had used organic, inorganic nano- and microsized phase polymer composites had been used. There had been selected SiO_2 and BaTiO_3 with 70–100 nm sizes as inorganic nanophas. There had been used $\text{Pb}(\text{TiZr})\text{O}_3$ PZT piezoelectric materials with various (R_e , T, R_e+T) structures as microsized piezoceramic phase. We had took polar and nonpolar PE and PVDF polymers as organic phases. There had been used IR spectroscopy, thermodepolarizing current method and barrier type electric gas discharge technology.

RESULTS AND DISCUSSION

There had been developed more effective immobilization technology by used barrier type electric gas discharge. We had used metal-dielectric-gas gap – polymer solution-dielectric-metal structure (fig. 1). We have chose this system that in wide range to regulate energy of gas discharge in plasma channels. Realy, in offered dielectric structure we can modify parameters of electric gas discharge in wide range by changing of electric-physical parameters of dielectric, gas gap, solution, composite and geometric sizes.

One of the necessary steps of new piezoelectric forming problem based on the hybrid of polymer matrix composites with nano- and microsized phases is obtainning nanostructured polymer solution, deposition on the piezosubstrate and prediction. First of all, we obtain polymer solution, then structure by BaTiO_3 and SiO_2 nanoparticles with size of 70 nm under the action of electric gaz discharge plasma. As solvent we used toluene and xylene. The process of dissolution we had carried out under the simultaneous action of temperature and electric gas discharge at frequency of 50 Hz and amplitude of 25000 V. For increasing the rate of polymer dissolution we divede polymer macromolecule to small fragments under the action of electric gas discharge and as result we provide necessary variation of polymer dissolution in toluene. The destruction of macromolecule we have carryied out under the simultaneous action of synthesized in plasma channel high energy electrons, ions, ionizing radiation and oxygenous small molecule active compounds. Under the action of high voltage the electric discharge is formed in gas gap between polymer solution and dielectric anod. So, polymer solution is acted by uninterrupted electric gas discharge. The plasma of barrier electric gas discharge is formed in cell shown in fig.1: the structure of cell is metal=dielectric-gas-polymer solution-piezoelectric substrate-metal. The change of polymer structure is shown in fig.2. As we can see that the PE phase of composite is not acted sharp structure change and there have been formed various oxygen small

molecular compounds in polymer chain. The process of polymer dissolution in toluene and nanostructurization have been carried out at temperature of 20-40 K low than boiling temperature. Then one of the main stages is immobilization of preliminarily encapsulated BaTiO_3 and SiO_2 nanoparticles with size of 60-70 nm.

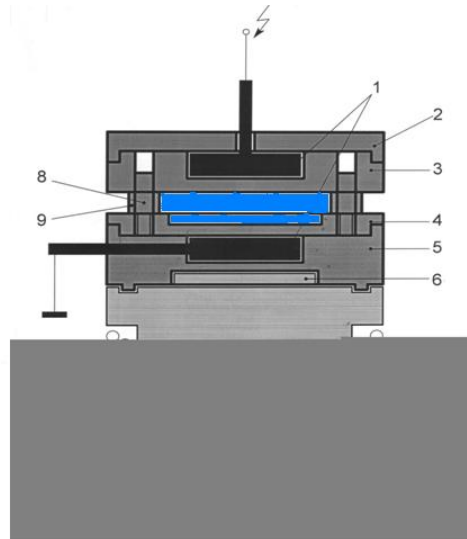


Fig 1. The offered cell for polymer solution nanostructurization.

1 – electrodes, 2 – dielectric washer, 3 – dielectric anode, 4 – dielectric cathode, 5 – insulator, 6 – metal cylinder, 7 – heating element, 8 – guiding, 9 – dielectric distance limiter. $E_p=3,6 \text{ MV/m}$; $T_p=383 \text{ K}$; $t_p=0,5 \text{ hours}$.

In addition to that there have been formed active gas products, ionizing radiation, high energy electrons, ions and mechanical waves during electric discharge in gas gap of the structure of dielectric-gas-polymer solution. Under the action of these the process of nanoparticle mobilization is broke, and in another hand there have been formed a new immobilization centers. On of the pozitive side of application of dielectric structure isn't point stabilization of plazma channels on the dielectric structure surface but providing uniform distribution of them. The main reason of this there have been formed electric spots on the dielectric surface by creation of each discharge channels. During formation of each local discharge we can observe a stabilization of electric charges in zone of their channels contacts with dielectric. From this reason, the second plazma channel is formed as possible far from of the first one. At satisfaction of this prinsipe for following microdischarges the final result is an uniform distribution of microdischarges on the dielectric surface. That is, there have been provided uniform probability of immobilization process onto whole volume of polymer solution. At this time, the volume of taken polymer solution is practically under acted of electric discharge and in this volume the probability of mobilization effect formation is broken. It should be note that the efficiency of used method is an optimization of technological parameters. For this we have to determine the dependence of characteristics of electric gas discharge plasma on the characteristic parameter of immobilization. The characteristic parameter of immobilization effect, as we assume, is a multicomponent function.

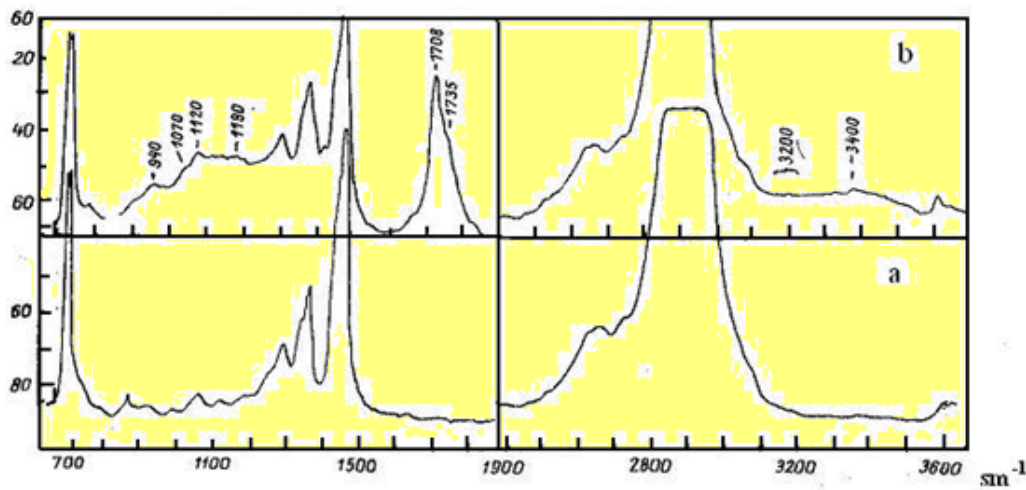


Fig. 2. IR spectrum for modified PE: a – initial PE; b – modified PE; air gap d = 4mm, voltage applied to cell U = 10 kV, p = 10⁵ Pa, modification duration t = (0,25-1) hours.

In the work we have offered a new method of connection between characteristics of the spectrum of thermostimulated depolarization (TSD) current for hybrid composites under the action of electric gas discharge plasma channels. Based on this method we have to determine a dependence of TSD spectrum characteristics: ΔT corresponded to difference of maximum and minimum values of TSD graph, transferred electric charge Δq . There has been presented the dependence of ΔT on ΔW in figure 3. The main result obtained from this experiment is that increasing temperature corresponding maximum of TSD spectrum at increasing immobilization process. Also, the similar effect has been obtained for $\Delta q = f(\Delta W)$. Here, Δq is a transferred charge in discrete plasma channel, T_p is a temperature corresponding to TSD spectrum maximum and ΔW is an energy released in discrete plasma channel.

For understanding a diagnostics essence of TSD method of hybrid piezoelectric materials structurization by BaTiO₃, SiO₂ nanoparticles we should take account next factors:

- If there is an immobilization effect then in polarization process the action ranges of nanoparticles in polymer phase of composite are transformed to active centers (traps) for injected electric charges;
- Macromolecules motion is restricted around of active centers;
- The amount of electric charge carriers determined on the basis of TSD current spectrum is in proportion to the concentration of active centers formed during nanostructurization;
- There is a process of macromolecules decay to segments with small molecular mass at some energy of plasma channels ($\Delta W \geq 4,5 \cdot 10^{-6}$ C – $8,0 \cdot 10^{-6}$ C) formed in the system of test cell of dielectric anod-gas phase-polymer solution; and these macromolecules are stabilizers of nanoparticles that is stabilizers of ultradisperse state under the simultaneous action of plasma of electric discharge and temperature;

- There are enough differences between the maximums of temperature ($T_{\max}^{hib}, T_{\max}^{mk}$) corresponding to TSD spectrums for composites based on the only micrized phase and nano- and micro-sized phase hybrid composites.

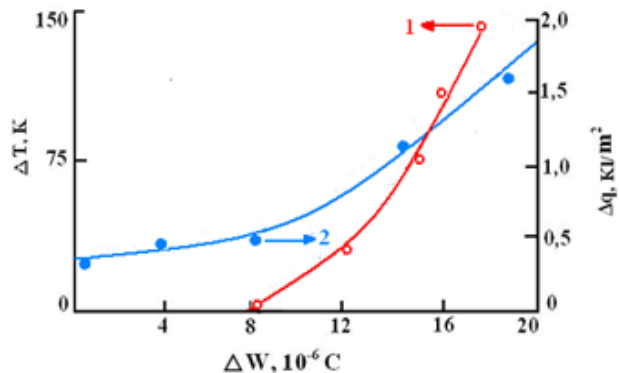


Fig.3. Dependences: $\Delta T = f(\Delta W)$ (curve 1); $\Delta q = f(\Delta W)$ (curve 2).

So, the analysis of obtained results indicates that using electric discharge plasma for immobilization effect in polymer composites is a good both technology and scientific method.

Up to now the forecast of composite nanostructurization isn't a solved problem. For this we used TSD spectrum. Shortly, the importance of this method is: it is adopted, if there isn't immobilization then microcomposites's TSD spectrum isn't differ from nanocomposites's one. It indicates that intercalated into polymer nanoparticles are mobilized as large clusters, that is, they like microparticles. If there is a nanostructurization in composite then TSD spectrums are differed and formed in spectrum the maximum of temperature shifts to high temperature. Parameter $\Delta T = T_{\max}^{nk} - T_{\max}^{mk}$ is used for determination of nanostructurization degree. TSD current spectrums for PE and PVDF matrix composites are shown in figures 4, 5 and 6. From analysis of these spectrums we can conclude:

- The same polymer matrix nano- and microcomposites's TSD spectrums are sharply differed. At least two maximums are observed in composites with microsized piezoelectric phase;
- There is a wide maximum in high temperature range in the same polymer matrix composites.

There have been exactly observed low temperature maximums for both PE and PVDF microsized composites. Their temperature ranges are due to temperature depended processes in initial polymer molecular structure not dispersed by piezoelectric ceramic particles. In TSD spectrum for composites dispersed by nanoparticles closed to polymer matrix melting temperature the formed maximum indicates that nanoparticles restrict a heat-motion intensivity of molecular chain. In figure 6 there is shown TSD current spectrum for nanoparticles volume distribution. The structure of TSD spectrum is changed when in composite a nanosized non-organic volume phase is changes, and we don't observe low temperature spectrums of microsized piezophase composite. There have been obtained the same but more complex spectrums for PVDF matrix composites. Spectrums are changed when the volume content of BaTiO_3 particvles in composite is changed, and, as result, there have been formed a single wide spectrum. The experimental results show that the change of volume content of BaTiO_3 particles leads to decreasing mechanical and physical properties of composite. Under the action of electric gas discharge physical and chemical effects are formed in polymer phase and control immobilization. There are next effects:

- under the action of electric gas discharge there have been formed active oxygen centers as result oxidation along polymer chain;
- IR spectroscopy demonstrates chemical changes in polymer phase after crystallization (figure 2).

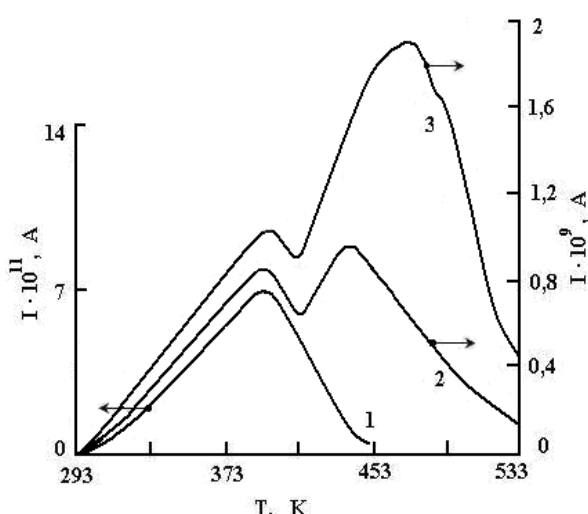


Fig.4. ASPE-50 vol.% PKR-7M micropiezocomposite's TSD current spectrum. 1– only ASPE; 2–ASPE-50 vol.% PKR-7M microcomposite; 3– polymer cryastalizad under the action of electric gas discharge. $E_p = 3,6 \frac{\text{MV}}{\text{m}}$; $T_p=383 \text{ K}$; $t_p=0,5 \text{ hours}$.

Obtained results show that under the action of electric gas discharge polymer phase is sharply oxidized and nanoparticles can become stable in oxidized centers. A small amount of these centers in polymer phase leads to decreasing process of immobilization formation and increasing probability of large clastes formation (see TSD current spectrum in figure 5).

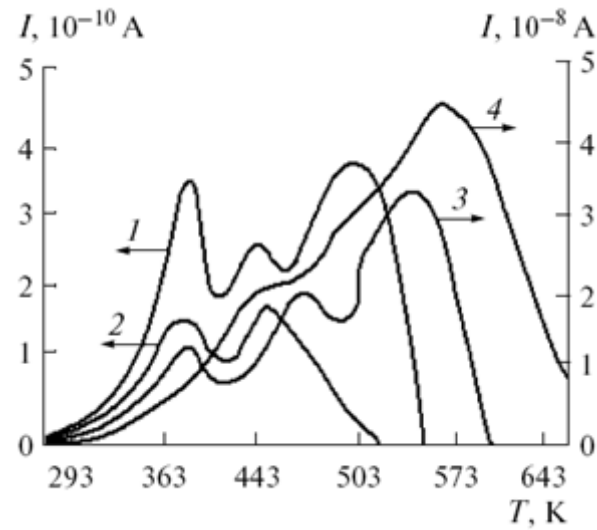


Fig. 5. TSD current spectrums for microsized and nanosized phase composites based on the PVDF. 1-PVDF; 2-PVDF+50 vol.% PZT-5A; 3-PVDF+0,1 vol.% nanosized BaTiO_3 +49,9 vol.% microsized PZT-5A; $W=26,3 \cdot 10^{-6} \text{ J}$; 4- PVDF+1 vol.% nanosized BaTiO_3 +49 vol.% microsized PZT-5A; $W=335 \cdot 10^{-6} \text{ J}$; Polarization condition: polarization electric field $E_p=3 \cdot 10^6 \text{ V/m}$, polarization temperature $T_p=413 \text{ K}$ and polarization duration $t_p=0,5 \text{ hour}$.

We can watch from spectrum that TSD spectrums for composites with BaTiO_3 nanoparticles are much depended on preliminary crystallization under the action of electric gas discharge. Really, we can see from TSD spectrum that oxygenous centers, which can be stability centers for nanoparticles, can change immobilization process.

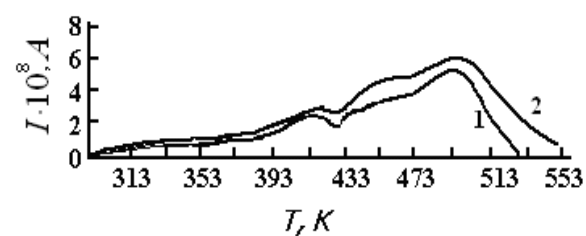


Fig. 6. TSD current spectrum for YSPE + SiO_2 +PKR-7M hybrid nano- and micropiezocomposit. 1–YSPE +0,2 vol.% SiO_2 +49,8 vol.% PKR-7M hybrid nano- and micropiezocomposit; 2–YSPE +0,4 vol.% SiO_2 +49,6 vol.% – PKR-7M hybrid nano- and microcomposit. $E_p = 3,6 \frac{\text{MV}}{\text{m}}$; $T_p=383 \text{ K}$; $t_p=0,5 \text{ hour}$.

ULTRA DISPERSE STATE OF POLYMER PHASE AS STABILIZER IN NANOSIZED BaTiO₃ AND POLAR AND NONPOLAR..

So, using TSD spectrums we can diagnose nanoparticles immobilization in composites. It should take an account two factors for increasing immobilization process:

- Use ultradisperse state of macromolecules as stabilizer;
- Formation of small molecules oxygenic combination having high polarization in polymer chain.

CONCLUSION

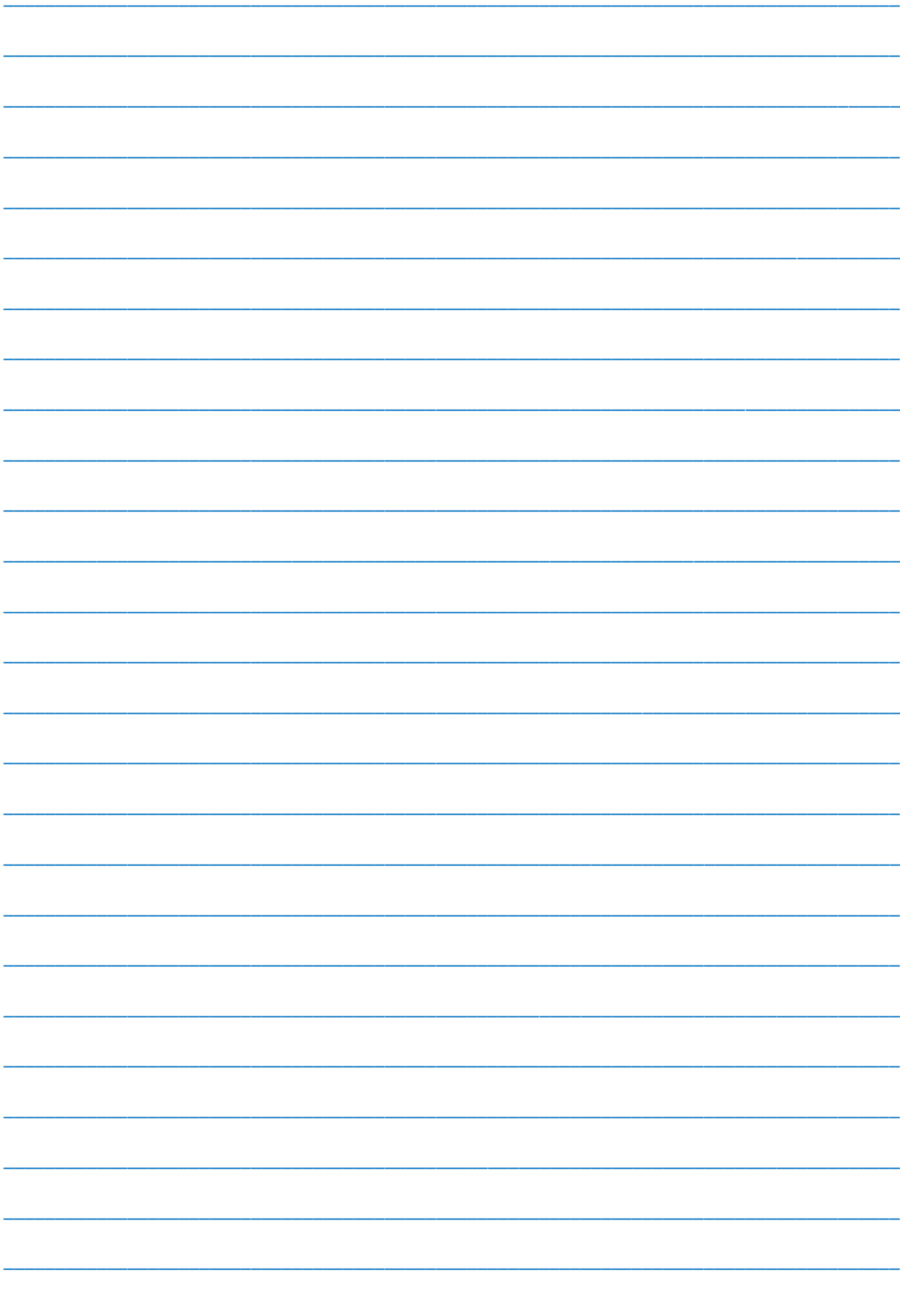
1. New technology of immobilization of SiO₂ and BaTiO₃ nanoparticles in polymer matrix have been developed;
2. It have been revealed that method of IR and TSD current spectrums is more efficiently for prediction nanostructurization of polymer-ferropiezoelectric composite.

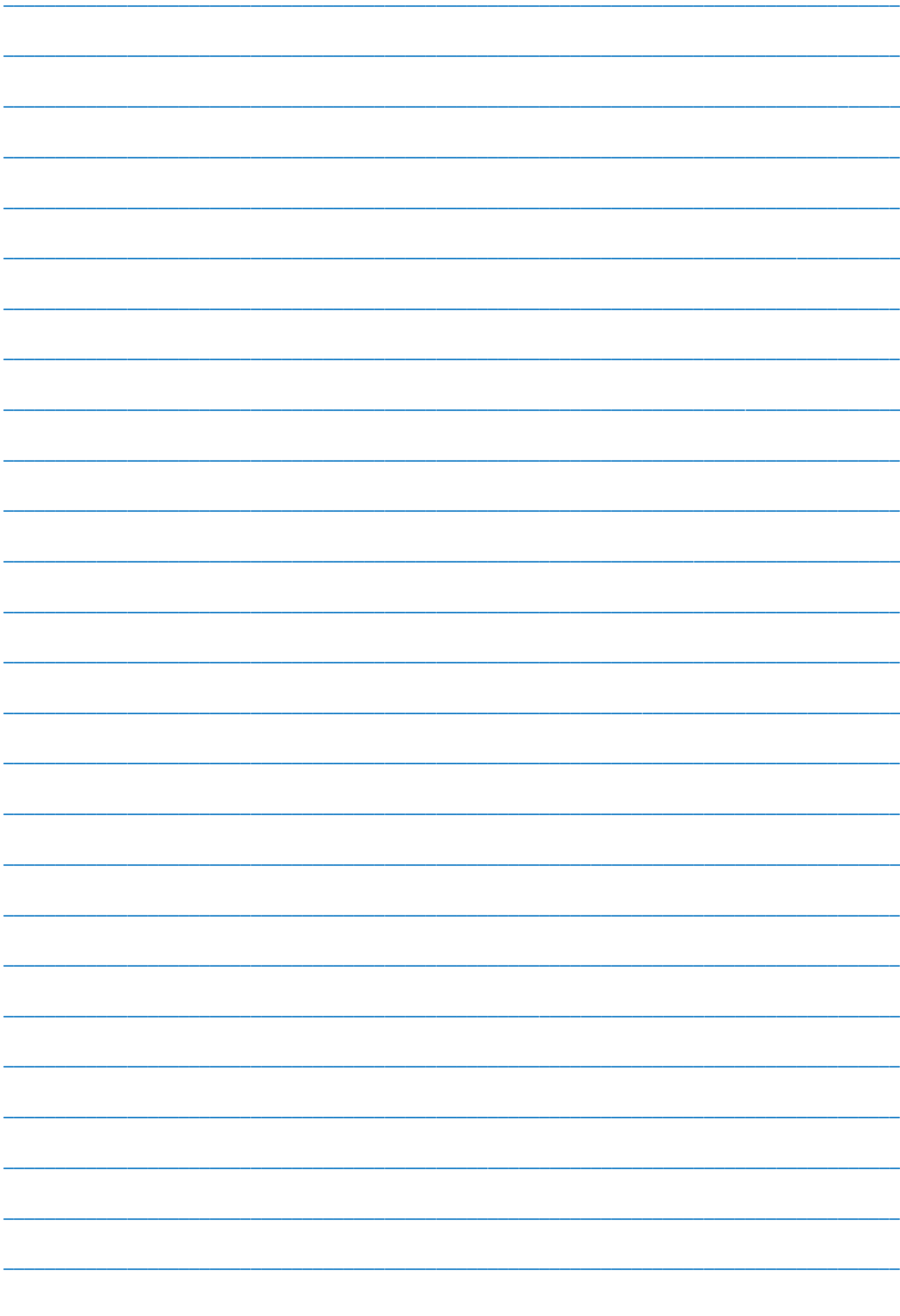
-
- [1] S.V. Glushanin, V.Yu. Topolov. Pisma JTF, 2001, v.27, is.15, p.15–21.
 - [2] V.V. Ermakin, A.E. Panich, V.G. Smotrakov, M.A. Kurbanov. Abstracts Books Inter. Scin.-Aplic. Conf. „Fundamental aspects of functional material sciences, piezoelectric devices and te chnology“. Piezotechnics, Rostof-na-Donu, 2005, p. 234–239.
 - [3] J.M.E. Lines, A.M. Glass Principles and application of ferroelectrics and related materials. Clarendo Press-Oxford, London, 1977.
 - [4] B.S. Aronov. Electromechanic transducers from piezoelectric ceramic, L., 1990, 272p.
 - [5] G.M. Sverdlin. Hydroacoustic transducers and antennas. L.: Shipbuilding, 1980. 232 p.
 - [6] I.S. RezPez, Yu.M. Poplavko. Dielectrics. Main properties and application in electronics. M.: Radio and communications, 1989, 288p.
 - [7] A.D. Pomogaylo, A.S. Rozenberg, I.E. Uflyand. Metal nanoparticles in polymers. M.: Chemistry, 2000. 672 p.
 - [8] J.E. Smay, J.I. Cesarano, A.B. Tuttle, J.A. Lewis. J. Appl. Phys., 2002, v. 92, No 10, p. 6119 – 6127.

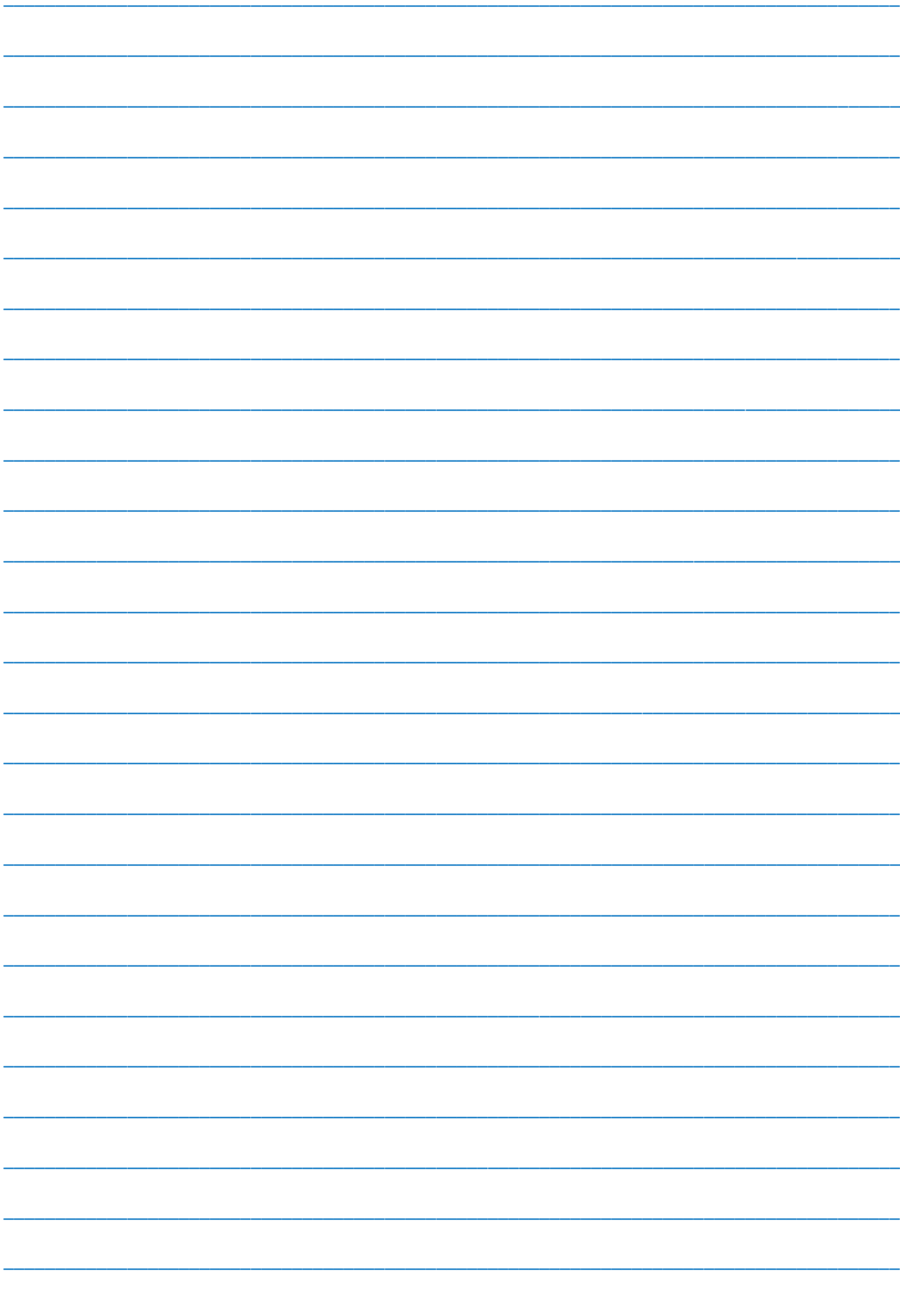
Received: 17.03.2014

CONTENTS

1.	The Analysis Of Main Artifacts In Scanning Probe Microscopy (III) S.D. Alekperov	3
2.	About possibility of using a dual-frequency liquid crystal for selective modulation of radiation T.D. Ibragimov, A.R. Imamaliyev, A.K. Mammadov, G.M. Bayramov	7
3.	The spectra of optical parameters of Bi_2Te_3 single crystals and film compounds N.Z. Jalilov, G.M. Damirov	10
4.	The study of phase equilibrium in $\text{TlSe}-\text{FeSe}$ system, electric and thermal properties of TlFeSe_2 F.M. Seidov, E.M. Kerimova, R.G. Veliyev, N.Z. Gasanov, K.M. Guseynova	18
5.	Energy spectrum of charge carriers in single crystal alloys $\text{Bi}_{1-x}\text{Sb}_x$ ($0, \leq x \leq 0,25$) at temperature $T=77-300\text{K}$ B.A. Tairov, H.A. Gasanova, V.I. Eminova, F.H. Mammadov	21
6.	A microscopic theory of local spin excitations in a rectangular ferromagnetic semiconductor nanowires V.A. Tanriverdiyev, V.S. Tagiyev	26
7.	Theoretical models of the isobutanol molecule conformations microwave spectra G.I. Ismailzadeh, I.Z. Movsumov, M.R. Menzeleyev, A.S. Qasanova, S.B. Kazimova	31
8.	Influence of gamma radiation on monocrystalline silicon solar cells Davud Mostafa Tobnaghi and Rahim Madatov	52
9.	Ultra disperse state of polymer phase as stabilizer in nanosized BaTiO_3 and polar and nonpolar polymer composites M.A. Kurbanov, A.A. Bayramov, F.N. Tatardar, F.F. Yahyayev, A.A. Nuraliyev, Z.A. Dadashov, B.Kh. Khudayarov	55









www.physics.gov.az